universität wien

DISSERTATION

Titel der Dissertation

„Biochemistry meets sequence analytics - investigation of predicted posttranslational lipid modifications and characterization of a predicted acetyltransferase“

Verfasser

Mag. Wolfgang Benetka

angestrebter akademischer Grad

Doktor der Naturwissenschaften (Dr. rer. nat.)

Wien, 2009	
Studienkennzahl lt. Studienblatt:	A 091 419
Dissertationsgebiet lt. Studienblatt:	Dr.-Studium der Naturwissenschaften Chemie
Betreuerin / Betreuer:	Dr. Frank Eisenhaber

Acknowledgments

First and most important, my thanks go to my family, especially my wife Patricia who always raised my spirits when a day at the lab had left nothing but dark clouds over my head, my parents who gave me the opportunity to go to university and always supported me, and my son Felix whose smile made me forget any problems occupying my thoughts.

Second, I want to express my gratitude to all the colleagues who accompanied me during my PhD. Manfred Koranda and Michaela Sammer were my lab colleagues during the first half of my PhD. Manfred was my direct contact person for a long time and Michaela provided the results my work concerning mec-17 was based upon and also participated in the experiments on the localization of NFAT5 and now continues this project. I want to thank Birgit Eisenhaber, Sebastian Maurer-Stroh, Maria Novatchkova, Alex Schleiffer and all other members of the Eisenhaber group from the Institute of molecular pathology (IMP), who provided the basis for my work and always found a reason to get together and enjoy some Belgian cherry beer and chocolate or other delicious food. In addition, I want to thank the group of Cecile Brocard, especially Sophie Merich and Johannes Koch, who shared the lab and their experiences and ideas with me during the second half of my PhD, as well as the members of the lab of Andreas Hartig.

Special thanks go to my supervisor Frank Eisenhaber who always valued my work and provided me with the opportunity to finish my PhD in Vienna.

I also want to thank all the people who contributed to my work by providing material or a helping hand. Egon Ogris from the Department of Medical Biochemistry provided a mouse brain cDNA library, the yeast strain EGY48 as well as the bacterial strain KC8 and a LexA antibody. Andreas Hartig kindly provided all plasmids needed in the yeast two-hybrid screen. James E. Samuel from the Texas A&M Health Science Center provided all cDNA clones from *Coxiella burnetii* (*C. b.*). The cDNA encoding Epb4.1l3 was provided by John Conboy from the Ernest Orlando Lawrence Berkeley Laboratory in California, and the cDNAs encoding numb-A and neur-B from *Drosophila melanogaster* (*D. m.*) were provided by Jürgen A. Knoblich from the Institute of Molecular Biotechnology. His group also helped with the localization experiments in transgenic flies, especially Jörg Betschinger and Ralph Neumüller.

Abstract

Sequence analytical tools can provide predictions of aspects of protein function such as enzymatic activities or sites of posttranslational modifications in protein sequences. Generally, an experimental verification is needed for these predictions. In the case of lipid posttranslational modifications, the standard experimental techniques are time-consuming and laborious. In this work, a new *in vitro* assay based upon the detection of incorporation of radioactively labeled lipid anchor precursors into *in vitro* translated proteins with a thin layer chromatography scanner was developed. This method drastically reduces time effort, it combines protein yield and anchor incorporation testing in a single experiment, and it is both applicable for prenylation and myristoylation. This assay has been used for investigation of prenylation and myristoylation of selected candidate proteins. Localization studies with GFP fusion proteins were used to verify the *in vivo* relevance of the results. The general potential of prenylation motifs in bacterial proteins to be modified by eukaryotic prenyltransferases was demonstrated *in vitro* for a so far uncharacterized, ankyrin repeat containing protein from *Coxiella burnetii*. The localization studies also suggest prenylation of an F-Box containing protein from *Legionella pneumophila*. The influence of SNPs on the functionality of prenylation motifs was investigated and found significant in the case of W353G in human ALDH3B2. Myristoylation of fly proteins important in asymmetric cell division and neuronal development (numb-A, neuralized B and C and Par-1 isoform Q) as well as homologous proteins from mouse (neuralized-like 1 and 2) was demonstrated. The importance of distinguishing between isoforms with differing capabilities for posttranslational modifications is discussed. Myristoylation of the human transcription factor NFAT5-A was shown to influence localization to the nucleus suggesting a new mechanism for regulation of nuclear shuttling of transcription factors.

Sequence similarities with the HATs from the GNAT superfamily suggested a function as histone acetyltransferase for mec-17 from *C. elegans* as well as homologous proteins from other organisms. Preliminary results of enzymatic activity tests and localization studies indicated that the protein has N-acetyltransferase activity; yet, histones might not be the primary substrate for acetylation by mec-17. A yeast two-hybrid screen revealed several proteins interacting with mouse mec-17 that could be either substrates or members of a multiprotein complex. Interaction with one of the found proteins, Kctd13, was verified biochemically by co-immunoprecipitation.

Zusammenfassung

Sequenzanalytische Methoden ermöglichen die Vorhersage verschiedener Aspekte der Funktion von Proteinen, wie enzymatische Aktivität oder die Position von posttranslationalen Modifikationen in Proteinsequenzen. In den meisten Fällen bedürfen diese Vorhersagen experimenteller Überprüfung. Im Fall von posttranslationalen Lipidmodifikationen ist die gängige Methodik zeit- und arbeitsaufwendig. In dieser Arbeit wurde deshalb ein neuer *in vitro* Assay entwickelt, der auf der Detektion des Einbaus radioaktiv markierter Vorläufermoleküle der Lipidanker in *in vitro* translatierte Proteine mittels eines Dünnschichtchromatographie-Scanners basiert. Diese Methode reduziert den Zeitaufwand merklich, sie kombiniert die Bestimmung der Proteinausbeute und des eingebauten Lipidankers in einem einzelnen Experiment und ist für die Untersuchung von sowohl Prenylierung als auch Myristoylierung anwendbar. Diese Technik wurde zur Untersuchung von Prenylierung und Myristoylierung ausgewählter Proteine verwendet. Lokalisationsstudien mit GFP-Fusionsproteinen wurden zur Bestätigung der *in vivo* Relevanz der Ergebnisse herangezogen. Die prinzipielle Möglichkeit der Modifikation von Prenylierungsmotiven bakterieller Proteine durch eukaryotische Prenyltransferasen wurde *in vitro* am Beispiel eines bisher nicht charakterisierten Proteins aus *Coxiella burnetii* gezeigt, welches so genannte Ankyrin repeats enthält. Die Lokalisationsstudien legen auch die Prenylierung eines Proteins mit einer F-Box-Domäne aus L*egionella pneumophila* nahe. Weiters wurde der Einfluss von SNPs auf die Funktionalität von Prenylierungsmotiven untersucht und im Fall von W353G im humanen Protein ALDH3B2 als signifikant bewertet. Die Myristoylierung von Fliegenproteinen mit biologischer Bedeutung in asymmetrischer Zellteilung und Entwicklung des Nervensystems (numb-A, neuralized B und C und Par-1 Isoform Q) sowie deren homologen Mausproteinen (neuralized-like 1 und 2) wurde gezeigt. Die Wichtigkeit der Unterscheidung zwischen Isoformen mit unterschiedlichem Potential für posttranslationale Modifikationen wird diskutiert. Die Myristoylierung des humanen Transkriptionsfaktors NFAT5-A sowie deren Bedeutung für dessen nukleare Lokalisation wurden gezeigt und legen einen neuen Mechanismus für die Regulierung des Kerntransports von Transkriptionsfaktoren nahe.

Ähnlichkeiten der Sequenz von mec-17 aus *C. elegans* und homologen Proteinen aus anderen Organismen mit HATs aus der GNAT-Familie deuteten auf eine Funktion als Histon-Acetyltransferase hin. Die Ergebnisse von Experimenten zur Enzymaktivität und

Lokalisation des Proteins zeigen N-Acetyltransferase-Aktivität. Allerdings scheinen Histone nicht das bevorzugte Substrat zu sein. Mit einem Yeast 2-Hybrid Screen wurden daher einige Interaktionspartner des Maushomologs identifiziert. Diese kommen als Substrat oder Bestandteile eines Multiproteinkomplexes in Frage. Die Interaktion mit einem der Kandidaten, Kctd13, wurde durch Co-Immunopräzipitation biochemisch bestätigt.

Table of contents

1 Aim of the thesis

The ultimate goal in the so-called life sciences is to get to an understanding of the principles that make life possible at the molecular level. To achieve this, there are two classical approaches: one is the genetic approach with mutagenesis, looking for phenotypes and defining participation of gene products in certain pathways, resulting in what is often called “arrow”-science because there is no information about the kind of the interaction symbolized by the arrows. On the other hand, there is the biochemical approach with protein purification, *in vitro* tests, and structural analysis where few proteins are characterized in depth, but the capacity for large scale investigations is often limited. A combination of both ways can lead to a quite complete understanding of biochemical processes, but will take a lot of time. A third approach might help to speed up this process: the application of computational power on biochemical questions is able to support the classical research. With the availability of complete sequenced genomes, the scope of the applicability of sequence analysis tools has expanded. Genome wide *in silico* screens produce many, increasingly reliable predictions that, generally, require dedicated experimental efforts for their verification. Unfortunately, this is often not compatible with the way classical research labs work. This raises the need for request-based biochemistry specializing on experimental investigation of sequence analytical predictions. Based on predictions of the sequence analytical unit of our group, two projects were topic of my work.

1.1 Development and application of an *in vitro* assay for the investigation of lipid posttranslational modifications

Cell signaling is of crucial importance to every multicellular organism. This becomes even more evident from the observation that defects in signaling pathways are the major cause for cancer. Posttranslational modifications play an essential role in signaling. Lipid modifications act together with other factors to attach signaling proteins to membranes where they get in contact with their respective receptors. From there, signals have to be relayed to the appropriate targets in the cell, most often the nucleus where transcriptional adjustments take place in response to extracellular signals. This is often achieved by phosphorylation cascades, underscoring the importance of another posttranslational modification.

Focusing on lipid modifications, their importance in signaling makes proteins carrying lipid anchors as well as the enzymes attaching them to possible drug targets for the treatment of cancer and other diseases. Identification of a number of lipid modified proteins also permitted development of sequence analytical tools for identification of additional candidate proteins which could enlarge our knowledge about these proteins and the impact of their modifications and also broaden the range of applications for already available inhibitors targeting lipid modifications. Of course, these predictions need to be verified experimentally. A fast and reliable *in vitro* assay for the detection of prenylation has been developed previously in our lab. The goal in the first project was to apply this assay for the investigation of predicted prenylation candidates of special interest, e.g. proteins with prenylation motifs predicted to be influenced by single nucleotide polymorphisms and bacterial proteins. According to the current knowledge, bacteria do not possess prenyltransferases themselves. However, pathogenic bacteria could utilize the prenyltransferases of their eukaryotic hosts, a strategy that has already been observed for myristoylation. Furthermore, the scope of lipid modifications under investigation should be expanded by development of a similar tool for the detection of protein N-myristoylation and application for the investigation of selected candidate proteins predicted to carry this modification. Lipid–modified transcription factors are of special interest as membrane attachment via lipid modifications would imply a so far unknown mechanism for the regulated mobilization and nuclear shuttling of transcription factors. This issue was exemplarily studied with human NFAT5 isoform A[a].

1.2 Characterization of a predicted protein N-acetyltransferase

Based on sequence analysis, there is not only the possibility to predict the sites of posttranslational modifications, but based upon conservation of critical residues between similar proteins as well as comparison of critical features of protein structures or 3D models, prediction of the function of unknown proteins is possible under certain circumstances. In our group, a rather uncharacterized protein form *Caenorhabditis elegans* (*C. e.*) called mec-17[b] was predicted to act as a histone acetyltransferase (HAT).

[a] Nuclear factor for activation of T cells

[b] Mechanosensory abnormality

Homologous proteins were found in fly, mouse, and human. Preliminary results of enzymatic assays with recombinant protein and histone tail peptides were promising since they supported the working hypothesis of mec-17 homologues having protein N-acetyltransferase activity, but the native substrates could not be identified. It is notable that the large family of proteins commonly termed histone acetyl transferases includes a lot of proteins also or exclusively targeting other proteins than histones. Therefore, it was decided to look for protein interaction partners of mouse mec-17 that might shed some light upon the functional impact of the protein and also reveal the true substrate.

1.3 Summary of aims

No case of a prenylated bacterial protein has been reported so far. Thus, the prenylation status of bacterial proteins with a predicted prenylation site from *Coxiella burnetii* (ankyrin repeat protein) and *Legionella pneumophila* (F-Box protein) will be investigated *in vitro* to check the general potential of bacterial proteins to be subject to prenylation by enzymes of eukaryotic host cells. Experiments with GFP fusion proteins will be performed to analyze the importance of prenylation for subcellular localization of the proteins in eukaryotic cells.

Predictions indicate that the recognition of potential prenylation substrates by prenyltransferases might be affected by SNPs in the relevant region of the substrate sequence. The influence of SNPs on the *in vitro* prenylation of the human proteins ALDH3B2, BEX2, UTP14A, and FLJ20364 as well as the impact on localization of the different variants in human cells will be studied.

Myristoylation plays an important role in the proper localization of proteins involved in asymmetric cell division and neuronal development. The prenylation assay will be adapted for the investigation of protein N-myristoylation and applied on the proteins numb A, Par-1 Q, and Neuralized B and C from *Drosophila melanogaster* as well as neuralized-like 1 and 2 from *Mus musculus*. In addition, the influence of myristoylation on localization of these proteins will be studied in transgenic flies and in murine cells, respectively.

Prediction of myristoylation sites in the sequence of transcription factors suggests a new mechanism for mobilization and subsequent translocation of these proteins to the nucleus. To test this hypothesis, the *in vitro* myristoylation status and the influence on the localization of NFAT5-A will be analyzed exemplarily.

Mec-17 is predicted to be a histone acetyltransferase. Its N-acetyltransferase activity was demonstrated *in vitro*. A yeast 2-hybrid assay will be used to identify potential substrates as well as other members of a putative multiprotein complex. The interaction of these proteins with mec-17 will be further characterized with biochemical methods.

This work features several topics that are mainly connected via the combined efforts of sequence analytics and biochemistry. For the sake of readability, the discussion of the results will follow their presentation for each topic separately. Thus, no extra section is present for the discussion. The main text is ended with a Conclusion section summarizing the findings, main conclusions, and the outlook. The work is completed with an Appendix that contains Materials and Methods for all experimental procedures, lists of Figures and Abbreviations as well as the Curriculum Vitae and the list of scientific publications of the applicant relevant for this work.

2 Introduction

Posttranslational lipid modifications that were subject to investigation include protein prenylation and myristoylation. Additionally, a putative N-acetyltransferase is the topic of the second part of my work. An extensive review on protein prenylation co-authored by the applicant has been published recently. Therefore, this material is not repeated here, and the reader is referred to the journal[1]. An overview of protein N-myristoylation as well as acetyltransferases will be given to provide the background information on the research topics discussed in this work.

2.1 Myristoylation

Protein N-myristoylation is the covalent attachment of the 14 carbon saturated fatty acid myristate to N-terminal glycine residues[2-5] via an amide bond[6]. Myristoylation of lysine ε-amino groups has been observed, too, but is not topic of this work. Protein N-myristoylation is specific for myristic acid over the more abundant palmitic acid[7], usually occurs co-translationally[8,9] after removal of the initiator methionine by cellular methionylaminopeptidases and is irreversible[10], but exceptions exist: Posttranslational myristoylation has been shown for a protein from *Dictyostelium discoideum*[11], and several proteins were shown to be myristoylated posttranslationally on internal glycine residues after caspase-mediated proteolytic cleavage leaving the glycine in an N-terminal position[12-15]. Contrary to the proposed irreversibility of myristoylation, an activity de-myristoylating MARCKS[a] has been described[16]. The enzyme catalyzing protein N-myristoylation is N-myristoyltransferase (NMT), a member of the Gcn5[b]-related N-acetyltransferase (GNAT) superfamily of proteins. It catalyzes transfer of the myristoyl moiety of Myristoyl-Coenzyme A (CoA) to the free amino-group of the N-terminal glycine residue of the peptide substrate[17].

2.1.1 Function in membrane attachment

The primary function of the lipid modification in most myristoylated proteins is promotion of membrane attachment. Myristoylation alone only provides a weak and reversible association with cellular membranes and, thus, is required but not sufficient for stable

[a] Myristoylated alanine-rich C kinase substrate

[b] General control of amino acid synthesis

membrane binding. This seems to be a wanted feature and important aspect of the function of myristoylation as NMT is highly selective for myristic acid, especially against the longer palmitic acid which would promote much stronger membrane association[18].

For a stable interaction with membranes, additional membrane attachment factors (MAFs) are needed which is in analogy to the two-signal model proposed for prenylation (C-terminal modification by polyisoprenoids). Palmitoylation of one or more nearby cysteine residues increases the hydrophobic interaction with the membrane lipids[19]. Palmitoyl acyl transferases (PATs) are described as membrane bound[20]. Thus, the weak membrane binding provided by myristoylation is a prerequisite for subsequent palmitoylation. Positive charge clusters in vicinity of the myristoyl anchor often referred to as polybasic region (PBR) can enhance the interaction with the surface of membranes by electrostatic interaction with negatively charged phospholipid head groups[21,22]. Other examples of MAFs would be phospholipid binding domains, transmembrane regions, and direct protein-protein interactions with otherwise membrane-bound targets.

2.1.1.1 Regulation of membrane binding

Depending upon the additional factors strengthening membrane attachment, several mechanism exist for the regulation of reversible membrane association[23]. Palmitoylation, in contrast to myristoylation, is a reversible lipid modification easily removed by palmitoyl thioesterases. Thus, the localization to and the release from membranes is controlled via cycles of palmitoylation and de-palmitoylation.

On the other hand, proteins harboring a myristoyl anchor in conjunction with a PBR can reversibly associate with membranes by a mechanism called “myristoyl switch”. Some proteins can change between two conformations with the myristate sequestered in a hydrophobic pocket of the protein in one state, but pointing outward ready for membrane insertion in the other conformation. There are different types of myristoyl switches classified upon the way the switch is triggered. Recoverin exposes its myristoyl anchor upon Ca^{2+}-binding[24], and Arf[a] releases its myristoyl moiety upon guanosine triphosphate (GTP) binding[25]. These proteins are examples of ligand switches. Another possible trigger

[a] Adenosine diphosphate (ADP) rybosylation factor

is proteolytic cleavage as is the case for HIV-1[a] Gag. It is synthesized as a 55 kDa polyprotein precursor and associates with the plasma membrane mediated by myristoylation and a nearby positive charge cluster. After proteolytic cleavage, the myristate is buried in a pocket of the 17 kDa product[26,27]. A similar mechanism is found in the reovirus membrane-penetration protein Mu1[28]. The third class is the so called electrostatic switch. For MARCKS, release from the membrane is triggered by phosphorylation of serine residues within the PBR disrupting the electrostatic interaction with the acidic phospholipid head groups[29,30]. Hisactophilin utilizes a pH-dependent switch with a histidine cluster that loses its positive charge above pH 7[31].

2.1.1.2 Specific membrane targeting

Combined use of different MAFs is not only necessary to provide stable membrane attachment but also to specify the exact targeting of lipid modified proteins to different membrane compartments. Localization studies with lipid modified GFP[b]-chimeras revealed that myristoylation excludes GFP from the nucleus and enables association with intracellular membranes, but plasma membrane localization requires a second signal[32]. A large fraction of myristoylated proteins is associated with the plasma membrane, but some are also localized to the endoplasmatic reticulum (ER), Golgi, mitochondrial membranes, or the nuclear envelope. There is even evidence for extracellular localization of a myristoylated protein[33]. To predict the final localization of a protein depending on the presence of different MAFs is not an easy task, especially when protein-protein interactions are involved. Furthermore, membranes are not a homogenous sea of lipids. The membranes of different compartments differ in lipid composition and, consequently, also in fluidity. There are even specific microdomains within membranes which are often referred to as lipid rafts.

The targeting specificity of proteins harboring a myristoyl moiety in conjunction with a palmitoylation to the plasma membrane is explained by the so called kinetic bilayer trapping hypothesis[34]. The proteins are myristoylated co-translationally enabling them to reversibly associate with a variety of membranes. But only when they reach the plasma membrane, they get in contact with membrane-bound PATs adding the second fatty acyl

[a] Human immunodeficiency virus

[b] Green fluorescent protein

anchor stabilizing their interaction with the plasma membrane[35,36]. As membrane dissociation is much slower for doubly lipid modified proteins, they are kinetically trapped there. After they are stably bound at the plasma membrane, these proteins often become enriched in lipid rafts. These membrane microdomains are defined by resistance to extraction with nonionic detergents and a high content of sphingolipids and cholesterol. Since the lipids in raft-like membranes contain primarily saturated fatty acyl chains, they are present in the liquid ordered state (in contrast to the more fluid liquid crystalline phase)[37]. Therefore, it seems plausible that proteins modified by saturated fatty acyl chains preferably localize to lipid rafts while proteins with prenyl anchors are excluded due to their bulky branched structure[38,39]. It remains unclear whether myristoylated/palmitoylated proteins are preferably partitioned to preformed microdomains or their interaction with the membrane induces the formation of these rafts. Anyway, enrichment of N-terminally fatty acylated proteins in a sub-membranous microenvironment might provide increased local protein concentrations and thus facilitate protein-protein interactions[40].

A good example for the effect of different lipid anchors and localization to specific membrane microdomains are heterotrimeric G proteins[41]. Gα subunits are N-terminally acylated by myristate and/or palmitate while the βγ-dimer is prenylated at the C-terminus of the γ-subunit[42,43]. The βγ-dimer seems to dominate membrane binding characteristics of heterotrimeric G-proteins. In model membranes, they are found in non-lamellar phases rich in phosphatidylethanolamine[44]. The same microenvironment is preferred by G-protein coupled receptors (GPCRs). Actually, the prenyl anchor of the βγ-dimer as well as transmembrane helices of the GPCRs seem to actively influence the behavior of the lipid phase[45,46]. In contrast to the heterotrimer, the Gα subunit which is monomeric after nucleotide exchange induced by receptor activation prefers pure lamellar membrane structures excluding it from the microenvironment of the receptor and the βγ-dimer. Monomeric $G\alpha_i$ and $G\alpha_s$ were found to localize to lipid rafts while $G\alpha_q$ was concentrated in caveolae[47]. This translocation might facilitate interaction with effector proteins located in these membrane microdomains.

Another interesting case of membrane targeting via fatty acyl modification was found in *Leishmania major*. Localization of HASPB[a] to the extracellular face of the plasma

[a] Hydrophilic acylated surface protein B

membrane was found to depend on N-terminal myristoylation and palmitoylation. This suggests a novel pathway for translocation of proteins to the surface of eukaryotic cells. This pathway seems to available also in higher eukaryotes[33].

2.1.2 More functions

In addition to membrane targeting, several other functions for myristoylation have been reported in certain cases. Involvement of the myristoyl moiety in direct protein-protein interactions has been shown for the interaction of calmodulin with the protein kinase C substrates MARCKS and BASP1[a] as well as the HIV-1 protein Nef[48-50]. A role in protein stability and structural integrity has been described for the myristoyl moieties of calcineurin[51]. Finally, myristoylation is involved in regulation of enzymatic activity of Pto, a serine/threonine kinase from tomato[52] and the c-Abl tyrosine kinase[53,54].

2.1.3 Function and clinical relevance of myristoylated proteins

The first myristoylated proteins identified were cyclo-adenosine monophosphate (cAMP) - dependent protein kinase[3] and calcineurin B[2]. As more and more myristoylated proteins were discovered, it became clear that N-terminal modification with myristic acid is common for proteins from eukaryotes as well as their viruses. Some myristoylated proteins are also found in bacteria. Classification of known myristoylated proteins shows that there are only few large protein families with a conserved myristoylation motif. These are primarily involved in signaling and include the Gα subunits, Arfs, serine, threonine, and tyrosine kinases, and EF hand calcium binding proteins. Many smaller families exert specialized functions.

Some members of the Gα family are myristoylated and palmitoylated[42,43]. Myristoylation is clearly required for membrane attachment but might also play a role in localization to specific membrane microdomains[47], interaction with GPCRs[55], and Gα structure[56].

Myristoylated tyrosine kinases also depend on the lipid modification for proper membrane localization and, in consequence, for their signaling function[57]. For c-Abl, an auto-inhibitory mechanism utilizing a myristoyl/phosphotyrosine switch has been described[53,54].Tyrosine kinases are of special clinical interest as mutations in this signaling

[a] Brain abundant, membrane attached signal protein

proteins are often associated with the development of cancer[58,59]. Since tyrosine kinases depend on myristoylation for signaling, increased NMT activity might be needed by cancerous cells. Indeed, elevated NMT activity was observed in early colonic carcinogenesis[60] suggesting NMT as a target for chemotherapeutic drugs as well as a diagnostic marker[61,62]. The potential role of NMT in cancer has been reviewed recently[63].

A regulatory role of myristoylation has been described for the serine/threonine kinase Pto from tomato. It is involved in race specific resistance to *Pseudomonas syringae*. Kinase activity is repressed by intramolecular binding of the myristoyl moiety. Effector proteins of the intruder target the same region of Pto, thereby displacing the myristate and activating kinase activity resulting in induction of defense responses including hypersensitive cell death[52].

Calcineurin B was among the first proteins known to be N-terminally myristoylated[2]. Recently, the importance of myristoylation for membrane targeting has also been demonstrated for calcineurin B-like proteins from *Arabidopsis thaliana*[64]. Furthermore, a role of NMT and calcineurin in epilepsy was suggested[65].

Proteins that are myristoylated posttranslationally after caspase-mediated proteolytic cleavage build another interesting group. A previously internal myristoylation motif becomes N-terminal and, thus, accessible for NMT. Several such cases are known now. For the pro-apoptotic protein BID[a], myristoylation is involved in targeting to mitochondria followed by release of cytochrome c and programmed cell death[12]. A myristoylated fragment of cytoskeletal actin is also targeted to mitochondria after cleavage by caspase, but the functional role of this translocation remains unclear[13]. The myristoylated cleavage product of gelsolin is not targeted to mitochondria, but displays anti-apoptotic activity[14], while myristoylation of the cleavage product of p21-activated protein kinase 2 potentiates late apoptotic events[15]. Taken together, this indicates an important role for posttranslational myristoylation in regulation of apoptosis.

As mentioned above, NMT was suggested as therapeutic target in the treatment of cancer and epilepsy, but this is not the only application for drugs targeting NMT. NMT is essential for growth and survival of several human parasites including the fungi *Candida*

[a] BH3 interacting domain death agonist

albicans[66], *Cryptococcus neoformans*[67], and the protozoa *Leishmania major* and *Trypanosoma brucei*[68,69]. Exploiting divergent peptide substrate specificity of NMTs from different species, some specific inhibitors targeting the NMTs of pathogenic organisms have been designed already[70-75]. Based upon a comprehensive analysis of different NMTs, the list of potential targets for selective NMT inhibition has been continued with *Histoplasma capsulatum, Plasmodium falciparium, Aspergillus fumigatus, Trypanosoma cruzi, Giardia intestinalis, Entamoeba histolytica, Pneumocystis carinii, Strongyloides stercoralis,* and *schistosoma mansoni*[76].

Myristoylation also has an important impact on various functions of many viral proteins as well as some from bacteria[77]. The large surface antigen of hepatitis B virus[78,79], µ1 of reoviruses[28], VP4 of picornaviruses[80], and VP2 of polyomaviruses[81] are myristoylated and the lipid anchor is required for viral entry into host cells. A mechanism with insertion of myristate into the host membrane has been proposed for some of them. Another function of viral proteins that can be dependent upon myristoylation is the assembly of viral particles. This has been shown for poliovirus[82] and several mammalian retroviruses[83-85], especially HIV[27,86]. There is also a conserved myristoylation motif in a superfamily of proteins from large deoxyribonucleic acid (DNA) viruses. One member of this group, the myristoylated transmembrane protein LR1 of Vaccinia poxvirus, is located in the first envelope and involved in acquisition of the second envelope[87]. Myristoylation is also found in non-homologous proteins of other large DNA viruses with similar membrane arrangements. Last but not least, myristoylated viral proteins are involved in manipulation of host cell signaling like the transforming protein of Rous sarcoma virus[88] and the Nef protein of lentiviruses (including HIV) which requires myristoylation-mediated membrane binding for interactions with the endocytic machinery and signaling proteins to adjust host cells to optimal viral replication conditions[89]. As an example from bacteria, three type III effector proteins from *Pseudomonas syringae* need myristoylation for efficient membrane targeting and function[90]. NMT inhibitors have been suggested for antiviral therapy[91], but, since viral and bacterial pathogens usually utilize the host NMT, it is much more complicated to achieve a specific effect on infected cells.

2.1.4 N-myristoyltransferase

The enzyme catalyzing the N-terminal myristoylation of proteins is called N-myristoyltransferase (NMT). NMT is ubiquitous among eukaryotes, and in higher

eukaryotes there are two gene copies named NMT1 and 2. Homology between NMT1 and NMT2 is lower than between NMTs of one type in different species indicating two distinct families. Additionally, posttranslational modifications (PTMs) or alternative splicing seem to account for differing NMT isoforms varying in molecular weight and cellular localization[92].

The best characterized N-myristoyltransferase is *Saccharomyces cerevisiae* (*S. c.*) Nmt1p. It consists of 455 residues with an apparent molecular weight of ~ 55 kDa[93]. It was shown to be a cytosolic monomeric enzyme with a slightly alkaline pH-optimum (8.0) and no requirement for divalent cations. At least one histidine residue seems to be critical for activity which is consistent with the fact that at pH 6.0 and below the enzyme is inactive. Nmt1p has no intrinsic aminopeptidase activity[94]. Thus, it is dependent on the action of methionylaminopeptidases in advance.

The structure of *S. c.* Nmt1p has been solved without and with substrates and/or substrate analogues. The Nmt fold consists of a saddle shaped mixed β-sheet surrounded by several α-helices. The protein has an internal pseudo-two fold symmetry with the N-terminal half responsible for myristoyl-CoA binding, while the C-terminal half predominately harbors the peptide binding site[95]. Based on kinetic studies, a Bi Bi reaction mechanism has been proposed with binding of myristoyl-CoA prior to peptide followed by release of CoA first and myristoylpeptide afterwards[96]. Consistent with this mechanism, the affinity of peptide substrates is much greater for the myristoyl-CoA-Nmt1p complex than for the apoenzyme suggesting either a direct contribution of myristoyl-CoA to the peptide binding site or a conformational change in the enzyme induced by myristoyl-CoA binding[97].

Resolution of the crystal structure of the enzyme as a binary complex with myristoyl-CoA revealed binding of the first substrate in a conformation resembling a question mark. Upon myristoyl-CoA binding, residues 34 – 55 are rearranged resulting in formation of the 3_{10} Helix A'. This helix, forming a positive dipole, and especially residues H38, K39, F40, and W41 contact the 3' phosphate group of CoA. Amide nitrogens and side chains of the eC loop and the αC helix provide hydrogen bonds with the pyrophosphate group of CoA inducing also a first bend in the myristoyl-CoA conformation[98]. Interactions of the adenosine -3'-monophosphate-5'-diphosphate group have been suggested to provide mainly the binding energy for positioning of catalytically important regions of CoA substrates [99]. This has been confirmed by binding studies of a substrate missing the 3'-

phosphate and is also consistent with the fact that acyl-CoAs outside the catalytical specificity of Nmt can bind to the enzyme with high affinity and also generate a functional peptide binding site, but catalytic activity is markedly reduced due to improper positioning of the reactive group [100]. Water mediated intramolecular hydrogen bonds between the O5p of pantetheine and the N6a amine of adenine induce a second bend directing the chain towards the active site. There, the reactive thioester carbonyl is hydrogen bonded to the backbone amides of F170 and L171, forming the so called oxyanion hole, providing the polarization of the carbonyl required for catalysis. Furthermore, the sulfur atom is located close to the N6a amine in hydrogen bonding distance.

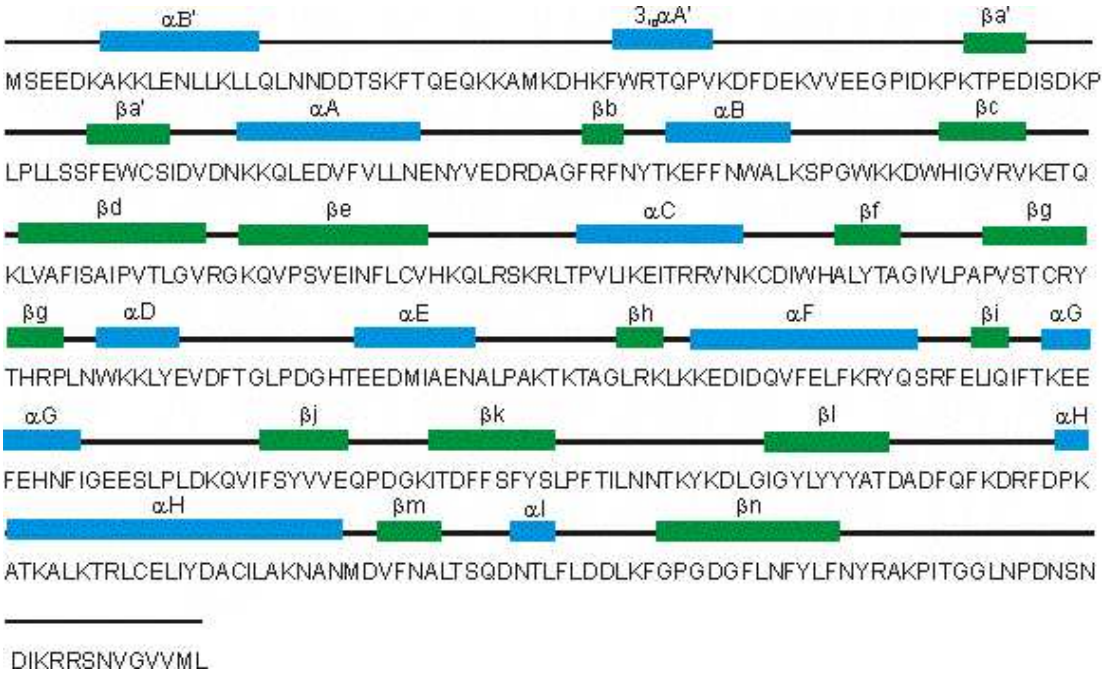

Figure 1: Secondary structure of ScNMT

Position of secondary structure elements in the sequence of ScNMT according to the crystal structure[101], with α-helices shown in blue and β-strands in green.

This intramolecular interaction could stabilize the CoA thiol during the reaction. Additionally, release of CoA after the reaction is easier as a compact globular product. A third bend after C1m leads the acyl chain around the adenine where the side chains of W41, I168, I187, and Y204 block its way producing a fourth bend at C6m forcing the remaining stretch of C7 – C14 into a deep pocket within the protein core. Its depth is limited by side chains from V194, A202, and F425 and main chain atoms from T191, W200, and H201 providing an explanation how Nmt discriminates between substrates of

different chain length [98]. In conclusion, three features act together to allow measurement of the acyl-CoA substrate length: The positioning of the reactive thioester carbonyl in the oxyanion hole, the block forcing the bend at C6m in the acyl chain, and the depth of the pocket. The requirement for a bent conformation of myristoyl-CoA is also confirmed by kinetic studies [102].

A critical role was suggested for the Ab loop. Binding of myristoyl-CoA in the correct conformation alters its conformation through interactions via the loop B'A' as well as direct interactions between myristoyl-CoA and the Ab loop. These interactions seem to stabilize the Ab loop in an open conformation and thus expose part of the peptide binding site [98,101]. Beyond this function, the Ab loop is not likely to be directly in involved in peptide recognition and binding.

The binding of the peptide substrate has been elucidated by the crystal structure of a ternary complex of Nmt1p with a myristoyl-CoA analogue and a peptide of the sequence GLYASKLA. The conformation of the bound model peptide reveals contact between the side chain of Leu2 and the myristoyl-CoA analog bending the peptide towards a binding groove. The path of the peptide is blocked at Ala4 by a large hydrophobic cluster forcing another bend that leaves the peptide main chain in a parallel β-sheet with strand βn of Nmt1p. This configuration is stabilized by several interactions with the enzyme as well as intramolecular hydrogen bonds, especially between Tyr3 carbonyl and Ser5 amide. The environment of the peptide also explains the amino acid restrictions observed: Leu2, Tyr3, and Ala4 experience a rather hydrophobic/aromatic environment with some potential hydrogen bonding partners for residues 2 and 3. Position 2 does not allow charged or bulky residues, while at position 3 and 4 there is enough space to accommodate all amino acids. Serine is strongly preferred at position 5. Ser5 is able to build hydrogen bonds with H221 and backbone amides of G418 and D417. Importance of H221 for peptide binding, but not for catalysis, has also been shown by mutation studies [103]. Position 6 shows a preference for lysine, but all residues except for proline are allowed. The ε-amino group of Lys6 is coordinated by D417 as well as D22 and D23 [101], and its aliphatic part is embedded in an hydrophobic/aromatic environment. The residues at position 7 and 8 have only few contacts giving the peptide binding groove an open-ended character and enabling it to accommodate nascent polypeptide chains for co-translational myristoylation [98]. It is noteworthy that most residues involved in peptide binding are highly conserved in

mammalian NMTs, and substitutions might account for species specific substrate differences.

With both substrates bound, the stage is set for the transfer of the myristoyl moiety to the peptide. Several prerequisites have to be fulfilled for a successful reaction: The thioester carbonyl of myristoyl-CoA needs to be polarized. This is achieved by interaction with the oxyanion hole. Hydrogen bonds with the main chain amides of F170 and L171 result in a partial positive charge of the carbonyl carbon facilitating a nucleophilic attack. The nucleophil is provided by proton transfer from the Gly1 amino group of the peptide substrate to the C-terminal carboxylate of Nmt which is consistent with the effect of C-terminal deletions on catalytic activity [103]. The hydroxyl group of T205 as well as the carbonyl group of N169 seem to stabilize the nucleophil and are conserved in all Nmts. Tyr3 of the peptide seems be involved, too. At this stage, the distance between the nucleophilic nitrogen of Gly1 and the electrophilic carbon is 6.3 Å. For the nucleophilic attack, a rotation by 180° around Ψ is required which gives a good explanation for the absolute requirement for an N-terminal glycine for myristoylation. It is needed to provide rotational flexibility. Consistent with this model, mutation of glycine to alanine as well as proline and aromatic residues at position 2 result in poor substrates. After rotation, the interactions of Gly2 are replaced by even stronger ones with the carbonyl of N169 and the hydroxyl and carbonyl group of T205. Upon nucleophilic attack on the polarized thioester carbon, a tetrahedral intermediate is generated followed by release of free CoA. This anionic reaction product is stabilized by an intramolecular hydrogen bond between the sulfur atom and a nitrogen atom of the adenine moiety providing a compact leaving group. The final step is release of the myristoylpeptide [98]. Product release also seems to be the rate-limiting step in protein N-myristoylation [104].

Comparative studies demonstrated that the myristoyl-CoA binding site is highly conserved in NMTs from different species while there are some substitutions in the peptide binding pocket accounting for differences in substrate specificity[105,106]. Phylogenetic analysis yielded three clusters representing plant, fungal, and metazoan NMTs. Protozoa are in one group with fungi. This finding is consistent with the observations in substrate specificity. The altered tolerance for amino acids at position 3, 4, 7, and 8 of the substrate can be exploited for development of species-specific inhibitors[72].

2.1.5 Sequence requirements for myristoylation

Based upon analysis of the sequences of experimentally verified myristoylation substrates, NMT substrate specificity studies utilizing oligopeptides, and structural data or models of NMT from various organisms, the sequence requirements for protein N-myristoylation were refined[76]. It turned out that a simple model of amino acid restrictions at certain positions is not sufficient. Instead, a certain pattern of physical properties is required for recognition by NMT where compensatory effects among the sequence positions of the substrate make the context more important than single residues. Based upon the intensity of the interaction with NMT, the substrate sequence motif has been divided in three segments.

The residues 1 to 6 have to fit into NMTs peptide binding pocket and are most restricted due to a multitude of specific interactions. Most NMT residues involved in recognition of substrate positions 1 to 6 are highly conserved. At position 1, glycine is absolutely required. This is due to the rotational flexibility required by the reaction mechanism of NMT as discussed previously. As position 2 and 5 show a tendency towards small amino acids compared to the average peptide, side chain volume seems to be an important factor there. Volume compensation is possible to some extent between 2 and 3. Polarity is preferred at 2 and 3, but fungal NMTs are more tolerant towards hydrophobic residues than NMTs from higher eukaryotes. At position 4, large and hydrophobic amino acids are preferred with the exception of certain fungal NMTs that have a smaller binding site there. Like position 2, residue 5 should be small and polar, but serine and threonine are preferred as they are additionally stabilized by hydrogen bonding. Furthermore, backbone flexibility is required between position 3 and 5. At position 6, lysine and threonine are preferred since the polar head group is stabilized by hydrogen bonds and the aliphatic region of the side chain by hydrophobic interactions.

The second segment consists of residues 7 to 11. These show weak interactions with the surface of the enzyme at the mouth of the catalytic cleft. The lack of tight specific interactions comes along with no clear amino acid preferences but a more general requirement for certain physical properties. At position 7, turn-like residues are preferred while bulky hydrophobic residues are disfavored, but volume compensation is possible between residues 7 and 9. Position 8 shows an increased occurrence of basic amino acids, but there is no obvious reason for this from the interaction with the enzyme. This

phenomenon rather seems to reflect the fact that myristoylation often acts in concert with a PBR. For both position 7 and 8, negative charges are not well accommodated by the enzyme, but NMTs of fungi and protozoa are more restrictive against them than NMTs of higher eukaryotes. Position 9 is preferably occupied by polar amino acids with flexible backbone. There is a general trend towards small and polar residues until position 11, especially between 8 and 10 only limited hydrophobicity is allowed.

Positions 12 to 17 fulfill the function of a spacer connecting the bulk of the substrate protein (which is likely to adopt a globular conformation) to the modified stretch. Since this segment of the motif is exposed to the aqueous cytosolic environment (or to hydrophilic membrane lipid head groups later on), a certain content of polar residues is required. Again, a limited amount of hydrophobic residues can be compensated for. For entering of the N-terminus of the substrate into the catalytic pocket of NMT, the whole stretch from 7 to 17 requires conformational flexibility to adopt an extended conformation. It has to be easily unfolded or permanently without secondary structure. Such a linker segment seems to be a general requirement for posttranslational modifications. In case of internal modifications, two linker regions are needed flanking the site of the modification. The length of the linker is determined by the roughness of the surface of substrate and enzyme[107].

2.1.6 The MYR-Predictor

Based upon the refinement of the sequence motif for protein N-myristoylation, a predictor has been developed and is available online at http://mendel.imp.ac.at/myristate/index.html[108]. Both amino acid preferences and required physical property pattern were implemented into a scoring function. Thus either many small deviations of the requirements or one drastic can be responsible for classification of query sequences as no myristoylation target. The contributions of different terms are summed up in the scoring function facilitating identification of the critical terms. Separate prediction functions were implemented for fungal as well as for eukaryotic and viral sequences to take the differences in substrate specificity between NMTs from different species into account. It is also possible to look for putative internal myristoylation sites. In this case, the potential protease cleavage site preceding the glycine is compared to documented cases of internal myristoylation after proteolytic cleavage.

Application of the predictor to protein databases yielded lots of interesting putative myristoylation targets[109]. 34 new potential myristoylation targets in fungi were added to the 22 fungal proteins present in the learning set, and 266 new putative targets were identified in higher eukaryotes and viruses. Many predictions add new members to protein families with known myristoylation targets like 16 α-subunits of G proteins, 7 tyrosine – protein kinases, and 12 serine/threonine-protein kinases. Of special importance seems to be the combination of calcium import and myristoylation as indicated by 34 known and 32 predicted myristoylation targets with annotated calcium binding sites. Some of the new candidates might also utilize a calcium-myristoyl-switch mechanism. These large families are examples of a myristoylation motif conserved over several species. This strengthens the predictions and suggests importance of the myristoylation for the biological function of the protein families. The evolutionary conservation of predicted myristoylation motifs has been evaluated in groups of homologous proteins. The results are available as MYRBASE at http://mendel.imp.ac.at/myristate/myrbase/ [110]. Several large protein families probably representing the oldest cases of myristoylation are found in opposition to a lot of families with only few members that might carry out specialized functions.

The candidates with no similarity to the known cases are especially interesting as they expand the functional spectrum of myristoylated proteins. A new group of proteins predicted to be subject to myristoylation are plant specific disease resistance proteins. Parasitic bacteria inject avirulence proteins that are often myristoylated into host cells via the type III secretion system. Myristoylation of the disease resistance genes could be necessary for the interaction with the avirulence proteins required for induction of the adequate immune response. Recently, the regulation of a disease resistance protein from tomato by myristoylation has been shown[52]. A role for myristoylation in ubiquitination is suggested by prediction of a myristoylation motif for several ubiquitin-specific proteases as well as proteins containing putative RING zinc finger domains commonly found in ubiquitin ligases. One example of this group is the Notch pathway protein neuralized, a peripheral membrane protein involved in establishing signaling asymmetry[111]. The myristoylation status of the mouse and fly homologues of neuralized was investigated in this work, and the myristoylation motif is also conserved in human, frog, and worm. A myristoylation motif is also conserved for TOM40[a] involved in protein import into

[a] Translocase of outer membrane

mitochondria which is quite surprising for an all-β integral membrane protein. The role of myristoylation in the function of voltage gated potassium channels also remains unclear. A channel as well as a group of modulatory proteins interacting with these channels is predicted to be myristoylated, and proteins of this group that are not subject to myristoylation are palmitoylated instead indicating the importance of lipid modification[112]. While GTPases are usually prenylated, an interferon-γ induced GTPase involved in mammalian immune response is predicted as a substrate for myristoylation.

This finding adds another example to the assumption that the myristoylation motif is used as an exchangeable module in evolution together with other MAFs. There are already several known cases supporting this idea. Gα-subunits carry myristoyl and/or palmitoyl anchors in different number[42]. In *Arabidopsis thaliana*, a protein of the Rab/Ypt GTPase family was found that lacks the typical C-terminal prenylation motif, but harbors N-terminal sites for myristoylation and palmitoylation instead[113]. Functional replacement of the N-terminal double acylation with myristate and palmitate by a transmembrane domain was demonstrated for endothelial nitric-oxide synthase[114]. A phosphoinositide-specific phospholipase C from Trypanosoma cruzi is N-terminally myristoylated and palmitoylated replacing the pleckstrin homology domain usually mediating membrane interactions of these proteins[115]. Of course, these exchanges of MAFs often come along with differences in function and/or localization. Furthermore, while it is well established that palmitoylation or PBRs act synergetic with myristoylation in membrane attachment, other MAFs like lipid-binding domains, transmembrane regions, and protein-protein interaction domains are clearly overrepresented in the predicted substrates. The functional importance of these combinations needs further investigation.

To sum up, a multitude of new myristoylation targets are predicted and await experimental verification. Of course, some of them might deserve elaborate investigation of their function and the impact myristoylation has on it, but to make a pre-selection it would be convenient to have a fast and reliable method for testing protein N-myristoylation at hand. Furthermore, the simple experimental verification of the ability of proteins to be a substrate for myristoylation gives the opportunity to enlarge the learning set available for the prediction function which both helps in improvement of the quality of the predictions as well as development of more species-specific prediction functions in addition to the ones available for fungi and higher eukaryotes. Thus, a new *in vitro* assay for investigation of protein N-myristoylation was developed and applied on selected candidate proteins.

2.2 Mec-17 – histone acetyltransferase or not?

2.2.1 Chromatin structure

DNA is nature's medium for storage of information. The building plan for the proteins that carry out most biological processes required for life is encoded in DNA by linear combination of four bases. This information is present in every single cell. As one can imagine, storing all this information in a linear code of just four elements yields quite a long string. Somehow this string, which is about 1 -2 meters long in eukaryotic cells, has to fit into the nucleus of the cells and be available at the same time for fundamental cellular processes. Transcription is required for protein synthesis, replication for proliferation, and DNA repair to maintain the integrity of the genome. In a review, the problem is depicted very nicely: "Imagine trying to stuff about 10.000 miles of spaghetti inside a basketball. Then, if that was not difficult enough, attempt to find a unique one-inch segment of pasta from the middle of the mess, or try to duplicate, untangle and separate individual strings to opposite ends"[116]. Thus, it is obvious that a sophisticated mechanism is required to store DNA in a convenient way. In a way, the comparison of DNA with spaghetti also fits for the method that is used for compaction of DNA to fit into the nucleus. Most people tend to wrap the spaghetti around a fork, and this is what is basically done in the first step with DNA, too. In the so called nucleosome core, the smallest unit for organization of DNA, 147 base pairs (bp) in a left-handed superhelix are wrapped 1.65 times around a histone octamer. These nucleosome cores are repeated with 10 – 60 bp of linker DNA in between resulting in a fiber with a diameter of ~10 nm that presents the characteristic look of "beads on a string"[117,118]. The linker histone H1 seems to neutralize the negative charges of the linker DNA backbone reducing the electrostatic repulsion between the DNA strands and changing the exit path of the DNA from the nucleosome core to allow a more compact folding. Together, the core histones with the DNA wrapped around it as well as the linker DNA and the linker histone build a nucleosome. Interactions between the nucleosomes lead to the assembly of higher order structures that are stabilized by the linker histones resulting in formation of a compact 30 nm fiber. Fiber-fiber interactions increase the compaction of DNA to ~100 nm thick chromonema fibers. The maximum level of condensation is achieved during mitosis when the chromosomes are separated into the daughter cells. Metaphase chromosomes are ~1400 nm thick. It is tempting to view packing of DNA into chromatin similar like protein

structure: the primary structure is the linear arrangement of nucleosomes, the secondary structure would be the 30 nm chromatin fiber, and chromonema-like fibers represent the tertiary structure[119].

2.2.1.1 Histones

The nucleosome core is the basic unit of chromatin structure with DNA wrapped around a histone octamer. This multimeric protein is built of two copies of each of the core histones H2A, H2B, H3, and H4. Four so called "histone-fold" dimers assemble stepwise into the complete octamer. Two H3-H4 dimers associate to build a tetramer which then interacts with two H2A-H2B dimers. All four core histones consist of two functional domains, the "histone-fold" motif which accounts for histone-histone interactions required for octamerization as well as histone-DNA contacts, and the so-called histone tails which are the site of various posttranslational modifications and involved in interactions with linker DNA and between nucleosomes[120].

The histone-fold domains of the different core histones share a common structural motif that consists of three α-helices connected by two loops. These are the basis for assembly of the crescent-shaped heterodimers via a "handshake motif". The interactions between the heterodimers are mediated by 4 helix bundles. One such interaction between the H3 histones of the H3-H4 dimers leads to assembly of the tetramer. Subsequently, the full octamer is put together by 4 helix bundles between the H4 and H2B histones. The two H2A-H2B dimers are not connected this way leaving the respective helices in H2A unused. These would be available for internucleosome interactions, although current models for higher order structure would not fit to such an interaction.

Each heterodimer is able to bind about 2.5 turns of DNA double helix bent around the curvature of the structure. Summing up over the octamer, the histone fold domains are able to harbor 121 bp of DNA with 27 – 28 bp bound to each dimer and 4 bp in between as a linker[121]. Although binding of DNA to histones occurs primarily via the negatively charged phosphodiester backbone, the positioning of the nucleosomes is at least partially dependent on the DNA sequence. The wrapping of DNA around the histones requires a certain degree of flexibility or bendability. Additionally, some direct contacts between the histones and base pairs could also account for sequence selectivity.

The second functional domain of the core histones are the histone tails. These are segments at the N-terminus of the core histones with a length of 20 to 35 residues rich in basic amino acids. H2A has an additional 37 residue C-terminal tail. The histone tails do not significantly contribute to nucleosome structure and stability, they seem to emanate radially from the nucleosomes. They were shown to contribute to sequence dependent nucleosome positioning[122], but their main function seems to lie in higher order compaction of chromatin which is underscored by the result that removal of the tails blocks condensation at the level of the 10 nm fiber[123,124]. The condensation mediated by the histone tails is stabilized by linker histones that are not structurally related to the core histones, which seems to be required for further compaction[125,126].

2.2.2 Regulation of chromatin structure

Assembly of DNA and histones into nucleosomes and higher-order structures provides the compaction necessary to store the whole genome in the nucleus of a single cell. However, the challenge is not over at this point, it has just begun. Certain pieces of DNA must be accessible at specific time points for replication, transcription, and repair. These processes require the stepwise assembly of large protein complexes which can be viewed as molecular machines. But it is hard to imagine how the protein machinery required for these processes could target specific sequence stretches and attach to them to carry out their tasks in the fully condensed state. In fact, cells use the compaction of DNA regions into heterochromatin to keep them transcriptionally silenced. Thus, chromatin can not be a rigid structure, but has to be a highly dynamic construct undergoing regulated unfolding and folding.

For fully condensed metaphase chromosomes, fiber diameters up to 300 nm were shown[127]. At mitotic exit to interphase, regional decondensation down to chromonema fibers with 60 to 80 nm diameter was observed[128]. In a model system, activation of transcription resulted in decondensation to 80-100 nm fibers which were suggested as basic higher order structure allowing gene expression[129]. A second model in a more natural context lead to observation of at least fully condensed 30 nm fibers in regions of active transcription[130]. Thus, it seems not necessary to fully untangle DNA from the histones to provide the accessibility required. However, regulated chromatin remodeling is certainly needed. Several mechanisms act together to achieve this goal.

First of all, chromatin is not only built of the canonical nucleosomes. There are several histone variants with special functions in chromatin structure. One of them has been shown to be essential for centrosome assembly and function, and an H3 variant replaces canonical H3 during transcription. Several variants of H2A have been found, one of them involved in X-chromosome inactivation. H2AZ, another variant of H2A, has a different tail sequence[131] and is involved in transcriptional activation and repression[132,133]. It seems to exert a role in chromatin folding as it prevents further condensation of 30 nm fibers[134]. However, not much is known at present about the targeting of these histone variants to specific regions of chromatin. In addition, also non histone proteins were shown to bind to nucleosomes. These so-called high mobility group proteins (HMG) also seem to affect chromatin structure[135].

In addition to incorporation of variants of histones into chromatin for special functions, two major mechanisms act together in chromatin remodeling. Proteins of the Swi2 superfamily use the energy of adenosine triphosphate (ATP) hydrolysis to modify the chromatin structure. The second mechanism is based on posttranslational modification of the histone tails. Both activities are present in protein complexes often recruited by transcriptional activators[136]. It is not clear whether there is some sort of order for the action of these mechanisms. ATP-dependent remodeling has been shown to be prerequisite for posttranslational histone modifications in the case of genes transcribed during mitosis when the genome is highly condensed. On the other hand, the reverse order is observed for cell-cycle independent genes[137].

2.2.3 Histone tail modifications

Histones are subject to a multitude of posttranslational modifications, most of them occurring at the histone tails. In fact, it seems like almost every solvent accessible residue of histones is modified in one way or another. From the already highly conserved histones, the tail regions are evolutionary conserved most indicating the importance of the presence of the residues that are target of covalent modifications. Posttranslational modifications of histones include acetylation, methylation, phosphorylation, ubiquitination, sumoylation, glycosylation, and ADP-ribosylation with the first three of the modifications occurring most frequent. Acetylation and methylation can occur at the side-chain amino groups of lysine and arginine. For methylation, complexity is increased by the fact that arginine residues can carry two methyl groups and lysine up to three. Phosphorylation takes place

on serines and threonines, and the small protein ubiquitin as well as the related SUMO[a] are attached to lysine side chains. A wide variety of functions has been addressed to these modifications. Acetylation is generally associated with transcriptional activation, although there are exceptions[138]. The various methylation marks were shown to be involved in both activation and repression of transcription depending on the site and number of methyl modifications[137]. For histone phosphorylation, a role in transcriptional activation and chromosome condensation in mitosis was shown[139]. Reversible ubiquitination of core histones H2A and H2B is associated with transcriptional activity.

2.2.3.1 The histone code

Given the multitude of modifications, the existence of a histone "code" was proposed. This word is rather misleading as it implies that a certain modification does always have the same function. But the functional impact of histone modifications seems to be the result of the interpretation of a whole pattern of modifications depending on the gene and the cellular context[140]. Some marks are needed for further modification while others may block modification of nearby residues. Two roles have been postulated for the histone code. The first is to provide heritable chromosome-specific epigenetic marks. Somehow a cell passes on the pattern of active and silenced genes to its daughter cells. Some sort of marks has to survive DNA replication and segregation of chromosomes during mitosis. Histone modifications have been suggested to be involved in this process, especially methylation as it is viewed as a rather stable modification in contrast to others, although enzymes responsible for removal of methyl marks have been discovered recently[116,141,142]. However, to which degree histone modifications are responsible for epigenetic memory is still controversial and needs further investigation[143]. On the other hand, the combinatorial function of posttranslational histone modifications in localized control of events on chromatin including transcriptional activation and repression as well as histone deposition in S-phase or chromosome condensation in mitosis is out of question.

2.2.3.2 Targeting of histone modifications

A multitude of cellular processes are influenced by one or the combination of several histone modifications. Thus, their placement needs to be precisely targeted. This is

[a] Small ubiquitin-related modifier

achieved in part by the inherent substrate specificity of the enzymes responsible for the modifications but also by their recruitment to specific loci via association with gene-specific activators or repressors or with the RNA polymerase II holoenzyme complex. Enzymes involved in DNA repair were shown to be recruited directly by DNA lesions. A special case is the methylation of histone 3 lysine 9 which seems to be targeted by small non-coding ribonucleic acids (RNAs) via the RNA interference (RNAi) pathway resulting in formation of heterochromatin required for centromere function[116]. Apart from the precisely targeted modifications required for specific functions, there are bulk chromatin modifications, too, involved in histone deposition after passage of a replication fork or chromosome condensation in mitosis. For example, the non-targeted action of histone acetyltransferases and deacetylases seems to maintain some sort of equilibrium level of histone acetylation in yeast[144]. After targeting of the histone modifying enzymes to certain loci, the exact point of modification is determined by their substrate specificity but also by cross-talk with other marks that are already present. These can promote or inhibit further modifications, some types of PTMs might rival for the same residue. Thus, a pattern coding for a specific function can be built up sequentially.

2.2.3.3 Function of histone modifications

When the modifications are finally in place, they somehow have to exert their function. Two models have been proposed. The first is based upon the change of the charge of histone tails by PTMs. Elimination of positive charges from the overall basic histones could weaken the interaction with the negatively charged DNA backbone. However, a lot of modifications would be necessary to significantly reduce the overall charge of histones given the number of basic residues present. Furthermore, hyperacetylation did not release histone tails from DNA *in vitro*. It seems more plausible that removal of critical charges destabilizes internucleosome contacts disrupting the higher-order structure of chromatin and, thus, reducing DNA compaction[145].

In the second model, PTMs modify the surface for protein interactions creating new binding sites for proteins which then in turn exert the functions mediated by the PTMs. Evidence for this model comes from the discovery of specific binding domains. Bromodomains were shown to bind to acetylated lysines. Some of them are even specific for a certain acetylated lysine residue. However, it is not clear whether all bromodomains bind acetyllysine. Bromodomains are present in many transcription and chromatin

regulators like histone acetyltransferases (HATs) or ATP-dependent chromatin remodelers[146,147]. The chromodomain was discovered as methyl-lysine binding domain, but later on chromodomains were shown to interact with diverse targets including histones, DNA, and RNA. Chromodomains are present in many regulators of chromatin structure[148,149]. Tudor-, MBT-, and PHD-domains recognize methyllysines, too[150]. The model of histone modifications as protein binding sites also gives a nice explanation for cross-talk as neighboring PTMs could easily influence the binding of these specific domains. Several modifications could act together to give a certain function in different ways. Either a specific pattern of modifications is recognized by a single binding protein which would require that they are on the same histone tail or at least the same nucleosome. On the other hand, each modification could be recognized separately by individual proteins which then interact physically or functionally. This would allow the modifications to be quite distant from each other. In each case, the binding proteins could be the basis for the assembly of multiprotein complexes that exert the specific functions. However, the basic coding unit could either be a single nucleosome or a chromatin stretch of undefined size[143].

Taken together, both proposed models how posttranslational modifications of histone tails influence chromatin structure provide some explanations. Furthermore, they are not exclusive, so it is very likely that reality is more closely to a combination of both models.

2.2.4 Histone acetylation

The first hint on a role for histone acetylation in transcriptional control came from the observation that actively transcribed regions tend to be hyperacetylated whereas transcriptionally silent regions tend to be hypoacetylated[151]. All core histones except H2A have four or five potential acetylation sites giving a total of 26 sites for acetylation on a nucleosome. Acetylation of histone tails was shown to disrupt higher order chromatin folding[152] resulting in better accessibility for proteins interacting with DNA. Furthermore, acetylation maintains the unfolded structure of transcribed nucleosomes[153], and acetylation of 46% of all acetylation sites is sufficient to facilitate transcription. Despite the obvious link between histone acetylation and transcription, it is important to distinguish different types of acetylation. Partial chromatin decondensation induced by broad histone acetylation does not directly correlate with active transcription, but rather marks regions of transcriptional competence. In this state, promoters are accessible for the transcription machinery and transcription elongation is supported, too. In contrast to broad acetylation,

activation of transcription often comes along with targeted histone acetylation at promoters and could function in recruitment of other chromatin remodeling activities[154].

The two models described previously also fit for the description of the function of histone acetylation. Neutralization of positive charges by acetylation could weaken the interaction with the DNA backbone as well as interactions required for higher order chromatin structure. Additionally, acetylated residues could act as docking sites for proteins that, in turn, carry out the functions mediated by histone acetylation. The best characterized module for this purpose is the bromodomain which is able to recognize acetyllysine[155]. This domain is present in many regulators of transcription and chromatin structure[156]. Bromodomains were shown to play a role in five functions so far. First, they are important for chromatin acetylation by HATs. Bromodomains present in several HATs are required to anchor them to acetylated chromatin. Second, ATP-dependent chromatin remodeling complexes like SWI/SNF and RSC require their bromodomains for acetylation dependent chromatin remodeling. The third function is in organization of chromosome and chromatin domains. Brd proteins build a physical barrier between euchromatin and heterochromatin, associate with acetylated chromatin regions in interphase and/or mitosis, and reorganize chromatin. Fourth, bromodomains also recognize acetylated non-histone proteins. Several transcription factors and chromatin remodelers are subject to lysine acetylation. In some cases, it has been shown to promote association of these proteins with HATs. Finally, bromodomains can act as regular protein- or DNA-binding modules[157].

2.2.5 Histone acetyltransferases

Although the connection between reversible histone acetylation and transcriptional control has been known for quite some time, it took until the 90s to identify the enzymes responsible. The breakthrough was the discovery of a protein from *Tetrahymena thermophila* that has histone acetylation activity and is related to the yeast protein Gcn5[158]. Gcn5 was known before as a transcriptional coactivator, and the demonstration of its HAT activity established the connection between histone acetylation and transcriptional regulation. Since then, several transcriptional co-activators and co-repressors were shown to possess histone acetylation and deacetylation activity, respectively[159].

2.2.5.1 HAT families

Histone acetyltransferases are grouped in several families which display high sequence similarity between families but poor to no similarity between families[159]. These are named Gcn5/PCAF[a], p300/CBP[b], MYST[c], SRC[d], $TAF_{II}250$[e], Hat1, and ATF-2[f]. The members of these families combine HAT domains of different size with other protein domains like the bromodomain in the case of Gcn5/PCAF, CBP/p300, and $TAF_{II}250$, the chromodomain and a cysteine-rich zinc-binding domain in MYST as well as cysteine-histidine rich domains in CBP/p300. ATF-2 differs from the others because it is the only sequence specific DNA-binding transcriptional activator with HAT activity. The diversity of HAT families enables them to exert various functions including a role in transcriptional activation and silencing, formation of leukemic translocation products, and dosage compensation in *Drosophila melanogaster*. A subgroup of cytoplasmic enzymes also called B-type HATs acetylate newly synthesized histones prior to their incorporation into chromatin. The best studied example is Hat1[160]. The HATs with nuclear localization involved in transcriptional control are also called A-type HATs.

2.2.5.2 HAT structure and mechanism

Some HATs were shown to belong to the Gcn5 related N-acetyltransferase (GNAT) superfamily, a family of proteins with diverse functions. In addition to HATs, the GNAT superfamily also includes aminoglycoside N-acetyltransferases, serotonin N-acetyltransferase, glucosamine-6-phosphate N-acetyltransferase, mycothiol synthase, protein N-myristoyltransferase, and the Fcm family of acyltransferases. Members of this family display limited sequence homology in four segments called motif A, B, C, and D. Although the pairwise sequence identity between the different members of the GNAT family ranges only between 3 and 23%, they all share a structurally conserved fold consisting of an N-terminal β-strand, two α helices, three antiparallel β strands, a "signature" central helix, a fifth β strand , a fourth α helix, and a final β strand[161].

---

[a] p300/CBP associated factor

[b] CREB binding protein

[c] Named after the founding members MOZ, Ybf2/Sas3, Sas2 and Tip60

[d] Steroid receptor coactivator

[e] TBP associated factor

[f] Activating transcription factor

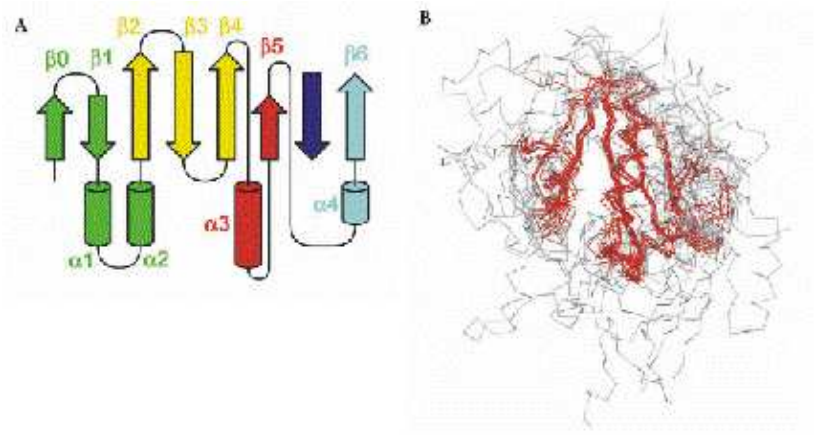

Figure 2: Conserved fold of Gcn5 family members

(A) Topology of the core GNAT fold. From N- to C-terminus, structural elements are colored green, yellow, red, and blue. The N-terminal strand β0 is not completely conserved and the deep blue C-terminal strand may be contributed by the same or another monomer. (B) Superposition of 15 GNAT structures. Residues with root medium square deviation < 2,7 Á are shown in red[161].

The histone acetyltransferases of this family, including Gcn5, PCAF and CBP/p300, show no significant homology in motif C, but motifs A, B and D form a structurally conserved domain involved in binding of CoA. Other HATs which do not belong to the GNAT superfamily were suggested to contain a structurally similar motif for CoA interaction. The A-D motif consists of three antiparallel β-strands followed by a helix underneath the sheet in parallel orientation. The similarities in HAT structures extend this motif with a conserved loop – β-strand C-terminal of the helix. Together, this structural element is approximately at the center of the HAT proteins and viewed as core domain. It is believed to play a role in Acetyl-CoA binding and catalysis. Coenzyme A is bound in a bent conformation. Motif A makes most of the contacts, especially with the pantetheine chain and the pyrophosphate group of CoA. A catalytical role has been suggested for a conserved glutamate residue (E173 in yGCN5) and confirmed by mutagenesis[162]. It seems to act as general base to facilitate deprotonation of the substrate lysine and is surrounded by non-polar residues raising the pK_a value. Structural superposition of HATs from different families reveals corresponding conserved glutamate residues in similar arrangement in MYST and Hat1 families[160].

In contrast to the core domain, the domains at the N- and C-terminus seem to mediate histone substrate binding. The sequence divergence found in these regions might account for different substrate specificities of the HATs. Nonetheless, superposition of the core

domains reveals an N-terminal helix-loop and a loop-helix motif in the C-terminal domain found in other HATs, too. Furthermore, these regions play a critical role in substrate binding and contain residues highly conserved in the respective families. The substrate is bound in a long channel in a random coil conformation. Most interactions with the enzyme occur via main chain atoms of the substrate and thus do not contribute to substrate specificity. Selectivity is provided by extensive interactions of few critical residues as well as by the requirement of the substrate to adopt the needed conformation. Other histone modifications were shown to play a role in selectivity, and to some degree the substrate specificity is also determined by other proteins present in multisubunit complexes harboring the HATs as catalytic subunits.

Despite the structural similarities between different HATs, their mechanisms differ. The kinetic mechanism of Gcn5 and P/CAF is ordered Bi-Bi. Acetyl-CoA binds first followed by the histone substrate. CoA binding was shown to induce localized conformational changes in the enzyme, especially the histone substrate binding groove is widened[160]. The carbonyl of Acetyl-CoA is hydrogen bonded to the enzyme polarizing it for nucleophilic attack by the amino group of the substrate and stabilizing the anionic tetrahedral intermediate[161]. After transfer of the acetyl moiety to the substrate, the acetylated histone is released prior to CoA[163,164]. In contrast, MYST HATs utilize a ping-pong mechanism where the acetyl group is transferred to a cysteine residue at the active site. After dissociation of CoA, the acetyl group is moved onto the histone substrate[165].

2.2.5.3 HAT complexes

Some conserved patches in HATs are not involved in substrate binding. These regions are likely to act as protein interaction sites. In fact, most HATs are in multisubunit complexes in vivo[157]. The complexes characterized best are the yeast SAGA[a]/human PCAF/Gcn5 and yeast NuA4[b]/human Tip60[c] complexes. Both have roles in regulation of transcription[166,167]. HAT proteins and their complexes have similar but distinct substrate specificity. Furthermore, the complexes are typically more active than the catalytic subunits alone. Thus, associated subunits are involved in regulation of the HAT activity as well as in

[a] Spt-Ada-Gcn5-acetyltransferase

[b] Nucleosome acetyltransferase of H4

[c] Tat interactive protein

recruiting substrates. For example, yeast Gcn5 alone can only acetylate free histones, but Gcn5 functions as a catalytic subunit in two native HAT complexes named ADA and SAGA, which acetylate nucleosomal histones[166]. Furthermore, Gcn5 alone acetylates predominately lysine 14 of histone H3 on free histones while ADA acetylates 9,14, and 18 and SAGA 23 in addition[168]. Ada2, Ada3, and Gcn5 form the catalytic core of these HAT complexes. Ada2 seems to potentiate the Gcn5 catalytic activity and Ada3 facilitates nucleosomal acetylation and expanded lysine specificity[169]. The SAGA complex also contains Spt gene products that are linked to TBP[a] function. This indicates the importance of histone acetylation during steps in transcription activation but also demonstrates that these modular complexes have multiple, independent functions in chromatin modification and TBP recruitment [166,170]. Some subunits of HAT complexes also contribute to transcriptional function in targeting the complexes to promoters. For example, the yeast HAT complexes SAGA and NuA4 contact several yeast activators through their only common subunit Tra1[171]. A similar functionality is observed for TRRAP[b] in human complexes. MYST HATs are part of large complexes and their activity and specificity is modified by the other subunits, too. Their subunits differ from the elements present in complexes of HATs of the GNAT superfamily and indicate a role in epigenetics and cell proliferation control for MYST complexes.

2.2.6 Non-histone-targets for acetylation

Up to now, many HATs were shown to have other protein substrates in addition to histones. The first non-histone protein found to be a target for HAT acetylation was p53, a tumor suppressor and sequence specific DNA-binding transcription factor that is acetylated by p300/CBP and deacetylated by HDAC1[c,172-174]. Acetylation occurs at several lysine residues at the DNA binding regulatory domain enhancing DNA binding and thereby increasing activation of target genes. In addition, acetylation seems to promote protein stability due to protection of lysine residues that need to be ubiquitinated for degradation. Since then, a multitude of transcription factors as well as several other cellular and also viral proteins were shown to be substrates for lysine acetylation[175].

---

[a] TATA-binding protein

[b] Transformation/transcription associated protein

[c] Histone deacetylase

2.2.6.1 Acetylated transcription factors

YY1[a] has multiple roles including sequence specific DNA binding and activation as well as repression of transcription. While acetylation at the zinc-finger DNA binding domain decreases DNA binding activity, acetylation at the repression domain affects transcriptional activition[176].

High mobility group (HMG) proteins are known to bind to distorted DNA and induce bending in linear DNA. Members of different subfamilies can be acetylated by p300/CBP and/or PCAF. Acetylation yields different effects depending on the specific protein and the lysine residue modified including increased or decreased DNA binding affinity, increase in transcriptional activation as well as influence on nuclear localization[177-180].

STAT3[b] is a latent cytoplasmic transcription factor and the downstream effector of cytokine signaling pathways. Acetylation of STAT3 by p300/CBP enhances dimerization which is required for nuclear translocation as well as DNA binding and activation of target genes[181,182].

c-MYC[c] is known as an oncoprotein. Although acetylation sites targeted by PCAF/GCN5 and Tip60 reside in the nuclear localization sequence and the leucine zipper domain, their modification has no effect on localization or interaction with proteins. Instead, acetylation seems to increase the stability of the protein by preventing ubiquitination of the lysine residues[183].

Nuclear receptors targeted by acetylation include the androgen receptor (AR) and the estrogen receptor α (ERα). Several HATs seem to be involved in the regulation of activation of AR[184,185], while acetylation of ERα at the ligand binding domain regulates hormone sensitivity without affecting induction by MAPK signaling[186]

Members of the GATA family of transcription factors associated with hematopoiesis are regulated by reversible acetylation, too. Acetylation increases transcriptional activation for GATA1, 2, and 3 as well as DNA binding for 1 and 2[187-189].

---

[a] Yin Yang 1

[b] Signal transducer and activator of transcription

[c] Myelocytomatosis

EKLF[a] is also involved in hematopoiesis. EKLF is acetylated by p300/CBP at two specific lysine residues located in the transactivation domain and the zinc finger domain. Interestingly, transactivation requires acetylation of the first residue but does not influence DNA binding, but rather enhances recruitment of the SWI/SNF chromatin remodeling complex[190,191]. Acetylation of the second residue is associated with function of EKLF as a repressor and recruitment of co-repressors[192].

MyoD[b] is critical for skeletal myoblast differentiation. Acetylation by PCAF and p300/CBP regulates its activity by enhancing DNA binding and also facilitates binding to p300/CBP via its bromodomain[193,194].

Acetylated members of the E2F family promote proliferation. Modification by pCAF and/or p300/CBP of residues conserved in E2F 1, 2, and 3 at the DNA binding domain enhances DNA binding and, in consequence, transactivation. Furthermore, protein stability is increased by preventing ubiquitination[195,196]. Acetylated E2F1 is recruited to pro-apoptotic genes as p73 which itself is a target for acetylation by p300. Again, acetylation prevents degradation and facilitates activation of other pro-apoptotic genes[197,198]. A direct binding partner of E2F, the tumor suppressor Rb[c], is also acetylated by p300 and pCAF which seems to regulate differentiation-specific functions like cell cycle exit[199].

The function of NF-κB[d] is regulated by acetylation by p300/CBP. Controversial results are available on the influence of acetylation on DNA binding, transactivation, and interaction with IκB[e,200-202]

HIF1[f] plays a role in adaption to changes in oxygen availability. Its stability is regulated by acetylation, but, in contrast to previous examples, in this case the modification promotes ubiquitination and subsequent proteasomal degradation[203].

---

[a] Erythroide Kruppel like factor

[b] Myogenic differentiation

[c] Retinoblastoma

[d] Nuclear factor of kappa light polypeptide gene enhancer in B-cells

[e] NF-κB inhibitor

[f] Hypoxia-inducible factor 1

Finally, Smad7 acetylation by p300 increases its stability by protecting it from ubiquitination and degradation induced by TGFβ-signaling[204].

2.2.6.2 Other acetylated proteins

Although the acetyltransferase responsible is not identified so far, acetylation of α-tubulin is known to play an important role in microtubule stability. While stable microtubules contain mainly acetylated α-tubulin, the opposite is true for dynamic microtubules[205,206].

Acetylation of importin-α by p300/CBP was shown to promote the interaction with importin-β, required for subsequent nuclear import of cargo proteins[207].

Ku70 is involved in the repair of double-strand breaks via the non-homologous end-joining DNA repair pathway and in regulation of apoptosis. Acetylation by PCAF and CBP was shown to impair the interaction of Ku70 with the pro-apoptotic factor Bax enabling initiation of apoptosis[208].

Acetylation of the molecular chaperone Hsp90[a] was shown to block its interaction with the glucocorticoid receptor (GR) preventing transcriptional activation by GR[209,210].

The adenoviral protein E1A is acetylated by p300/CBP and PCAF which was suggested to either influence interaction with the C-terminal binding protein resulting in transcriptional activation or localization by disrupting binding to importin-α3[211,212].

The small and large delta antigen of hepatitis delta virus both are targets for acetylation. Modification of the small antigen by p300 was shown to be required for its nuclear localization and viral RNA replication[213].

In conclusion, acetylation targets a multitude of non-histone proteins exerting various functions including regulation of DNA binding affinity, transcriptional activation, protein stability, and protein-protein interactions. In contrast to the widespread irreversible Nα-terminal acetylation that occurs co-translationally, posttranslational acetylation of the ε-amino-group of lysine residues is highly reversible. Thus, the non-histone acetylation targets are also substrates for deacetylating enzymes. In fact, most if not all histone deacetylases are able to deacetylate non-histone proteins. Together, the dynamic character

[a] heat shock protein

of lysine acetylation and the diversity of targeted proteins clearly suggest a role for acetylation beyond regulation of transcription. In fact, a general regulatory role for acetylation has been suggested similar to protein phosphorylation[214]. Anyway, this clearly demonstrates that prediction of a function as acetyltransferase by similarity to known HATs does not mean that the preferred substrate will be histones. Thus, extensive characterization of such a protein is indispensable.

3 Results and Discussion

For the longest time, sequence analytics has been viewed as a support unit for research groups. The work was more or less request-based. With the development of more and more prediction tools and the availability of fully sequenced genomes, the field of sequence analytics developed a new dynamics. Genome-wide screens produced lots of predictions and interesting suggestions for new topics of research. Some results that fitted into the scientific orientation of research groups were picked up by them, but other promising topics, sometimes of vital interest for further improvement of sequence analytical tools, remained untouched. Thus, it was decided to build up a new biochemical unit integrated into the sequence analytics group. This unit was designated to develop biochemical assays for the experimental confirmation of sequence analytical predictions and to also start follow up projects on promising results. This is where I came in at the start of my diploma work.

3.1 Development of an *in vitro* assay for investigation of the prenylation status of selected proteins

Lipid posttranslational modifications have been a main topic in our group for a while now. Prediction tools for glycosylphosphatidylinositol anchors (GPI)[215], protein N-myristoylation[109], and, last but not least, prenylation[216] have been developed. Large scale application of the prenylation predictor and clustering of hits into protein families revealed several groups of predicted prenylation targets with no experimentally verified member. Since experimental testing of lipid anchor incorporation is laborious, annotation of lipid modifications by similarity to known targets has been used widely over the database, although it is known that the existence of the modifiable residue alone (a C-terminal cysteine for prenylation and N-terminal glycine for myristoylation) is not sufficient without a proper sequence environment. At the same time, consistent prediction of lipid anchoring within a protein family with the PrePS and NMT/MyPS tools together with an experimentally verified member can be considered a safe indication for the respective lipid modification among that group of targets. Therefore, it was of vital interest to test representative candidates from these new protein families. Using well established prenylation targets as a positive control, I developed an *in vitro* assay for analysis of the prenylation status of proteins[217]. It was based upon a previously described method utilizing

in vitro transcription and translation in the presence of radiolabeled lipid substrate[218,219], but included several improvements. N-terminal GST[a]-fusions of the cDNAs encoding the candidate proteins were amplified by polymerase chain reaction (PCR, see Materials and Methods: PCR) and used as template for coupled *in vitro* transcription/translation with rabbit reticulocyte lysate in the presence of ^{3}H-labeled mevalonate (precursor for both types of prenylation, is converted to the final lipid substrates in the lysate), farnesylpyrophosphate (FPP), or geranylgeranylpyrophosphate (GGPP,). The translated protein was separated from other components of the lysate by GST-affinity purification and subjected to polyacrylamide gel electrophoresis under denaturing conditions (with sodium dodecylsulfate, SDS-PAGE). After electrotransfer of the protein to a nitrocellulose membrane, incorporated radioactive label was detected with a thin layer chromatography (TLC) linear analyzer followed by determination of total protein yield by a Western Blot with anti-GST-antibody (see Material and Methods: Biochemical techniques**)**.

This experimental setup has several advantages compared to the previous method. Without purification, the multitude of proteins in the rabbit reticulocyte lysate limits the amount of product analyzed in SDS-PAGE. The purification gives the opportunity to load the whole protein yield on a gel instead of just an aliquot. For proteins with weak expression, it is even possible to upscale the reaction volume to reach the desired amount of translation product. Furthermore, the purification step also reduces radioactive background increasing the signal to noise ratio. Thus, it is possible to detect prenylation of candidates that would have been classified as non-prenylated in the old setup. Another important improvement is the detection of incorporated radioactive label. While autoradiography or fluorography could take several weeks or even months, the TLC linear analyzer reduces the time effort to 20 minutes per lane. This makes it easier to repeat the experiments and optimize reaction conditions in reasonable time. Last but not least, the determination of the total protein yield is enhanced by the use of Western Blot. There is no need for a parallel reaction with [^{35}S]methionine. It is possible to directly check the yield of the reaction with the prenyl anchors. Due to the GST-tag, the same antibody can be used for all candidates.

This newly developed assay was used then successfully for the verification of selected candidate proteins from groups predicted to be subject to farnesylation with no

[a] Glutathione-S-transferase

experimental evidence so far[220]. The human proteins RasD2, Rab28, the hypothetical protein FLJ32421, and C-terminal peptides of Prickle1 and 2 were shown to be farnesylated *in vitro*. Furthermore, the wild-type versions of the candidates as well as modified sequences with mutated prenylation site were expressed as fusions to GFP in HeLa[a] cells to demonstrate the importance of prenylation for localization of the proteins.

3.2 Prenylation of bacterial proteins

In addition to these proteins, a bacterial protein was investigated, too. Although the prediction of the prenylation of YopQ from *Yersinia pestis* (NP_995392) was in the twilight zone of the algorithm, the protein was of special interest. According to current knowledge, there are no prenyltransferases in bacteria. No protein from bacteria has been shown to be prenylated, too. For myristoylation, there are cases of proteins from pathogenic organisms utilizing the hosts NMT. Thus, it was tempting to speculate that the same could be true for prenylation. Unfortunately, it turned out that YopQ is no prenylation target.

After my diploma work was finished, this topic was picked up again. Two more potential prenylation targets were selected for experimental investigation: an ankyrin repeat containing protein from *Coxiella burnetii* and a hypothetical protein from *Legionella pneumophila*.

3.2.1 Coxiella burnetii

A potential target for prenylation of a bacterial protein was identified in *Coxiella burnetii,* the cause of Q-fever. It is a hypothetical protein containing ankyrin repeats, hence it will be referred to as AnkRep protein for simplicity. Different versions of AnkRep are present in distinct strains. The respective proteins from the strains Dugway 7E9-12 (ZP_01298590) and RSA331 (ZP_0130976.1) are almost identical differing only in a single residue far away from the C-terminal prenylation motif. In the strain RSA493, the gene is split into two open reading frames by an insertion resulting in a much shorter prenylation target corresponding to the C-terminus of the longer version (NP_819396.1). The N-terminal fragment carries no prenylation motif. The strain Graves harbors a C-terminally truncated version lacking the prenylation motif.

[a] Henrietta Lacks

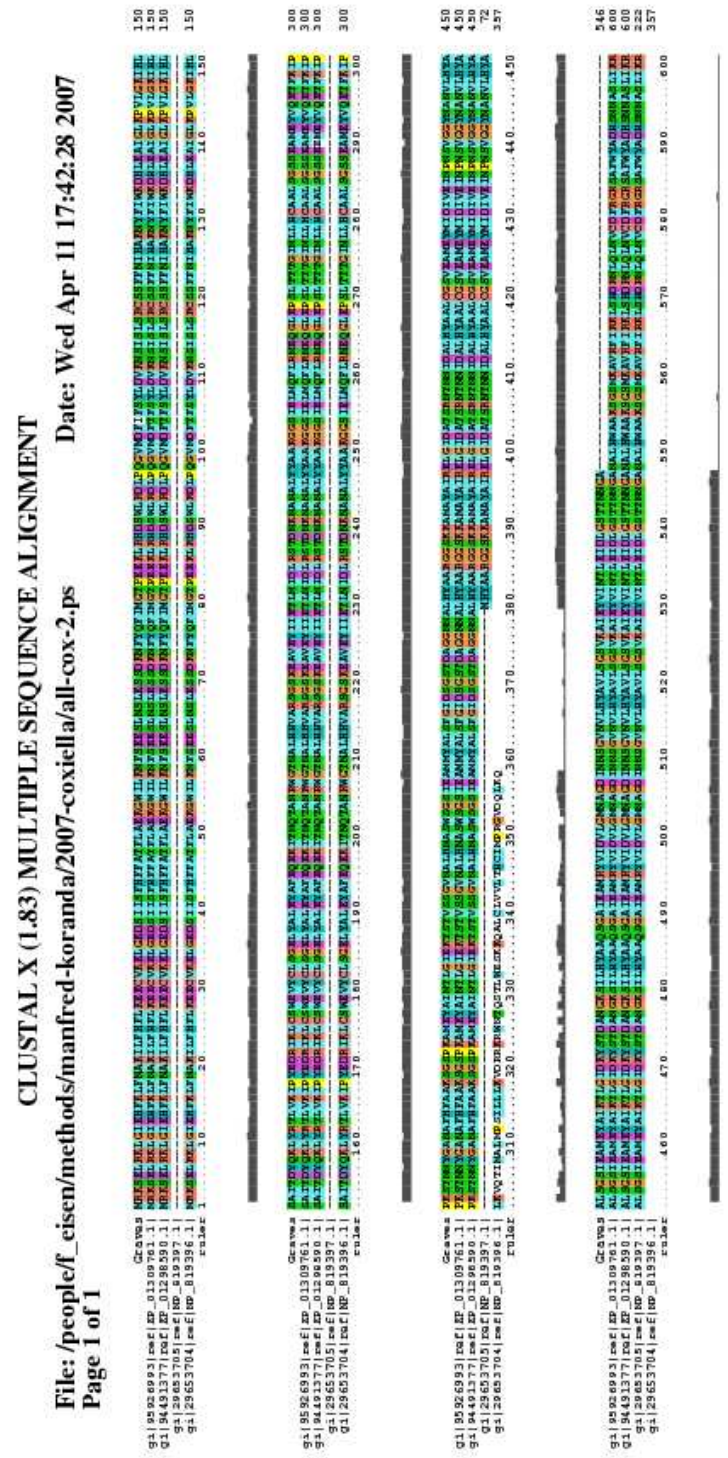

Figure 3: Sequence alignment of ankyrin repeat containing protein variants from different strains of *Coxiella burnetii*

Application of the prenylation prediction suite on these proteins classified them as substrates for both farnesyltransferase (FT) and geranylgeranyltransferase (GGT) type 1 (C-terminal peptide IKRVLAMPFEELMLETSIEEIKPSEDCLVM, FT score 0.165, P-value 4.9e-03, GGT1 score 0.862, P-value 2,2e-03). The *in vitro* prenylation assay has been used to investigate the prenylation status of these protein variants. GST-fusions of the wildtype protein and a cysteine to alanine mutation (preventing prenylation) of the shortest version, the C-terminal fragment from RSA493, has been subjected to coupled transcription/translation in the presence of ^{3}H-labeled mevalonic acid first to verify that the protein becomes isoprenylated, and subsequently with [^{3}H]FPP and [^{3}H]GGPP to identify which type of anchor is incorporated preferentially. The standard procedure was slightly modified. The elution buffer containing glutathione was not able to elute sufficient amounts of protein from the beads. Thus, the translated protein was eluted by addition of 50 µl 2 x sample buffer and incubation at 95°C for 5 min.

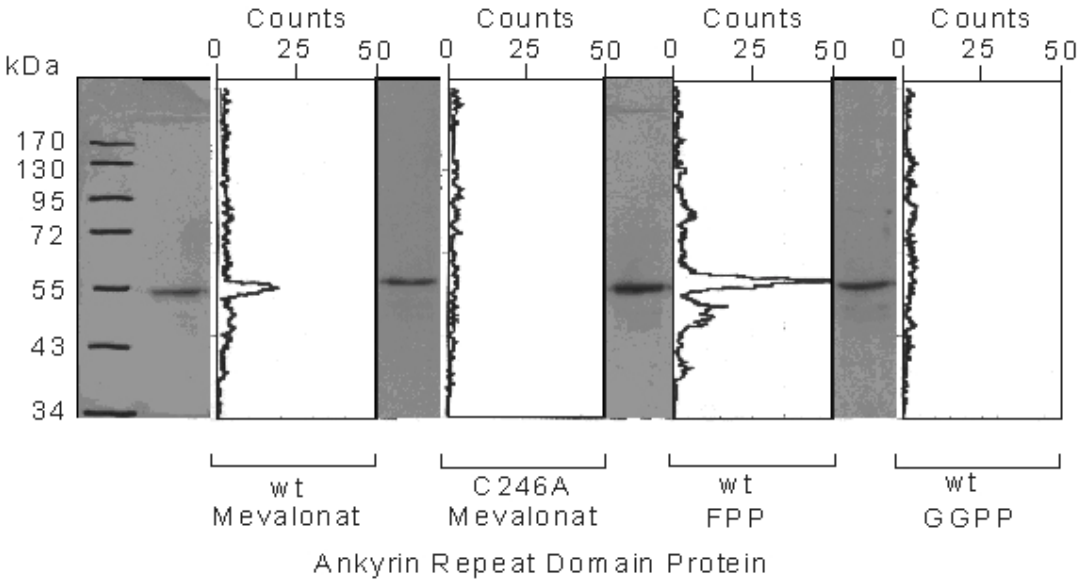

Figure 4: Western Blots and TLC scanning results for ankyrin repeat containing protein from *Coxiella burnetii* strain RSA493

Western blot and corresponding scans from TLC linear analyzer of wild-type GST-fusion protein translated with [^{3}H]mevalonate, the C246A-mutation with [^{3}H]mevalonate, as well as wildtype with [^{3}H]FPP and [^{3}H]GGPP.

It is clearly visible that the protein is farnesylated *in vitro* but, in contrast to the prediction, no geranylgeranylation was detected. Loss of the radioactive signal with the cysteine to alanine mutation demonstrated specific incorporation of the labeled isoprenoids. To rule

out influence of the additional amino acid sequence of the longer versions on the accessibility of the C-terminus for the farnesyltransferase, these proteins were also investigated. Both proteins from the strains Dugway 7E9-12 and RSA331 show clear and specific incorporation of a product of [^{3}H]mevalonic acid. The prenylation motif is identical in these proteins, so the specificity of the isoprenoid type is expected to be the same. Therefore, the test with FPP and GGPP was skipped. The C-terminally truncated version from the strain Graves was included as an additional negative control.

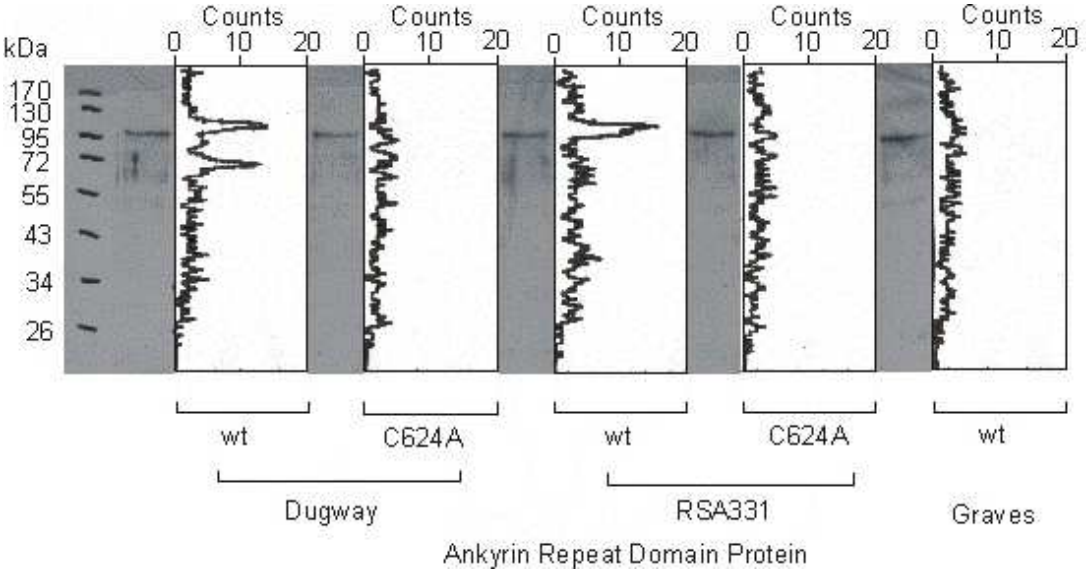

Figure 5: Western Blots and TLC scanning results for ankyrin repeat containing protein from *Coxiella burnetii* strains Dugway 7E9-12, RSA331 and Graves

Western blot and corresponding scans from TLC linear analyzer of wild-type and C624A mutated GST-fusion protein translated with [^{3}H]mevalonate from the strains Dugway7E9-12 and RSA331 as well as wildtype GST-fusion protein from Graves.

To check the potential influence of prenylation on the localization of the proteins in host cells, HeLa cells were transiently transfected with N-terminal GFP-fusions of the wildtype proteins and cysteine to alanine mutations (see Materials and Methods: Cell culture techniques). The cells were fixed, permeabilized, nuclei co-stained with 4′,6-Diamidino-2-phenylindol (DAPI) and analyzed by fluorescence microscopy (see Materials and Methods: Fluorescence microscopy of GFP-constructs). A diffuse cytosolic localization was observed. All variants except for the N-terminally truncated protein from the strain RSA493 were clearly excluded from the nucleus. No difference in localization was found for the mutations.

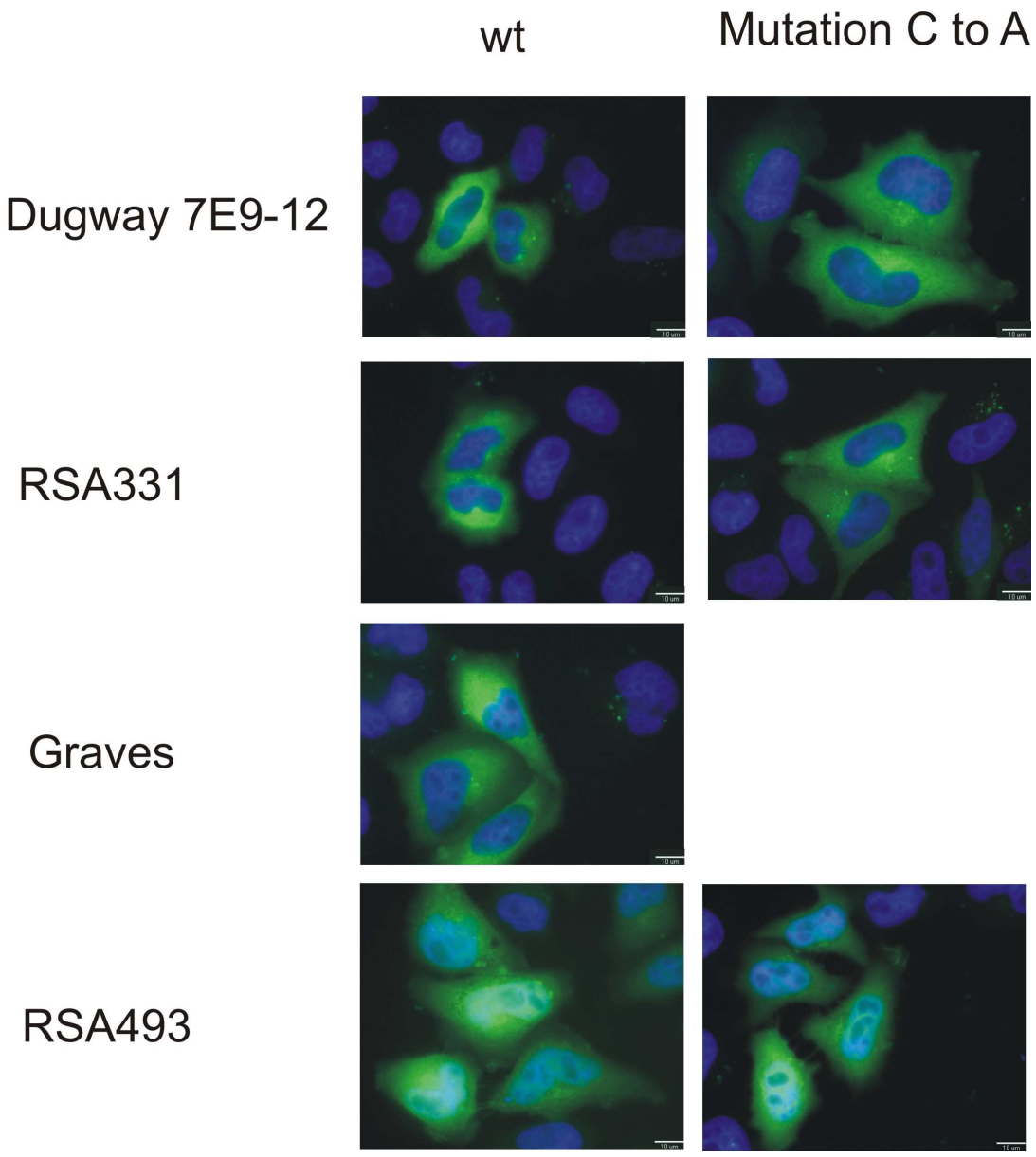

Figure 6: Localization of N-terminal GFP-fusions of ankyrin repeat containing protein from *Coxiella burnetii* strains Dugway 7E9-12, RSA331, Graves and RSA493 in HeLa cells.

Fluorescence microscopy of HeLa cells transiently transfected with N-terminal GFP-fusions. Nuclei co-stained with DAPI are blue, GFP is green. The white scale bars represent a size of 10 µm.

3.2.2 Legionella pneumophila

The second potential target for prenylation of a bacterial protein was identified in *Legionella pneumophila*. It is a hypothetical protein containing an F-box motif, thus it was named F-Box protein for convenience (YP_096532.1). The prenylation prediction suite predicts F-Box to be substrate for both farnesyltransferase and geranylgeranyltransferase type 1 (C-terminal peptide SQNLYINQDETIELFNKYTEEKTNNFCSIL, FT score 0.155, P-value 5.09e-03, GGT1 score 2.501, P-value 5.6e-04). Unfortunately, application of the *in vitro* prenylation assay on F-Box resulted in very low protein yields. A preliminary result indicated weak incorporation of a product of [^{3}H]mevalonic acid into F-Box but, due to the problems with the protein yield, the result was not reproducible. All attempts to improve the result by skipping the purification to minimize losses or by increasing the reaction scale were not successful. Thus, it was also impossible to identify the nature of the isoprenoid incorporated into the translated protein. In conclusion, prenylation of the protein can not be ruled out, but could not be demonstrated free of doubt.

As an alternative approach, the localization of N-terminal GFP-fusions of wildtype and cysteine to alanine mutation of F-Box in transiently transfected HeLa cells was investigated by fluorescence microscopy. The wildtype protein is clearly localized to some intracellular membrane compartments while the mutation shows a more diffuse distribution between intracellular membranes and the cytosol. This indicates that prenylation might be important for localization of F-Box, but of course this gives only indirect evidence for prenylation.

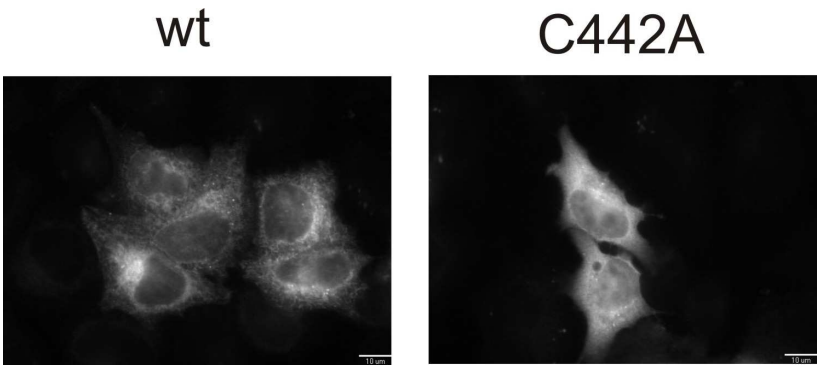

Figure 7: Localization of N-terminal GFP-fusions of F-Box containing protein from *Legionella pneumophila* in HeLa cells.

Fluorescence microscopy of HeLa cells transiently transfected with N-terminal GFP-fusions. The white scale bars represent a size of 10 µm.

3.2.3 Discussion

The *in vitro* prenylation assay clearly demonstrated that AnkRep from *Coxiella burnetii* is a substrate for farnesyltransferase. Localization studies using fluorescence microscopy of GFP-fusions showed no difference upon mutation of the prenylated cysteine. Thus, the protein might not become prenylated in HeLa cells, but it is also possible that other factors dominate the localization of AnkRep and the prenyl moiety is required for specific protein interactions or only in a certain context. For example, Ankyrin repeats are known to mediate protein interactions. Thus, an interaction partner could dictate the localization of AnkRep. For F-Box, *in vitro* prenylation was indicated by preliminary experiments but doubtless evidence for incorporation of an isoprenoid as well as identification of the type is missing. In this case, localization studies in HeLa cells suggest importance of the prenylation for subcellular membrane targeting. Of course, more data are needed to shed light on prenylation of bacterial proteins. For example, it will be important to address the question whether the proteins are secreted into host cells where they might get in contact with prenyltransferases. If they are not, the prenylation motifs could be an evolutionary curiosity that has arisen by chance because there is no negative selection against it in bacteria. If the proteins are accessible for a host prenyltransferase at least part of their lifetime, prenylation could be an important factor influencing localization and/or function. As a prerequisite for further experiments, an antibody was raised against a peptide common to all investigated variants of AnkRep. Unfortunately, it did not fulfill the requirements for the intended use. Nonetheless, both potential cases of prenylated bacterial proteins are still under investigation by other members of the lab. Recent results suggest secretion of the F-Box protein from *Legionella pneumophila* into the cytoplasm of macrophages (Hwei Ling Khor et al., 2008, to be published). Thus, prenylation of the protein *in vivo* seems plausible.

3.3 Influence of SNPs on prenylation

Single nucleotide polymorphisms (SNPs) are DNA mutations that have managed to survive in the gene pool of a population to a certain degree. They account for approximately 90% of all variations in the human genome. They are not distributed equally over the genome, but occur in differing frequency in certain regions. SNPs can alter the amino acid sequence of the proteins encoded by the DNA. Therefore, they can account for different susceptibility of individuals for diseases and/or drugs. Since the recognition motifs for prenyltransferases require a certain type of amino acid at some positions and at least a certain pattern of physical properties in general, SNPs are able to influence those motifs. An SNP could destroy a prenylation site by mutation of the modified residue or of a residue in its environment and influence the type of anchor that is preferably attached or the accessibility for the prenyltransferases. Thus, SNPs can be involved in both generation and destruction of functional prenylation motifs. By application of the prenylation prediction suite, several cases of human proteins were identified where the score of the prediction is significantly altered by an SNP. The candidates selected for investigation were ALDH3B2[a], BEX2[b], UTP14A[c] and the hypothetical protein FLJ20364.

Name	Accession	C-terminal sequence	FT-score	GGT1-score
ALDH3B2	NP_000686.2	TDWNQQLLRWGMGSQSCTLL	-2.761	-2.051
		TDWNQQLLRGGMGSQSCTLL	-1.485	-0.638
BEX2	NP_116010.1	RAVSTDPPHHDHHDEFCLMP	-2.768	-12.860
		RAVSTDPPHHDHHDEFCLMH	-1.912	-15.262
UTP14A	NP_006640.2	RNPKRITTRHKKQLKKCSVD	-2.692	-14.685
		RNPKRITTRHKKQLKKCSVG	-0.771	-10.423
FLJ20364	NP_060255.2	SHPILYVSSKSTPETQCPQQ	-1.870	-23.913
		LHPILYVSSKSTPETQCPQQ	-2.170	-24.213

Table 1: Selected candidate proteins with SNPs in the prenylation motif predicted to influence prenylation

[a] Aldehyde dehydrogenase 3 family, member 2

[b] brain expressed X-linked 2

[c] U3 small nucleolar ribonucleoprotein, homolog A

ALDH3B2 is suggested to become a better target for both FT and GGT1 after replacement of Trp375 with glycine. BEX2 and UTP14A show an improved score suggesting potential prenylation only for FT, and in the case of FLJ20364 the protein is predicted to be a worse farnesylation target due to the SNP.

All candidates were investigated by the *in vitro* prenylation assay in both variants. No prenylation for either version was detected in the case of BEX2 and UTP14A. Preliminary results indicated incorporation of a product of [^{3}H]mevalonic acid for FLJ20364, but no significant difference between the SNP variants. Finally, ALDH3B2 turned out to be an example of SNP-influenced prenylation. For ALDH3B2, N-terminal GST-fusions of the full-length protein did not yield a sufficient amount of protein. Therefore, it was decided to use a GST-fusion of a C-terminal peptide consisting of 25 amino acids instead since previous experiments had indicated better expression of shorter constructs. A significantly stronger signal from an incorporated product of [^{3}H]mevalonic acid was detected with Gly at the position corresponding to amino acid 375 of the full protein compared to Trp. Consistent with the prediction, the protein was modified by both FPP and GGPP. Specificity was demonstrated by loss of the signal with a cysteine to alanine mutation.

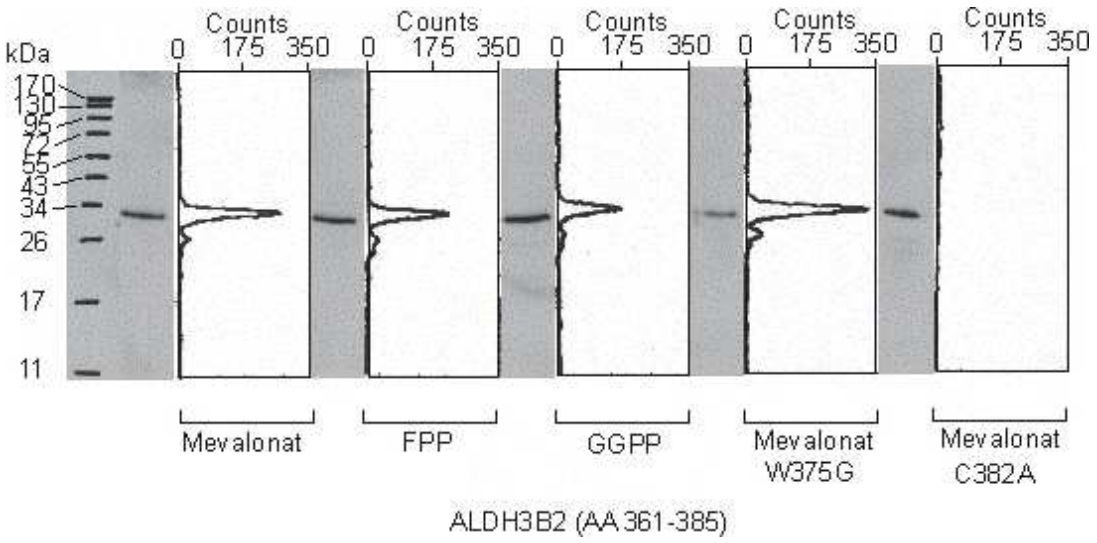

Figure 8: Western Blots and TLC scanning results for a C-terminal peptide of human ALDH3B2

Western blot and corresponding scans from TLC linear analyzer of a fusion protein consisting of GST as well as residues 361 – 385 from the C-terminus of ALDH3B2 with a Trp at position 375 translated with [^{3}H]mevalonate, [^{3}H]FPP and [^{3}H]GGPP, the W375G mutation with [^{3}H]mevalonate and the C382A-mutation with [^{3}H]mevalonate.

Localization studies were performed with HeLa cells transiently transfected with N-terminal GFP-fusions of both SNP variants of ALDH3B2, FLJ20364 and UTP14A. BEX2 was not included as its prenylation was already ruled out by the *in vitro* experiments at that time point. No significant difference in localization was observed between the SNP variants in any case.

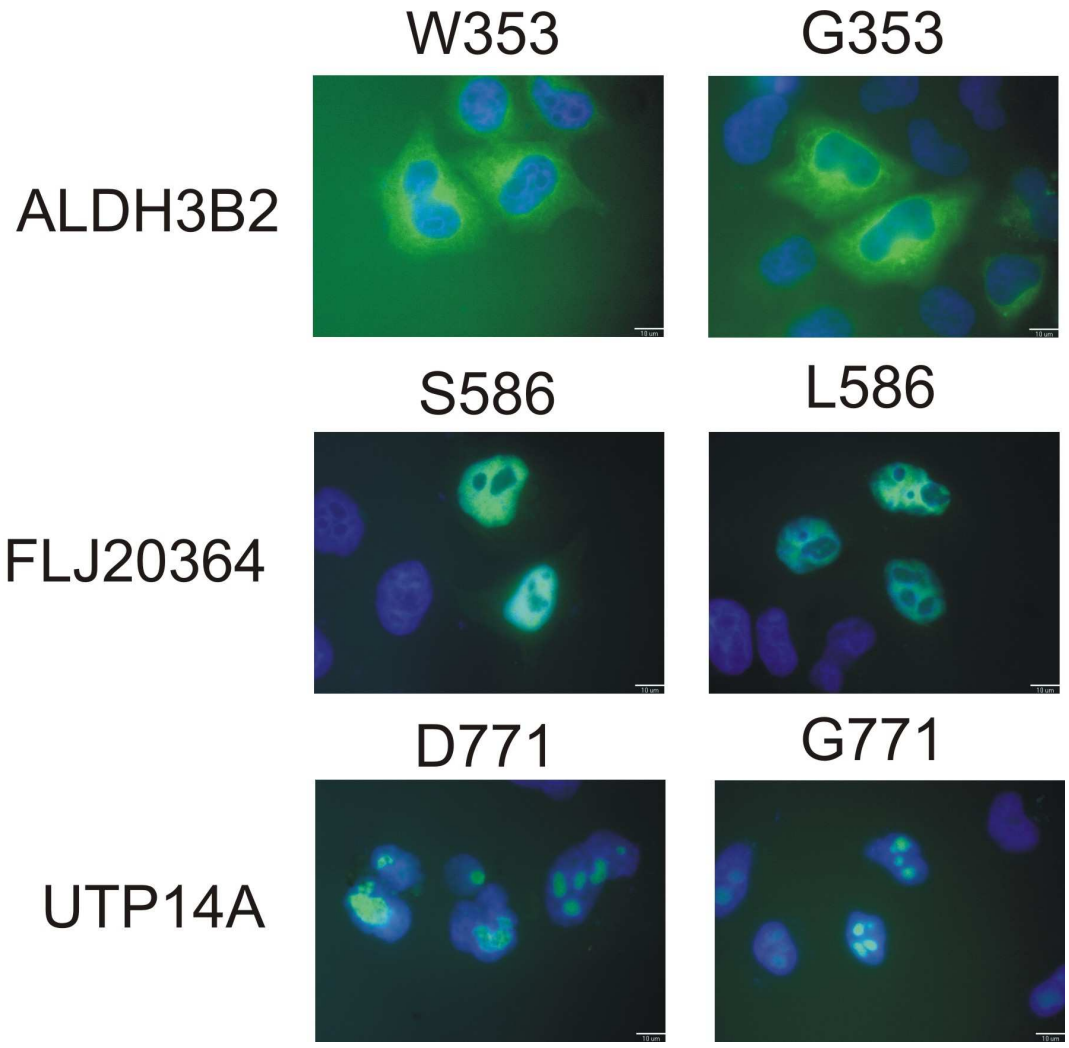

Figure 9: Localization of N-terminal GFP-fusions of SNP variants of ALDH3B2, FLJ20364 and UTP14A in HeLa cells.

Fluorescence microscopy of HeLa cells transiently transfected with N-terminal GFP-fusions. Nuclei co-stained with DAPI are blue, GFP is green. The white scale bars represent a size of 10 µm.

3.3.1 Discussion

The case of ALDH3B2 clearly demonstrates that SNPs can influence prenylation motifs. Thus, they might participate in the genesis (or destruction) of such motifs in the course of evolution. Of course, this example only shows us a snapshot of the whole process. The modification with isoprenoids is only slightly enhanced by the mutation W375G and thus it is not surprising that no influence on subcellular localization was observed. Until now, ALDH3B2 remains a theoretical example for the influence of SNPs on prenylation. Whether this SNP has any relevance *in vivo* is still unclear. The members of the aldehyde dehydrogenase family play a role in detoxification of aldehydes generated by alcohol metabolism and lipid peroxidation. The cDNA of ALDH3B2 (also named ALDH8) is highly similar to ALDH7, but contains a termination codon corresponding to the seventh amino acid in the ALDH7 sequence. Thus, ALDH3B2 is either a non-processed pseudogene or a functional gene if the stop codon is skipped or suppressed[221]. The mRNA has been shown to be expressed specifically in salivary gland, but protein expression has not been investigated so far. To address this question, an antibody has been raised against a peptide specific for ALDH3B2. Unfortunately, the antibody was not good enough to use it for testing expression of ALDH3B2 in tissue samples. A commercial antibody available for ALDH3B2 did not meet the requirements, too. Furthermore, it might be necessary to generate an antibody specific for ALDH7 in addition to ensure maximum specificity. In conclusion, investigation of the expression status of ALDH3B2 seems not to be an easy task, but the project is still continued by other members of the lab.

3.4 Experimental investigation of protein N-myristoylation

According to our focus on lipid posttranslational modifications, a sequence analytical tool for the prediction of protein N-myristoylation was developed in our group[109]. Another group at the institute showed interest in several potential myristoylation targets in *Drosophila melanogaster*, hence it was decided to try to adapt our *in vitro* assay for the investigation of protein N-myristoylation. In addition, our interest in "paradox"-targets, proteins showing a motif for a lipid posttranslational modification in a context where it is usually not found like the bacterial prenylation targets, prompted us to investigate a transcription factor predicted to be myristoylated.

3.4.1 Adaption of the assay for the detection of myristoylation

Since the main application of an *in vitro* myristoylation assay was the investigation of the candidates from fly, it was decided to use a positive control from this organism for setting up the assay. The perfect candidate for this purpose was igloo-L[a] (AAB32065.1). This protein was shown to be modified with myristic acid using *in vitro* transcription and translation, demonstrating that sufficient NMT activity is present in rabbit reticulocyte lysate[222]. Several modifications to the experimental setup used for the detection of prenylation were necessary. First of all, a C-terminal GST-tag had to be used since myristoylation occurs at the N-terminus. Due to the lack of commercially available vectors with C-terminal GST-Tag, a self-constructed plasmid was used (GST was amplified from pGEX-5X-1 and cloned into a pSK+-vector, the construct will be referred to as C-GEX). As radioactively labeled lipid substrate, [^{3}H]myristic acid was used. Furthermore, the reaction time had to be changed. While an incubation time of four hours (at least) yielded best results for prenylation, a reduction to two hours gave the best results with myristoylation. Longer incubation times did not increase the incorporation of radioactive label, but reduced the total protein yield. Since N-myristoylation occurs at the N-terminus and usually as a co-translational modification, it seems plausible that less time is needed than for prenylation which requires the C-terminus to leave the ribosome to be accessible for the prenyltransferase. The decrease of protein yield over time seems to be caused by adsorption of the hydrophobic myristoylated proteins to the reaction tubes. This effect was already observed with prenylated proteins and posed even more problems with the more

[a] Invertebrate GAP-43 like, the L symbolizes the larger isoform

hydrophobic myristoylated proteins. Therefore, also the purification step introduced successfully for the prenylated proteins had to be skipped in the myristoylation assay. No conditions were found that allowed elution of a satisfying amount of GST-fusion protein from the beads, even with increased glutathione concentration. Elution with SDS-PAGE sample buffer was also tested but yielded in co-elution of a lot of background radioactivity rendering the purification rather useless. Thus the direct application of unpurified reaction mix on the acrylamide gel turned out to be the best solution.

After elaboration of all necessary modifications, application of the final assay on igloo-L demonstrated functionality of the assay. The radioactivity measurement yielded a peak at a molecular weight corresponding to the band in the Western blot of igloo-L-GST, leaving no doubt about the incorporation of myristic acid. In contrast, the G2A mutant protein, which served as a negative control, gave no signal exceeding the background noise although the protein yield in the Western blot was even larger (another hint for loss of myristoylated protein). In conclusion, it was possible to apply at least some of the positive aspects of the improved assay also for protein N-myristoylation.

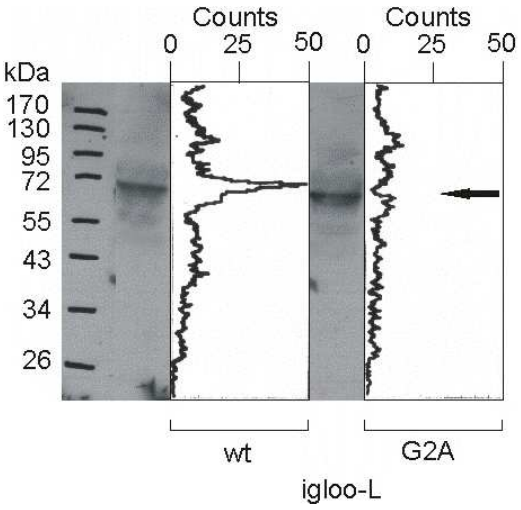

Figure 10: Western Blots and TLC scanning results for igloo-L

Western blot and corresponding scans from TLC linear analyzer of wild-type and G2A mutated C-terminal GST-fusions translated with [^{3}H]myristate.

3.4.2 In vitro myristoylation status of predicted myristoylation targets from Drosophila melanogaster

The *D. m.* numb protein is important in the development of the nervous system. Asymmetric distribution of the protein during mitosis is associated with cell polarity and, in consequence, determination of cell fate. During asymmetric cell division of the sensory organ precursor, numb is segregated to only one daughter cell where it antagonizes Notch signaling[223,224]. Two isoforms of the protein are known named numb-A (AAA28730.1) and B. Numb-B is an N-terminal truncation of isoform A lacking 41 residues including the glycine obligatory for myristoylation. The N-terminal sequence of numb-A (MGNSSSHTHEPLERGFTR) is predicted as a reliable myristoylation site (score 0.949, P-value 1.75e-03). C-terminal GST-fusions of wildtype and G2A mutated numb-A were transcribed and translated in the presence of [^{3}H]myristic acid. The proteins in the reaction mix were resolved by SDS-PAGE, transferred to a nitrocellulose membrane and analyzed by scanning with a TLC linear analyzer and Western Blot with anti-GST HRP-conjugated antibody. A clear signal of incorporated myristate is detected for the wildtype protein, but missing for the G2A mutant protein, indicating specific modification of the N-terminal glycine with myristic acid.

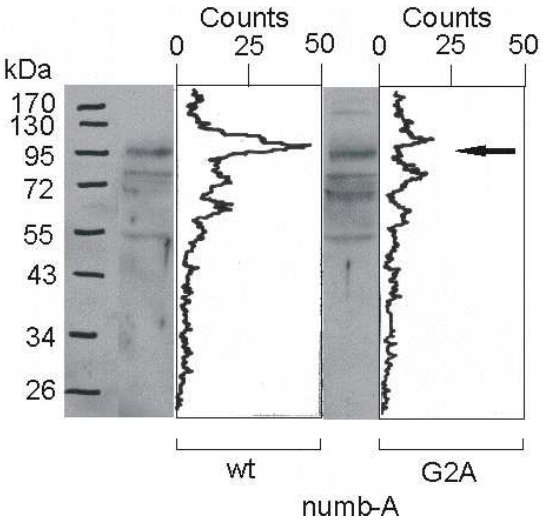

Figure 11: Western Blots and TLC scanning results for numb-A

Western blot and corresponding scans from TLC linear analyzer of wild-type and G2A mutated C-terminal GST-fusions translated with [^{3}H]myristate.

Par-1 is a serine/threonine kinase[225] expected to play multiple roles in *Drosophila* development. It is involved in oocyte fate determination and maintenance by establishing anterior-posterior polarity of the oocyte. The localization of Par-1 changes during oocyte development[226-228]. Consistent with multiple roles, fifteen different splice variants of Par-1 are described. Three different N-terminal sequences are present in those variants, but only one of them is a potential target for myristoylation. The sequence of this N-terminus (MGQTSSHRQM HHSSNNNN) is predicted as a reliable myristoylation site (score 3.596, P-value 2.46e-05). For convenience, the shortest protein harboring the myristoylation motif, Par-1 isoform Q (AAM75016.1), was chosen for investigation. Specific modification of the N-terminal glycine of Par-1 isoform Q was verified by application of the *in vitro* myristoylation assay on wildtype and G2A mutated C-terminal GST-fusions.

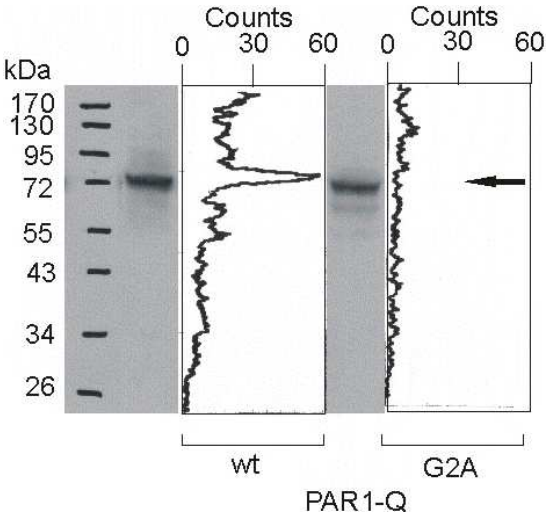

Figure 12: Western Blots and TLC scanning results for Par-1 isoform Q

Western blot and corresponding scans from TLC linear analyzer of wild-type and G2A mutated C-terminal GST-fusions translated with [^{3}H]myristate.

The third protein from Drosophila melanogaster selected for experimental investigation is neuralized (neur). Similar to numb, it plays a role in determining cell fate in development of the nervous system. While numb is segregated to one daughter cell of the sensory organ precursor inhibiting Notch signaling there, neur is inherited by the other daughter cell. In contrast to numb, Notch signaling is activated by neur[229]. Four different transcript variants are described for neur designated A, B, C, and D. Isoforms A and B as well as C and D are identical except for a glutamine which is present at position 672 in isoform A and in position 590 in isoform C but is missing in isoforms B and D. Since, according to current

knowledge, only the first 17 amino acids of a protein are of relevance for its myristoylation, only isoforms B (AAK93411.1) and C (AAO41451.1) were investigated. Neuralized B and C differ in their N-terminal sequence. While both of them harbor a glycine at position 2, only neur-C is predicted as a reliable myristoylation target (N-terminal sequence MGQSAGKIVRRSPSSCPG, score 1.407, P-value 9.69e-04) while isoform B is rejected by the predictor due to several negative physical property terms (N-terminal sequence MGLSDIPANYMQGSHPHL, score -12.466, P-value 4.75e-01). The hydrophobic leucine residue at position 3, a negative charge at position 5, and the hydrophobic residues with reduced backbone flexibility at positions 6 and 7 (isoleucine and proline) do not fulfill the requirements of the substrate binding pocket of animal NMT.

In agreement with the predictions, neither the wildtype protein of neur-B nor the G2A mutant negative control show incorporation of ^{3}H-labeled myristic acid in the *in vitro* assay, although a satisfying total protein yield is detected. In contrast, neur-C wildtype protein yields a clear radioactive signal while the G2A mutant protein gives no signal above background noise at comparable protein yield.

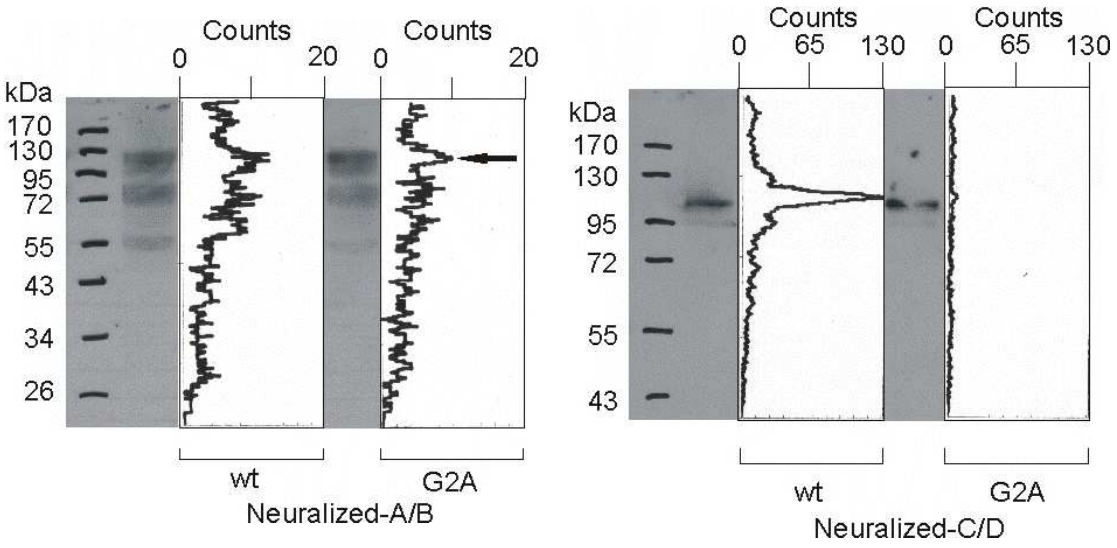

Figure 13: Western Blots and TLC scanning results for neuralized-B and C

Western blot and corresponding scans from TLC linear analyzer of wild-type and G2A mutated C-terminal GST-fusions translated with [^{3}H]myristate. As isoforms A and B as well as C and D are almost identical, the results can be expected to reflect the myristoylation status of all four isoforms. The band corresponding to the calculated molecular weight of neur-B is marked with an arrow.

3.4.3 Localization in fly embryos

To investigate the influence of myristoylation on the localization of the proteins *in vivo,* transgenic flies were generated expressing C-terminally myc-tagged constructs. These experiments were carried out in cooperation with the lab of Jürgen Knoblich (Institute for molecular biotechnology, IMBA). Fluorescence microscopy of embryonic epithelial cells revealed cortical localization of wildtype igloo-L while the G2A mutant was predominately cytosolic. For numb-A, the mutant still shows cortical localization but seems to be partially delocalized to the cytoplasm. Both wildtype and G2A mutant neur-B are localized cortical, consistent with the finding that neur-B is not myristoylated *in vitro*. Obviously, other factors determine the localization of neur-B. Unfortunately, no flies yielding satisfying results were generated for neur-C. For Par-1 isoform Q, cortical localization is clearly disrupted by mutation of the myristoylated glycine residue.

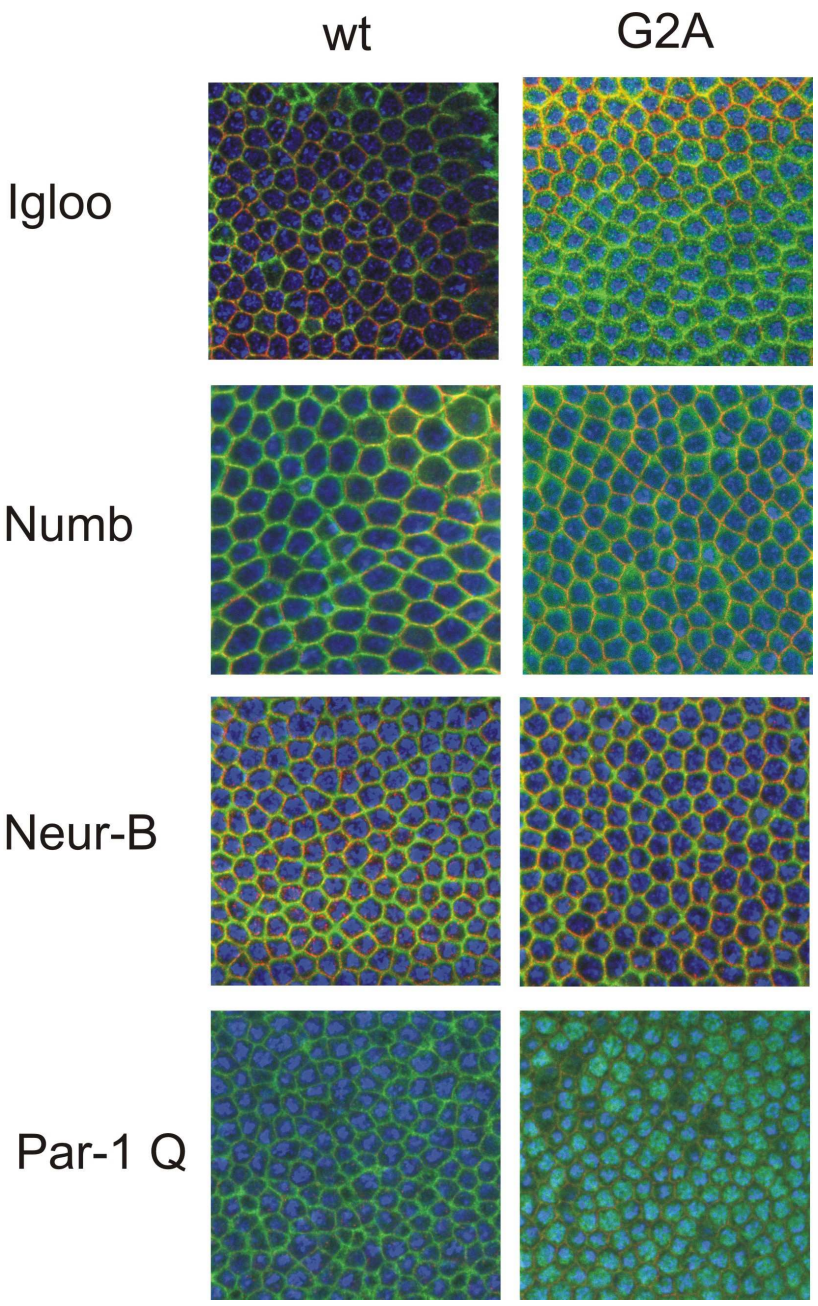

Figure 14: Localization of igloo-L, numb-A, neur-B and Par-1 isoform Q in embryonic fly epithelium

Fluorescence microscopy of embryonic fly epithelium expressing C-terminal myc-fusions of wildtype and G2A mutant candidate proteins stained in green. DNA is stained in blue and the cortical marker Miranda in red.

3.4.4 Myristoylation of proteins homologous to neuralized from mouse

Only two of the isoforms of neur in Drosophila are myristoylated *in vitro*¸ although all of them harbor a glycine at position 2. Other differences in the N-terminal sequences account for the selective myristoylation of isoform C and D. To get a more complete picture of selective myristoylation of neur isoforms, two homologous proteins from *Mus musculus* (*M. m.*), neuralized-like 1 (AAH58386.1) and 2 (AAK97495.1), were chosen for investigation additionally. Like the proteins from Drosophila, they are highly identical. In fact, except for the very N-terminal sequence, they are identical in all but one residue. In contrast to the proteins from Drosophila, reliable myristoylation sites are predicted for both isoforms (neuralized-like 1 with the N-terminal sequence MGNNFSSVSSLQRGNPSR with score 2.348, P-value 2.40e-04 and neuralized-like 2 with the N-terminal sequence MGGQITRNTIHDSIGGSF with score 1.124, P-value 1.141E-03). Both versions were investigated with the *in vitro* myristoylation assay. Unfortunately, no satisfying protein yields were produced with the GST-fusions of the full-length proteins. Since shorter sequences often tend to give better protein yields with *in vitro* transcription/translation, it was decided to use N-terminal fragments representing the first 262 amino acids of neuralized-like 1 and the first 245 residues of neuralized-like 2, respectively.

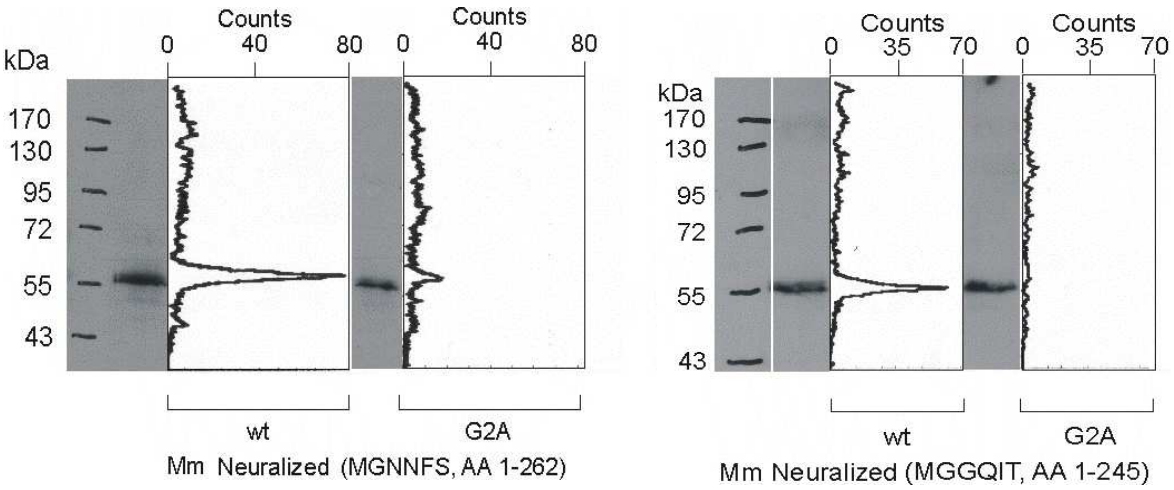

Figure 15: Western Blots and TLC scanning results for mouse neuralized isoforms

Western blot and corresponding scans from TLC linear analyzer of wild-type and G2A mutated C-terminal GST-fusions representing the first 262 and 245 amino acids of the mouse neuralized isoforms translated with [^{3}H]myristate.

With these truncations, glycine-dependent incorporation of myristic acid into both versions was clearly demonstrated.

To address the effect of myristoylation on the localization of the proteins, too, C-terminal GFP fusions of the full-length sequences were transiently transfected in mouse 3T3[a] cells. Fluorescence microscopy revealed membrane attachment of both wildtype versions while the G2A mutations were predominately present in the nucleus. Our result is in agreement with data in a recently published work on neuralized-like 1[230].

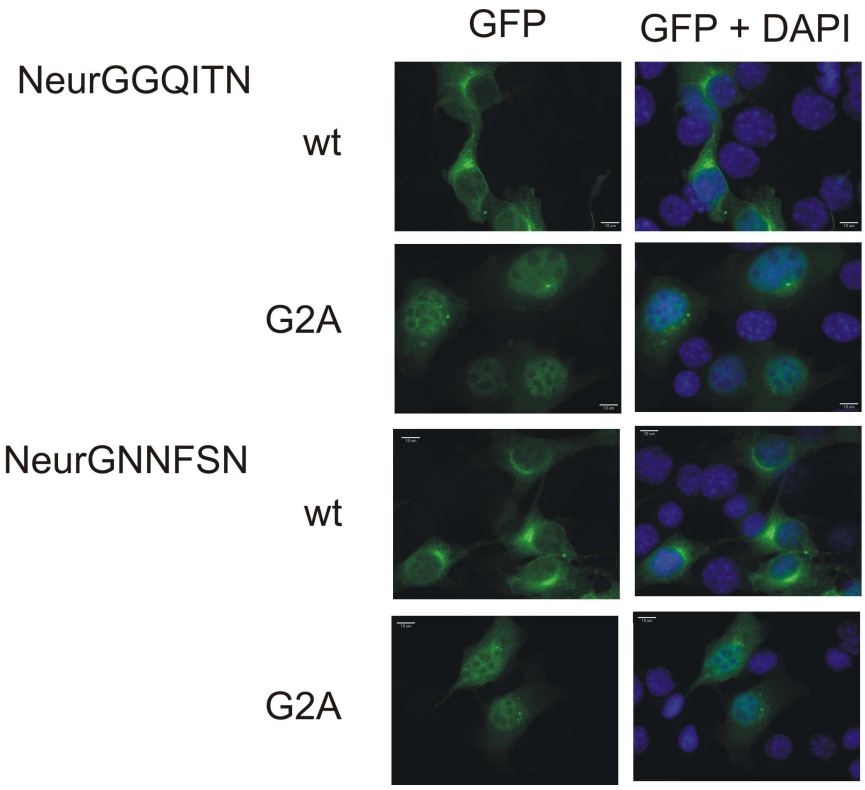

Figure 16: Localization of mouse neuralized isoforms in 3T3 cells

Fluorescence microscopy of mouse fibroblasts (3T3) expressing C-terminal GFP-fusions of wildtype and G2A mutant mouse neuralized isoforms. DNA is stained in blue.

[a] 3-day transfer, inoculum 3 x 10^5 cells

3.4.5 Discussion

The investigated candidates from *Drosophila melanogaster*, numb, Par-1, and neuralized, are three examples of proteins expressed in different isoforms. In all three cases, only some, but not all, different versions are subject to myristoylation *in vitro*. It is likely that the selective myristoylation of only a subpopulation of the proteins might be of importance *in vivo*. Different isoforms could exert different functions or a similar function but at different locations. Unfortunately, very little is known on the functional differences of the isoforms. Some phenotype rescue and localization experiments concerning Par-1 already gave a first hint[226,231], and it will be of growing importance in the future to separately investigate the different isoforms of a protein. Summing up the results gathered with the *in vitro* myristoylation assay on proteins from both fly and mouse, all predictions were verified experimentally indicating that the predictor is capable of distinguishing between the ability of N-terminal glycines in different context to become modified by NMT or not.

The localization studies underscore the importance of myristoylation for targeting of the investigated proteins. In the case of igloo-L and Par-1 Q as well as the mouse neuralized proteins, mutation of the site of attachment of the myristoyl moiety drastically changes the localization of the proteins. The smaller effect observed for numb-A indicates that several other membrane attachment factors might contribute to the correct targeting of the protein compensating the loss of myristoylation to some degree. As already discussed, myristoylation is believed to provide only transient interaction with membranes which have to be enhanced by other MAFs for stable membrane attachment. Numb could be part of a protein complex that is able to bind membranes without myristoylation of numb, too. This assumption remains to be verified experimentally. The cortical localization of *D. m.* neur-B seems to be determined by other factors, too, as it is not influenced by mutation of the N-terminal glycine.

3.5 NFAT5-A – a myristoylated transcription factor?

Two common mechanisms for regulation of translocation of transcription factors to the nucleus are widely accepted in the scientific community. One type are cytosolic transcription factors with the nuclear localization signal (NLS) masked by binding of an inhibitor protein like in the case of NF-κB. Upon activation of the appropriate signaling pathway, the inhibitor protein IκB is removed from the transcription factor exposing the NLS that guides translocation into the nucleus[232]. The second type of transcription factors has their NLS exposed all the time but is prevented from entering the nucleus by membrane anchorage via transmembrane regions like SREBP[a] which is attached to the endoplasmatic reticulum (ER). Upon activation, proteolytic cleavage releases the transcription factor from the membrane enabling it to enter the nucleus[233]. As membrane attachment is not only possible via transmembrane regions, an *in silico* screen was carried out to look for transcription factors predicted to be substrates for lipid modifications. As the most promising candidate derived from the screen, the human transcription factor NFAT5-A[b] (NP_619728) was chosen for experimental investigation. Again, this is an example of selective modification of proteins isoforms. The three variants of NFAT5 named A, B, and C (b: NP_619727, c: NP_006590) differ only in their N-termini where only the shortest isoform a harbors a glycine residue in the context required for myristoylation.

Expression of sufficient amounts of the full-length protein (158 kDa) fused to a C-terminal GST-tag was not achieved, hence it was decided to use a truncation representing the first 541 amino acids of NFAT5-A. The *in vitro* myristoylation assay indicated covalent attachment of radioactive myristate at the wild-type fusion protein, whereas the G2A mutated version yielded no radioactive signal despite similar protein yield.

[a] Sterol regulatory element binding protein

[b] Nuclear factor of activated T-cells 5, isoform a

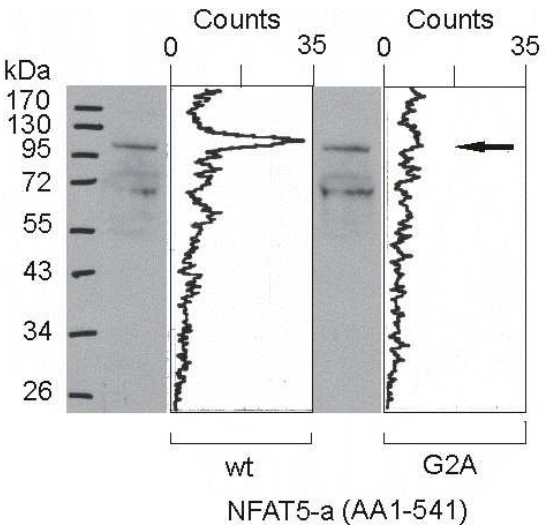

Figure 17: Western Blots and TLC scanning results for human NFAT5-A

Western blot and corresponding scans from TLC linear analyzer of wild-type and G2A mutated C-terminal GST-fusions representing the first 541 amino acids of human NFAT5-A translated with [^{3}H]myristate.

To check the impact of myristoylation on the localization of NFAT5-A, HeLa cells were transiently transfected with C-terminal GFP-fusions of wildtype and G2A mutated NFAT5-A. As expected, the wildtype protein accumulated at intracellular membranes while the mutated version that can not be myristoylated anymore is found predominately in the nucleus.

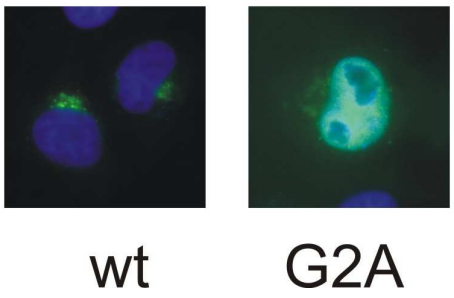

Figure 18: Localization of human NFAT5-A in HeLa cells

Fluorescence microscopy of HeLa cells transiently transfected with C-terminal GFP-fusions of wildtype and G2A mutant human NFAT5-A. DNA is stained in blue.

3.5.1 Discussion

NFAT5-A is the first example of a lipid modified transcription factor. Myristoylation has been demonstrated *in vitro*, and the relevance of the lipid anchor for intracellular localization has shown by fluorescence microscopy of GFP-fusions. This finding could represent a new mechanism for the regulation of nuclear import of transcription factors. Membrane attachment mediated by the myristoyl anchor seems to be required to prevent NFAT5-A from entering the nucleus. Different options come to mind for a mechanism including myristoylation of the transcription factor. As myristic acid is not able to provide stable membrane binding, other factors could enhance the membrane interaction of NFAT5-A. A cysteine residue is present at position 5 providing a potential site for palmitoylation. If NFAT5-A is indeed stably associated to the membrane via double acylation, it has to be released upon activation. This could be achieved by proteolytic cleavage in analogy to other membrane attached transcription factors. Alternatively, de-palmitoylation could weaken the membrane interaction facilitating detachment from the membrane. This could be enough to enable the myristoylated protein to enter the nucleus. In theory, one could also think of a switch mechanism where the myristoyl moiety is buried in a hydrophobic pocket of the protein after a conformational change.

If NFAT5-A is not palmitoylated to achieve stable membrane binding, the myristoyl anchor could act as brake delaying nuclear import. The other isoforms B and C are no substrates for myristoylation, but are kept outside the nucleus, too. A mechanism with active nuclear export of NFAT5 has been suggested[234]. This mechanism could also apply for NFAT5-A, but with the addition that nuclear import upon activation is delayed for NFAT5-A due to transient membrane interactions mediated by myristoylation. In this model, isoforms b and c would represent kind of a fast response to an activating stimulus while NFAT5-A could mediate a slower long-term response. Further experiments will be required to elucidate the impact of myristoylation on the function of NFAT5-A and a potential mechanism for release of lipid-anchored transcription factors. My lab colleague Michaela Sammer, who also participated in the localization experiments presented in this work, currently continues the investigation of NFAT5.

3.6 Mec-17 – an uncharacterized protein predicted to act as N-acetyltransferase

Mec-17 (NP_501337) was identified originally as a gene expressed in *Caenorhabditis elegans* (*C. e.*) touch receptor neurons[235]. The gene product seems to be required for maintained differentiation of these neurons. In mec-17 deficient animals, expression of mec-3, which seems to be a major determinant for differentiation, is lost during development[236,237]. A BLAST[a] search was carried out to search for homologous proteins in other species. In the course of analysis of conserved segments, the sequence stretch Q-R-X-G-X-G was found almost identical in all homologues and identified as part of motif A in histone acetyltransferases from the GNAT superfamily. This motif was well known from previous work in our lab with Eco1[238] and is part of the acetyl-CoA binding site. Subsequent alignment with other members of the GNAT superfamily revealed additional similarities in the unique motifs B, C, and D, too. Taken together, significant conservation was found including a common hydrophobic pattern, secondary structure (predicted for mec-17), and functional residues. Thus, an enzymatic function as N-acetyltransferase was suggested. This would provide a plausible explanation for the influence of mec-17 on the expression of others proteins as acetylation of histone tails or transcription factors is well known to be involved in regulation of transcription. The homologues mec-17 and w06b11.1 (NP_508981) from *C. e.*, 2610110G12Rik (BAC25866) from *Mus musculus* (*M. m.*) and c6orf134 (AAH25755) from *Homo sapiens* (*H. s.*) were selected for experimental investigation.

[a] Basic Local Alignment Search Tool

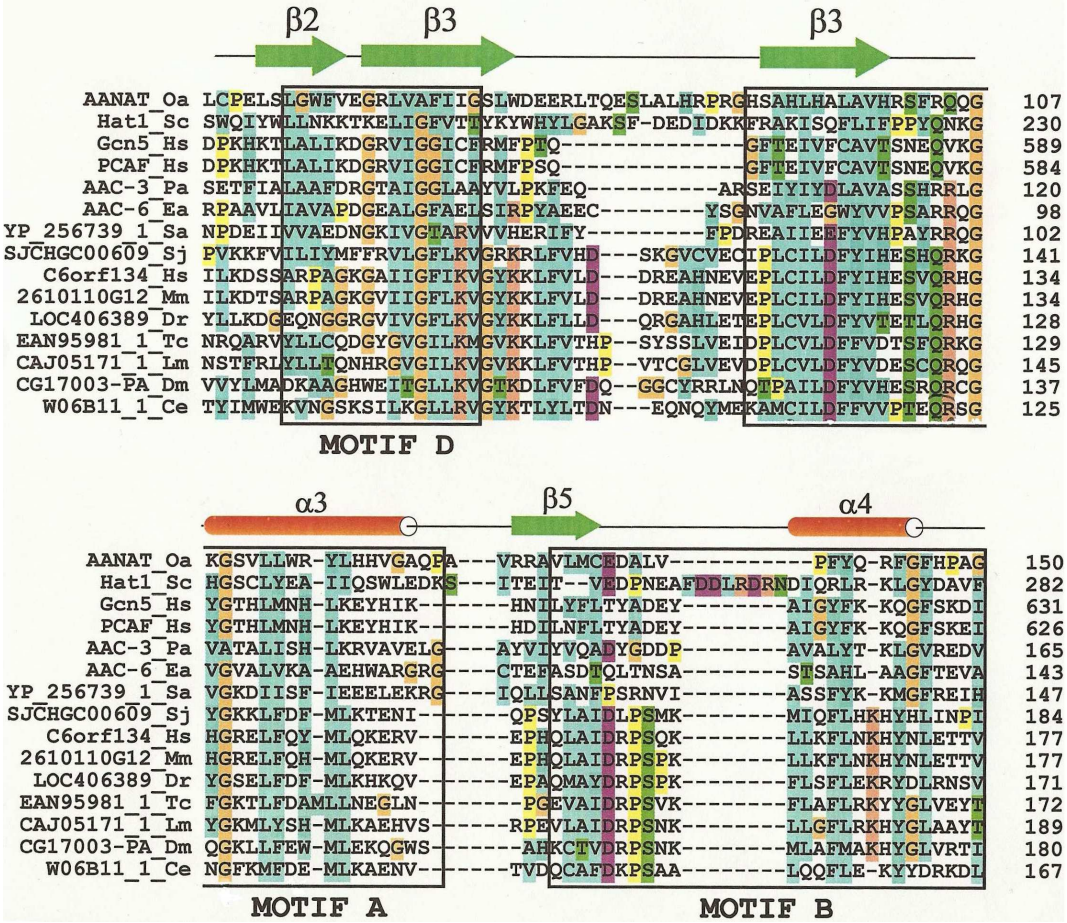

Figure 19: Alignment of mec-17 homologues with GNAT superfamily members

GNAT family members: AANAT (*Ovis aries*) Arylalkylamine N-acetyltransferase, Hat1 (S*accharomyces cerevisiae*), Gcn5 (*Homo sapiens*), PCAF (*Homo sapiens*), AAC-3 (*Pseudomonas aeruginosa*) aminoglycoside N-acetyltransferase, AAC-6 (*Enterobacter cloaca*), YP-256739.1 (*Sulfolobus acidocaldarius DSM 639*) Elp3 related protein; **homologous genes of mec-17**: SJCHGC00609 (*Schistosoma japonicum*), c6orf134 (*Homo sapiens*), 2610110G12Rik (*Mus musculus*), LOC406389 (*Danio rerio*), EAN95981.1 (*Trypanosoma cruzi*), CAJ05171.1 (*Leishmania major*), CG17003-PA (*Drosophila melanogaster*), wo6b11.1 (*Caenorhabditis elegans*)

3.6.1 Recapitulation of previous results on mec-17 function

The putative N-acetyltransferases were recombinantly expressed as GST-fusions in *Escherichia coli* (*E. coli*) and purified using affinity chromatography. An enzyme linked immunosorbent assay (ELISA) with immobilized histone tail peptides was used to test the HAT activity of the recombinant proteins *in vitro*. These experiments revealed intrinsic acetyltransferase activity for all four tested proteins, albeit the activity was weak compared to the known HAT PCAF as a positive control. Furthermore, mutation of conserved

residues in the acetyl-CoA binding site did not significantly reduce the activity, although the initial signals might have been too low to detect a partial loss of activity. Several explanations are possible for these results. Typically, histone acetyltransferases are part of multisubunit protein complexes. The other members of such complexes were shown to modulate both activity and substrate specificity of the HATs. Thus, the recombinant proteins might show only partial activity or insufficient substrate recognition. Alternatively, missing posttranslational modifications might cause reduced activity in the ELISA assay. Modifications of the enzymes or of the substrate peptides could be required for full activity as recognition of histone tails by modifying enzymes is strongly influenced by the PTMs already present on the histone tails. As a third explanation, histones might not be the preferred substrate for the putative acetyltransferases after all. Preliminary localization experiments with the homologues from mouse in N2A[a] cells and from human in HeLa cells, respectively, indicated localization of the proteins outside the nucleus supporting the assumption that non-histone proteins might be the true substrate. To address these questions, it would really help a lot to identify the proteins interacting with the homologues of mec-17. Due to the lack of experience and equipment for work with *C. e.* in our lab, it was decided to focus on the homolog from mouse, 2610110G12Rik, for further experiments. For simplicity, it will be referred to as *M. m.* mec-17 from now.

3.6.2 Expression profile of mec-17

According to RNA expression profiles, *M. m.* mec-17 is expressed strongest in the brain. To check the expression on the protein level, a Western Blot with total protein lysates from various tissues was done with a specific antibody raised against the first 194 residues of mec-17 (see Materials and Methods: Protein expression profile of M. m. mec-17). Indeed, of all tissues examined, prominent expression of mec-17 was only detected in the brain. Thus, the RNA profile seems to give a representative picture of the protein expression of mec17.

[a] Murine neuroblastoma

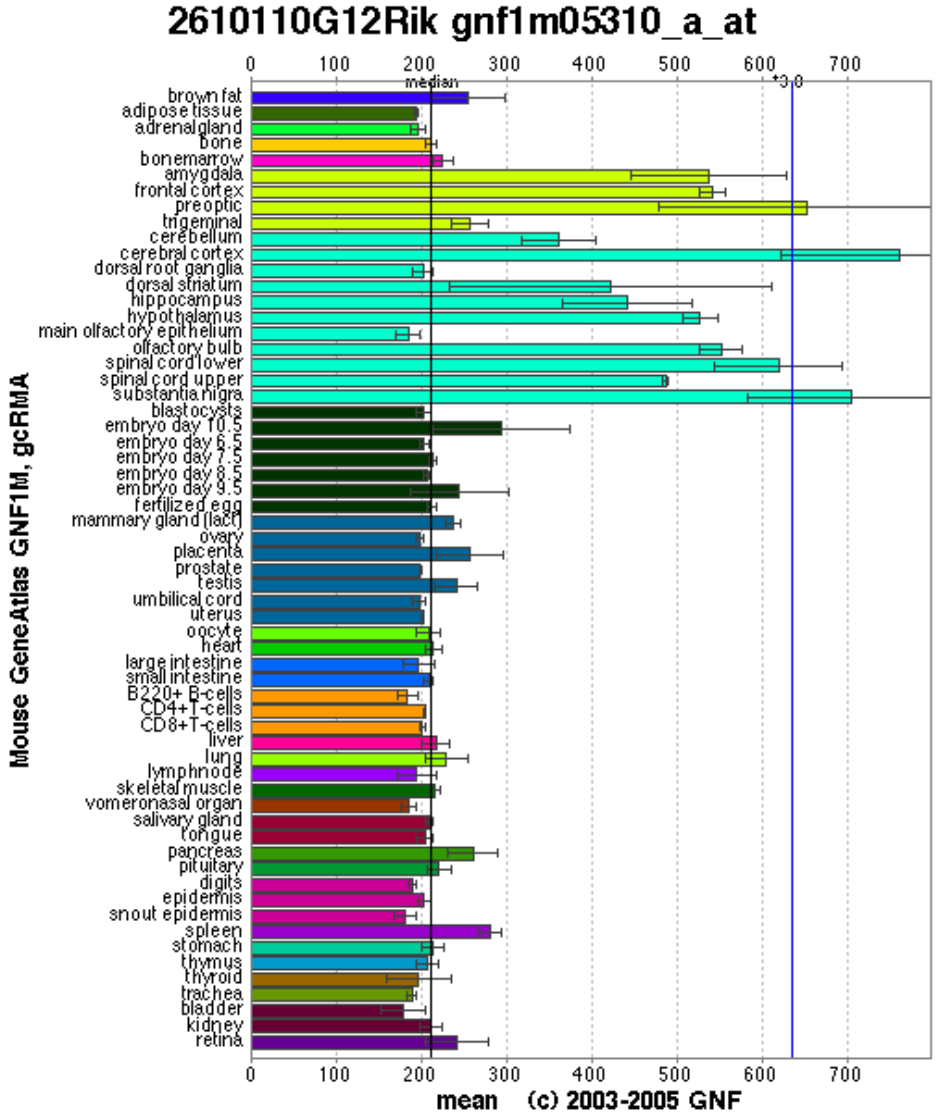

Figure 20: Transcription profile of 2610110G12Rik from GNF Symatlas

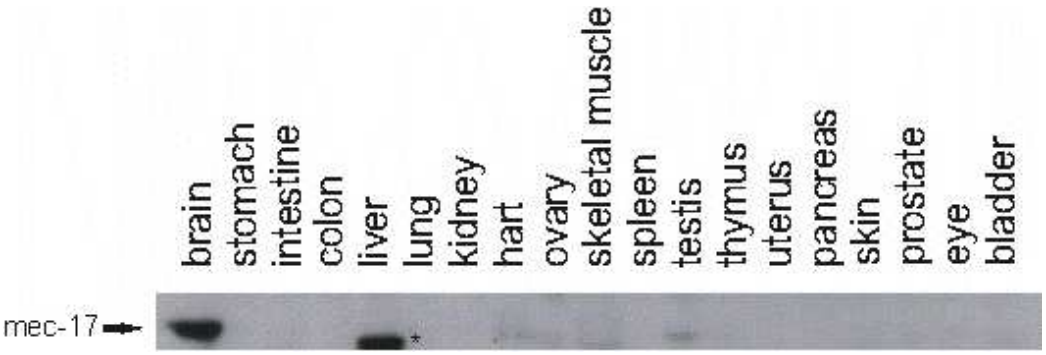

Figure 21: Mouse major tissue Western Blot with antibody directed against mec-17

The expected size of mec-17 is marked by the arrow. The band marked with an asterisk seems to be caused by a cross-reaction of the antibody.

3.6.3 Yeast-2-hybrid screen

To look for proteins interacting with mec-17, it was decided to carry out a yeast-two-hybrid screen. Mec-17 is primarily expressed in the brain as demonstrated above. Thus, a mouse brain cDNA library was used as prey. Since the library was cloned into a vector of the LexA-system and the other components were available at the institute, this system was chosen for the screen. The LexA-system uses a fusion of the protein of interest to the bacterial protein LexA as bait and a library fused to the transcriptional activator B42 as prey. Expression of the library is induced by galactose. An interaction reconstitutes a functional transcription factor binding to LexA-operators and activating transcription of downstream sequences. LEU2 is integrated as a reporter gene into the yeast strain providing growth selection, and a reporter plasmid carrying LacZ enables visual selection. A fusion of LexA to the yeast transcription factor GAL4 is used as positive control and a fusion to the *D. m*. protein bicoid as a negative control (see Material and Methods: Yeast 2-hybrid screen).

First of all, the library was amplified by transformation into *E. coli* and subsequent plasmid preparation from the bacteria to produce sufficient amounts of DNA (see Material and Methods: Amplification of the cDNA library).

To test the autoactivation potential of the bait LexA-mec-17, bait and reporter plasmid were co-transformed into the yeast strain EGY48 and plated onto selective medium. In addition, positive and negative controls were included. The yeast containing the bait plasmid was able to grow on medium selective for the plasmids, but not on medium requiring activation of the LEU2 reporter gene. A β-galactosidase filter assay was done additionally (see Materials and Methods: β-galactosidase filter assay). The positive control colonies turned blue after 5 – 10 min, the bait showed a faint blue color after 45 min, and the negative control was still white after 60 min. It was decided that the autoactivation potential of LexA-mec-17 is low enough for the screen.

Expression of the fusion protein was checked by Western Blot with anti LexA-antibody (1:20.000) from a total protein lysate of the transformed yeast and found satisfying (see Material and Methods: Total protein lysate from yeast). The ability of the fusion protein to enter the nucleus and bind to LexA-operators was tested by a repression assay. In this assay, a test plasmid harboring a constitutively active promoter preceding LexA operators

and the lacZ gene is co-transformed with the bait. When the bait protein is expressed, enters the nucleus, and binds to the LexA-operators, transcription of the reporter gene is blocked. Again, transcription of the reporter gene was tested by a β-galactosidase filter assay. Colonies expressing LexA, LexA-mec-17, or LexA-bicoid turned slower blue than colonies harboring only the test plasmid suggesting that the bait is able to enter the nucleus and bind the LexA operators.

For the screen, large scale transformation of the library is necessary. As transformation into yeast already carrying the bait and reporter plasmid failed to work with sufficient efficiency, it was done into yeast carrying only the bait plasmid (see Materials and Methods: Large scale yeast transformation). The transformed yeast was plated onto medium inducing expression of the library and selective for the plasmids and also for activation of the reporter gene due to interaction of the proteins. Transformation efficiency was monitored by plating a serial dilution on medium selective only for the plasmids. A total yield of 14 million colonies was measured for the screen. After 3 days, 164 colonies growing on –Leu were picked. Seven clones did not grow anymore after transfer to a new plate, and 5 clones could also grow on -Leu without induction of the library exposing them as false positives. These clones were eliminated. From the remaining 152 clones, plasmid DNA was isolated (see Materials and Methods: Plasmid isolation from yeast), transformed into a bacterial strain (KC8) allowing selection for the library plasmid by electroporation and plated onto minimal medium selective for the library plasmid. Plasmid DNA was isolated from the bacteria (4 minipreps for each clone) and inserts were checked by restriction digestion. Only 52 clones yielding the same pattern for all four minipreps were further characterized. These plasmids were retransformed into the yeast strain carrying bait and reporter plasmid. As a selectivity control, the same was done with the empty bait plasmid expressing only LexA instead of LexA-mec-17. Growth selection with and without induction of the library was repeated and, in addition, visual selection was done by a β-galactosidase filter assay (see Materials and Methods: Liquid β-galactosidase assay). 46 clones passed all tests. The plasmid inserts were sequenced and the results blasted against the mouse mRNA database. Only protein coding sequences creating an in-frame fusion with the activation domain were considered resulting in 11 potential interaction partners for mec17. A quantitative liquid β-galactosidase assay was done with these clones to estimate the strength of the interaction. LexA-mec17 alone was tested as an autoactivation control, a LexA-GAL4 fusion as positive control, and LexA-bicoid as

negative control. The empty library plasmid pJG4-5 was tested in combination with LexA-mec17 to exclude interaction of mec-17 with the activation domain. In addition, all candidates were tested also without inducing expression of the interaction partner as well as in combination with LexA alone instead of LexA-mec17 to exclude interaction of the candidates with LexA. All these controls yielded results in the same order of magnitude as the negative control.

LexA-mec17 (autoactivation control)		0,86	+/-	0,13	units
LexA-GAL4 (positive control)		2877	+/-	1570,1	units
LexA-bicoid (negative control)		1,21	+/-	0,18	units
pJG4-5 (specificity control)	+ LexA-mec17	1,26	+/-	0,31	units
Psmc5[a] (NP_032976)	+ LexA-mec17	450,95	+/-	268,68	units
Rps27a[b] (expressed as fusion to ubiquitin, NP_001029037)	+ LexA-mec17	355,2	+/-	165,02	units
Epb4.1l3[c] (NP_038841)	+ LexA-mec17	308,91	+/-	91,47	units
Kif5B[d] (NP_032474)	+ LexA-mec17	293,42	+/-	59,24	units
Immt[e], Mitofilin (NP_083949)	+ LexA-mec17	266,09	+/-	50,28	units
6330407J23Rik (NP_080414)	+ LexA-mec17	181,17	+/-	154,32	units
Dctn1[f] (NP_031861)	+ LexA-mec17	162,05	+/-	43,5	units
mRAS[g] (NP_032650)	+ LexA-mec17	139,02	+/-	27,68	units
Kctd13[h] (NP_766335)	+ LexA-mec17	107,06	+/-	85,48	units
Kif2A[i] (NP_032468)	+ LexA-mec17	83,15	+/-	30,15	units
Spnb2[j] (NP_787030)	+ LexA-mec17	50,78	+/-	9,1	units

Table 2: β-galactosidase activity of clones interacting with mec-17

[a] Proteasome 26S subunit, ATPase, 5

[b] Ribosomal protein S27a

[c] Erythrocyte protein band 4.1 like 3

[d] Kinesin family member 5B

[e] Inner membrane protein, mitochondrial

[f] Dynactin1

[g] Muscle and microspikes RAS

[h] Potassium channel tetramerization doman containing 13

[i] Kinesin family member 2A

[j] Spectrin β2

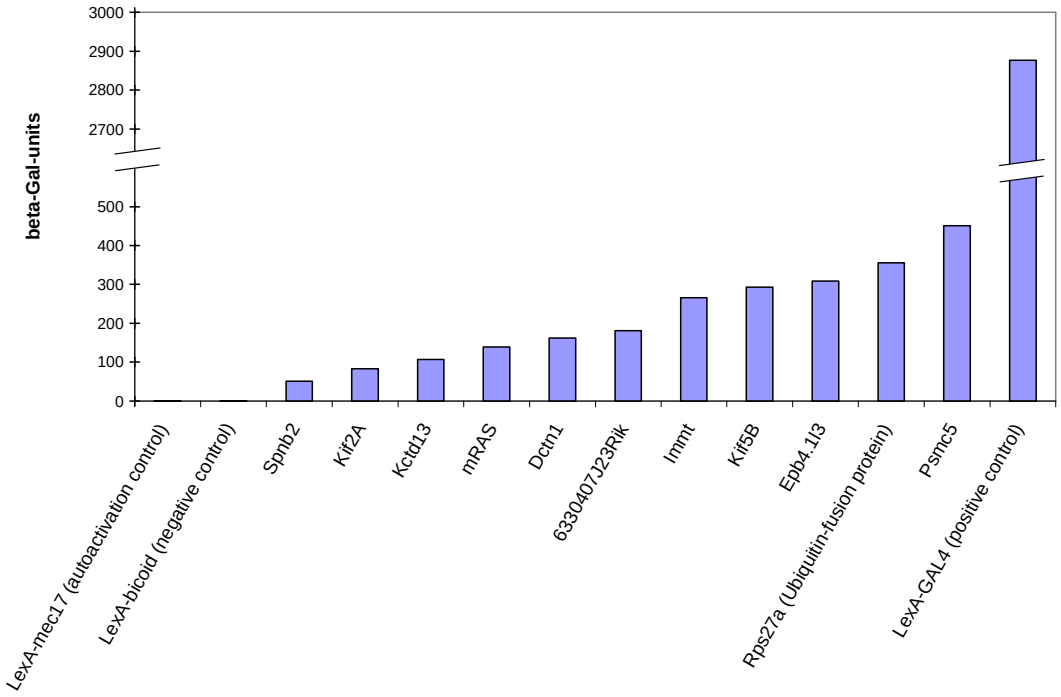

Figure 22: Column diagram of β-galactosidase activity

3.6.4 Co-Immunoprecipitation of mec-17 with interaction partners

To further strengthen the data from the screen, it was tried to co-precipitate mec-17 and its interaction partners from N2A cells. Therefore, cDNAs encoding the full-length sequences of the candidates identified were gathered. Unfortunately, no cDNAs representing the desired sequences of Dctn1, 6330407J23Rik, Kif2A, and Spnb2 were available. The others were cloned as N-terminal fusions with a FLAG-HA-Tag and co-transfected with an untagged mec-17 expression clone into N2A cells. One day after transfection, the cells were lysed and mec-17 precipitated with specific antibody bound to beads. After washing, proteins were eluted with sample buffer and resolved by SDS-PAGE. Proteins were detected by Western Blot with anti-mec-17 antibody for precipitated mec-17 and anti-HA-HRP-conjugate for co-precipitated interacting proteins (see Materials and Methods: Co-Immunoprecipitation). Immt, Kif5B, and Rps27a could not be detected in the lysate prior to precipitation and seem to be not expressed. Epb4.1l3, Psmc5, and mRAS were expressed, but not detected after precipitation. For Kctd13, co-precipitation with mec-17 was clearly demonstrated. As a control, the same procedure was done without antibody from the same lysate to exclude unspecific binding of Kctd13 to the beads. This experiment shows that Kctd13 is only precipitated together with mec-17 and not alone.

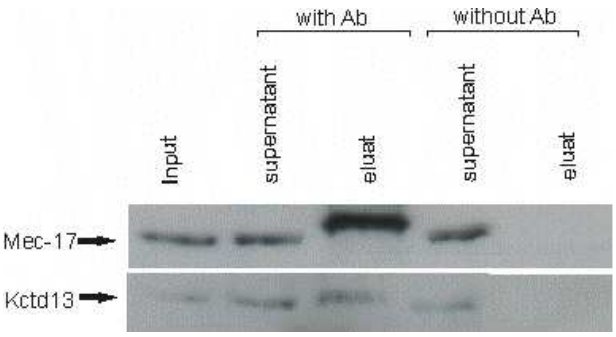

Figure 23: Co-IP of Kctd13 with mec-17 from transiently transfected N2A cells

3.6.5 Discussion

Several potential interaction partners of mec-17 have been isolated. Only one interaction could be confirmed by co-immunoprecipitation (co-IP), but this does not rule out a potential functional linkage to the other proteins. A co-IP requires a relatively stable association over the time needed for the experimental procedure. Thus, some of the proteins found in the yeast 2-hybrid screen could be substrates for mec-17 that interact with the enzyme only transiently.

Unfortunately, not much is known about the one confirmed interaction partner of mec-17. Kctd13 has been shown to interact with the small subunit of DNA polymerase δ and PCNA[a] simultaneously. Furthermore, Kctd13 stimulates DNA polymerase δ activity in the presence of PCNA. Nuclear localization was shown at replication foci suggesting a function in DNA replication[239]. This is consistent with a function of mec-17 in modulation of chromatin structure. Conflicting results on the localization of mec-17 previously gathered in our lab could be an artifact of overexpression of the protein or crossreactivity of antibodies. However, a function in replication shows no obvious correlation with the role in differentiation of neurons observed in *C. elegans.*

Psmc5 is known best as part of the 19S regulatory particle of the 26S proteasome. Additionally, involvement in transcriptional regulation has been suggested. This is consistent with the finding that Psmc5 is localized predominately at the nucleus, in fact, it has been shown to be part of the nuclear 26S proteasome. Interaction with several nuclear receptors/transcription factors has been demonstrated. Psmc5 could exert its effect on

[a] Proliferating cell nuclear antigen

transcription by targeting transcription factors for selective degradation by the proteasome or by modulating protein-protein interactions in transcriptional complexes[240,241]. Additional evidence comes from the yeast homolog SUG1. It has been shown to display helicase activity[242] and to enhance the interaction of the SAGA coactivator complex (which also harbors the HAT Gcn5) with other transcriptional coactivators and its recruitment to promoters[243]. Recently, direct involvement of Sug1 in regulation of transcription of MHC class II[a] by controlling promoter association of CIITA[b] has been demonstrated. Together with documented functions of other 19S ATPases, a role in regulation of transcription by controlling chromatin modifications seems plausible[244]. All these data are consistent with a role of mec-17 as an acetyltransferase involved in transcriptional regulation. Furthermore, Psmc5 has a potential acetylation site at Ala2 annotated. Thus, it could be a substrate for mec-17 giving an explanation for the failure to co-immunoprecipitate with mec-17 despite the interaction demonstrated in the yeast 2-hybrid screen.

The interaction of mec-17 with proteins associated with the cytoskeleton as Dctn1, Epb4.1l3, Spnb2 as well as Kif2A and 5B is consistent with a neuron-specific function for mec17 since the cytoskeleton is of special importance for the function of neurons. Consistent with this, in *C. e.* individuals harboring a mutation in mec-17 show a reduced number of cell-specific microtubules in touch receptors[236]. Dctn1 is part of the dynactin complex required for retrograde axonal transport in neurons[245]. A mutation of Dctn1 at the microtubule binding domain is linked to motor neuron degeneration[246]. Kif5B is involved in axonal transport of mitochondria and synaptic vesicle precursors[247]. For Epb4.1l3, a role in the interaction of axons with Schwann cells and maturation of axons and in myelinating glial cell-axon interactions has been suggested[248].

Immt (Mitofilin) is an integral membrane protein of the inner mitochondrial membrane[249]. Although it has been shown to be acetylated on a lysine residue[250], the interaction of an integral membrane protein in a yeast 2-hybrid screen seems questionable.

Rps27a is expressed as fusion to ubiquitin which is very likely subject to cleavage. Due to the architecture of the library plasmid used in the screen, mec-17 is probably interacting

[a] Major histocompatibility complex class II

[b] Class II transactivator

with the ubiquitin, not with Rps27a itself. The reasons for interaction of mec17 with ubiquitin could be manifold but it may be linked to the interaction with the proteasomal protein Psmc5.

For mRas, a role in cell survival of neural derived cells has been implicated[251]. The expression of mRas (also known as R-Ras3) is highly restricted to the central nervous system, and ectopic expression of the protein was shown to induce neuronal differentiation[252].

Summing up, the precise function of mec-17 was not unveiled by the interacting proteins found in the screen, but several candidates underscore a role in neuron development and/or function, and there are also some hints that mec-17 may indeed be involved in transcriptional control and/or regulation of chromatin structure.

4 Conclusion

For the first time, the functionality of prenylation motifs present in bacterial proteins has been demonstrated. The C-terminus of variants of an ankyrin repeat protein from different strains of *Coxiella burnetii* becomes farnesylated by the eukaryotic enzyme present in rabbit reticulocyte lysate *in vitro*. Thus, pathogenic bacteria seem to be able in principle to utilize the prenyltransferases of their eukaryotic hosts for prenylation of their proteins. Furthermore, localization studies in human cells indicated that prenylation of the *Legionella pneumophila* F-Box protein is important for targeting the protein to intracellular membrane compartments. Together with the recent result that F-Box is secreted into the cytoplasm of macrophages (Hwei Ling Khor et al., 2008, to be published), it is highly likely that prenylation of bacterial proteins is not just a freak of nature caused by the lack of prenyltransferases and, thus, lack of selection against prenylation motifs in bacteria, but a mechanism that might be important *in vivo* for the proper localization and function of secreted proteins. Further studies of other bacterial proteins with predicted prenylation sites will be needed to clarify whether this mechanism is widely used or just a rare occasion.

Prenylation motifs display specific sequence requirements needed for functionality, with restriction up to a single amino acid at the site of attachment. In the surrounding environment, at least a certain pattern of physical properties is needed. Thus, exchange of a single residue due to SNPs could influence the efficiency of recognition and modification by prenyltransferases. Among several protein candidates with SNPs predicted to influence the prenylation motif, prenylation of human ALDH3B2 turned out be significantly improved by exchange of W353 with glycine. This example can be viewed as a snapshot of evolution as prenylation motifs might be generated or destroyed by the accumulation of several mutations over time. Furthermore, SNPs are suggested to be the cause for individual differences in susceptibility to diseases and drugs which would be explained nicely by an influence on the posttranslational modification status of proteins. Therefore, the differential prenylation of the SNP variants of ALDH3B2 represents an exciting example for the influence of SNPs. Further investigations will be needed to explore the full impact of this observation on biochemistry and medicine.

Together with other membrane attachment factors, myristoylation is responsible for proper targeting and membrane attachment of a manifold array of proteins. One important group

consists of proteins involved in asymmetric cell division in neural development. Myristoylation of certain asymmetrically localized protein targets is suggested to be required for asymmetric distribution to daughter cells after mitosis. The proteins numb-A, neur-C, and Par-1 isoform Q from *Drosophila melanogaster* as well as neuralized-like 1 and 2 from *Mus musculus* were shown to be myristoylated *in vitro*. The impact of the modification on subcellular localization was studied in transgenic flies and in mouse cells, respectively. Interestingly, all of the fly proteins exist in more than one isoform but only a subset of these isoforms is myristoylated. Other N-terminal sequences of numb and Par-1 miss the obligatory glycine residue while neur-B is not myristoylated, despite the presence of an N-terminal glycine, due to other unfavorable residues in the sequence. The differential myristoylation of protein isoforms suggests that they might carry out different functions or the same function at different locations. These results also underscore the importance of distinguishing between isoforms with different potential for posttranslational modification in functional studies.

The human transcription factor NFAT5 is another exciting example of this phenomenon. While isoforms B and C do not possess an N-terminal glycine, isoform A is myristoylated *in vitro*. Furthermore, myristoylation was shown to be required to prevent translocation of NFAT5-A to the nucleus. Thus, this might be the first case of a transcription factor using a new mechanism for regulation of mobilization and nuclear shuttling. While the nuclear localization sequence of cytosolic transcription factor proteins is usually masked by inhibitor proteins that are removed upon activation, a second class of transcription factors has their NLS exposed all the time but is anchored by transmembrane domains and released by proteolytic cleavage. A similar mechanism could be utilized by a myristoylated transcription factor. Alternatively, reversible palmitoylation could be used as a switch for membrane attachment and release. In conclusion, a completely new mechanism is suggested for the regulation of localization of NFAT5-A. As the other isoforms are not myristoylated, they might exert divergent functions.

A function as histone acetyltransferase was predicted for mec-17 from Caenorhabditis elegans as well as homologous proteins from other species. N-acetyltransferase activity of these proteins was successfully demonstrated in our lab. However, histones turned out to be a weak substrate. HATs are usually part of multiprotein complexes. The other components of these complexes are known to influence activity and substrate specificity of the HATs. Furthermore, various non-histone proteins are acetylated by so-called HATs. A

yeast 2-hybrid screen was used to identify proteins interacting with mouse mec-17. These might be members of a complex or substrates for acetylation. The interaction with Kctd13 has been verified biochemically by co-immunoprecipitation. Together, the proteins identified indicate a function in transcriptional regulation and/or regulation of chromatin structure. Furthermore, the suggested role in neuronal development is underscored by the results.

5 Materials and Methods

5.1 Buffer Composition

DNA sample buffer

50% Glycerol
1 mM EDTA
0.25% Bromophenol blue
0.25% Xylene cyanol FF

EF-buffer

12.6 g K_2HPO_4
3.6 g KH_2PO_4
0.9 g Na-citrate
0.18 g $MgSO_4$
1.8 g $(NH_4)_2SO_4$
88 g Glycerol
for 1 L buffer

FSB buffer

10 mM KOAc, pH 6.2
10 mM KCl
50 mm $CaCl_2$
10% Glycerol

Glutathione elution buffer (GEB)

50 mM Tris-HCl, pH 8.0
10 mM reduced glutathione

Hunt-buffer

20 mM Tris-HCl pH 8.0
100 mM NaCl
1 mM EDTA
0.5% Nonidet P-40

Lysis buffer A

20 mM 4-(2-hydroxyethyl)-1-piperazineethanesulfonic acid (HEPES) pH 7.5 (with acetic acid)
100 mM KOAc
5 mM $Mg(OAc)_2$
0.1% Triton X-100

One-Step-buffer

200 mM LiOAc
100 mM Dithiothreitol (DTT)
40% PEG 4000
prepare fresh before use from stock solutions

P1

50 mM Tris-HCl pH 8.0
10 mM EDTA
0.01% RNase A

P2

0.2 M NaOH
1% Sodium dodecyl sulfate (SDS)

P3

3 M KOAc, pH 5.5

Phosphate buffered saline (PBS)

10 mM NaH_2PO_4/Na_2HPO_4, pH 7.4
150 mM NaCl

PBS-T

See PBS, + 0.1% Tween 20

SDS-PAGE running buffer

30 g Tris base
144 g Glycine
10 g SDS
for 1 L 10-fold buffer

SDS-PAGE sample buffer

60 mM Tris-HCl, pH 6.8
10% Glycerol
2% SDS
1% 2-mercaptoethanol
0.002% Bromophenol blue
use as 6-fold buffer

TBE-buffer

89 mM Tris base/boric acid, pH 8.3
2 mM EDTA

TE

10 mM Tris(hydroxymethyl)aminomethane (Tris)-HCl, pH 7.5
1 mM Ethylendiaminetetraacetic acid (EDTA)

TE/LiOAc

100 mM LiOAc
in TE

TE/PEG/LiOAc

100 mM LiOAc

40% PEG 3350

in TE

Z-buffer

60 mM Na_2HPO_3

40mM NaH_2PO_3

10 mM KCl

1 mM $MgSO_4$

(50 mM β-mercaptoethanol)

5.2 Composition of media

bacterial defined minimal medium

Autoclave 5 times 15 g agar in 800 ml dH_2O, cool to 50°C.
Dissolve
68.77 g K_2HPO_4
22.5 g KH_2PO_4
5 g $(NH_4)_2SO_4$
2.5 g Na-citrate . $2H_2O$
in 800 ml dH_2O, autoclave and cool to 50°C, add 50 ml each of URA, HIS and LEU (stock (4 mg/ml), 5 ml 1 M $MgSO_4$, 50 ml 20% glucose, 5 ml Kanamycin (stock 10 mg/ml), 0.5 ml Ampicillin (stock 100 mg/ml) and 2.5 mg thiamin-HCl.
Mix 200 ml of this solution with 800 ml of the agar solution and pour plates.

Luria Broth (LB)

1% Yeast-extract
1% Trypton
0.5% NaCl
0.1% Glucose

SC-X

0.67% Yeast nitrogen base (YNB) without amino acids
2% Glucose (or galactose, with additional 1% raffinose)
1% 100 x amino acid mix without X
for plates, add 3 % agar

SOB

0.5% Yeast extract
2% Trypton
10 mM NaCl
2.5 mM KCl
10 mM $MgCl_2$
10 mM $MgSO_4$

SOC

See SOB + 20 mM glucose

SOP-medium

	Dulbeccos modified eagle medium (DMEM)
10%	Fetal calf serum (FCS)
1%	Penicillin (stock 10.000 units/ml)
1%	Streptomycin (stock 10 mg/ml)
1%	Glutamine (stock 200 mM)

YPD

1%	Yeast Extract
2%	Pepton
2%	Glucose

5.2.1 100 x Amino acid stocks

Adenosine	3 mg/ml	Lysine	4 mg/ml
Uracil	4 mg/ml	Phenylalanine	5 mg/ml
Histidine	2 mg/ml	Tyrosine	2 mg/ml
Methionine	2 mg/ml	Isoleucine	2 mg/ml
Tryptophane	3 mg/ml	Valine	6.5 mg/ml
Threonine	15 mg/ml	Arginine	3 mg/ml
leucine	8 mg/ml	Asparagine	10 mg/ml

Do not autoclave Trp and Thr!

5.3 cDNA clones

organism	**name**	**Protein accession**	**source**
Coxiella burnetii (RSA493)	Ankyrin repeat containing protein, CBU_0356	NP_819396.1	J. E. Samuel
Coxiella burnetii (Dugway 7E9-12)	Hypothetical protein, CburD_01001505	ZP_01298590	J. E. Samuel
Coxiella burnetii (RSA331)	Hypothetical protein, CburR_01001221	ZP_01309761.1	J. E. Samuel
Coxiella burnetii (Graves)			J. E. Samuel
Legionella pneumophila	Hypothetical protein lpg2525	YP_096532.1	
Homo sapiens	ALDH3B2	NP_000686.2	IRAUp969B0231D6 (imaGenes)
Homo sapiens	BEX2	NP_116010.1	IRATp970G1018D6 (imaGenes)
Homo sapiens	UTP14A	NP_006640.2	IRAUp969B0312D6 (imaGenes)
Homo sapiens	FLJ20364	NP_060255.2	IRAUp969B0653D6 (imaGenes)
Drosophila melanogaster	Igloo-L	AAB32065.1	RE17162 (DGRC)
Drosophila melanogaster	Numb-A	AAA28730.1	LD45505 (DGRC), provided by J. Knoblich
Drosophila melanogaster	Neur-B	AAK93411.1	provided by J. Knoblich
Drosophila melanogaster	Neur-C	AAO41451.1	RE20876 (DGRC)

Drosophila melanogaster	Par-1-Q	AAM75016.1	GH14769 (DGRC)
Mus musculus	Neuralized-like 1	AAH58386.1	IRAVp968A02118D6 (imaGenes)
Mus musculus	Neuralized-like 2	AAK97495.1	Modified from neuralized-like 1 by PCR
Mus musculus	2610110G12Rik (mec-17 homolog)	NM_082752	RIKEN cDNA library
Mus musculus	Kctd13	NP_766335	RIKEN cDNA library
Mus musculus	Rps27a	NP_077239	RIKEN cDNA library
Mus musculus	Immt	NP_083949	RIKEN cDNA library
Mus musculus	mRAS	NP_032650	RIKEN cDNA library
Mus musculus	Psmc5	NP_032976	Mouse brain cDNA library
Mus musculus	Kif5b	NP_032474	IRAVp968G12160D (imaGenes)
Mus musculus	Epb4.1l3	NP_038841	Provided by J. Conboy

All cDNA clones were checked by sequencing. The cDNAs from *Coxiella burnetii* were kindly provided by James E. Samuel, Department of Microbial and Molecular Pathogenesis, College of Medicine, Texas A&M Health Science Center, College Station, TX. A mouse brain cDNA library was provided by Egon Ogris, Department of Medical Biochemistry, Max F. Perutz Laboratories, Medical University of Vienna. The cDNAs for numb-A and neur-B from *Drosophila melanogaster* were provided by Jürgen A. Knoblich, Institute of Molecular Biotechnology. A cDNA encoding Epb4.1l3 was provided by John G. Conboy, Life Science Division, Ernest Orlando Lawrence Berkeley Laboratory, CA.

5.4 Cloning procedures

For the *in vitro* prenylation assay, candidate cDNAs were amplified by PCR with appropriate primers (MWG Biotech) including the Stop-Codon. The PCR products were cloned into the pGEM-T Easy vector (Promega). Mutations were inserted by site directed mutagenesis. The constructs were subcloned into pGEX-5X-1 (Amersham). For localization studies, the same constructs were subcloned into pEGFP-C2 (Clontech).

For the *in vitro* myristoylation assay, candidate cDNAs were amplified by PCR without stop codon with primers adding a T7 promoter and Kozak consensus sequence directly prior to the start codon (aagcgtaatacgactcactatagggagaccacc).The PCR products were cloned into the pGEM-T Easy vector and subcloned into a self constructed vector for C-terminal GST-tagging. This vector was created by amplification of GST from the pGEX-5X-1 vector and insertion downstream of the multiple cloning site of the pSK+ vector (Stratagene). For localization studies in HeLa or 3T3 cells, the same constructs were subcloned into pEGFP-N3. For generation of transgenic flies, the candidate sequences were amplified by PCR without stop codon with primers containing attB recombination sequences for Gateway cloning. The PCR products were recombined into pDONR221 and subsequently recombined into a Drosophila pUAST gateway destination vector with a C-terminal myc-tag.

For the yeast 2-hybrid assay, the cDNA encoding *M. m.* mec-17 was amplified by PCR with appropriate primers including the termination codon, cloned into pGEM-T Easy and then subcloned into the bait vector pEG202.

For immunoprecipitation experiments, *M. m.* mec-17 including the termination codon was subcloned into the pEGFP-N3 vector for expression without tag. The cDNAs for mec-17 interaction partners from the screen were amplified by PCR including the Stop-Codon and cloned via pGEM-T Easy into pENTR4. These constructs were recombined into a Gateway destination vector harboring an N-terminal FLAG-HA double tag.

5.4.1 PCR

In a standard setup, a total amount of 10 pmol primers and ~20 ng plasmid DNA were used per reaction. PCR reactions for cloning were done with 1 µl deoxynucleotide mix

(Eppendorf) and 1 µl *Pfu*[a] Turbo polymerase (Stratagene) in a total reaction volume of 25 µl. Amplification of DNA for use in coupled *in vitro* transcription/translation was done with PuReTaq Ready-To-Go PCR beads (GE Healthcare). Standard reaction conditions were 30 cycles with a denaturing temperature of 94°C, annealing temperature usually 53°C (depending on the primer melting temperature), and extension at 72°C for one minute per kb product size. For TA-cloning of PCR products generated with *Pfu* polymerase, 1 µl of 50 mM $MgCl_2$, 1 µl 10mM ATP, and 1 µl *Taq*[b] polymerase were added subsequently and incubated for 15 min at 72°C. The samples were checked and purified by agarose gel electrophoresis.

5.4.2 Agarose gel electrophoresis

For a standard gel 1% agarose (Biozym) in TBE buffer was boiled in the microwave and cooled to ~50°C. Prior to pouring, 0.5 µg ethidium bromide per ml was added from a stock solution (10 mg/ml). DNA samples were mixed 5:1 with DNA sample buffer, loaded onto the gel, and run in TBE buffer at a constant voltage of 100 V. Subsequently, DNA was visualized by UV illumination. When agarose gel electrophoresis was used for purification, DNA fragments were excised from the gel with a scalpel blade and eluted with the QIAquick gel extraction kit (QIAGEN) according to the manual.

5.4.3 Ligation

Ligation of PCR-products into pGEM-T Easy (Promega) was done according to the manufacturers manual. Ligation of fragments created by restriction digestion was done with T4 DNA ligase (Roche) at room temperature (RT) for one hour or at 16°C overnight. Ligation products were transformed into chemically competent *E. coli* (strain DH5α) for amplification.

5.4.4 Transformation into chemically competent bacteria

Bacteria were inoculated into 3 ml LB-medium and incubated at 37°C overnight with shaking. 1 ml of the culture was diluted into 100 ml LB-medium and grown at 37°C to an

---

[a] *Pyrococcus furiosus*

[b] *Thermophilus aquaticus*

OD_{600} (optical density) of 0.5 – 1. Cells were pelleted by centrifugation at 4000 g for 10 min at 4°C, resuspended in 15 ml FSB buffer, and incubated for 10 min at 4°C. A second centrifugation step was followed by resuspension in 4 – 8 ml FSB (depending on the final OD). This suspension was used immediately or divided into aliquots and stored at -80°C.

Frozen aliquots of chemically competent bacteria were thawed on ice. 100 µl were used for each transformation. Ligation products (or plasmid in appropriate dilution) were mixed with the cells and incubated on ice for 30 min. The cells were heat-shocked at 42°C for 45 sec and then cooled on ice for 2 min. After addition of 1 ml LB-medium, cells were revived for ~ 1 h at 37°C with shaking. Cells were pelleted for 1 min at 13.000 rpm in a tabletop centrifuge. Medium was decanted and cells resuspended in the residual medium (~100 µl). The whole suspension was plated onto selective agar plates (containing the appropriate antibiotic) and incubated upside down at 37°C overnight. For blue/white-selection (with pGEM-T Easy), 100 µl of 0.1 M Isopropyl-β-D-thiogalactopyranosid (IPTG) and 20 µl of 5-Brom-4-chlor-3-indoxyl-β-D-galactopyranosid (X-Gal, 20 mg/ml) were plated prior to the cells.

5.4.5 Plasmid preparation from bacteria (Mini-Prep)

Single colonies were picked and inoculated into 4 ml of the appropriate selective medium. Cells were grown at 37°C overnight. If needed, stocks were prepared by mixing 500 µl of culture with 500 µl 2 x EF-buffer and stored at -80°C. 3 ml of culture were pelleted in a tabletop centrifuge at 13.000 rpm for 3 min. Plasmid DNA was prepared with the QIAprep Spin Miniprep kit (QIAGEN) according to the manufacturers manual. Alternatively, the alkaline lysis method was used. Cells were resuspended in 300 µl P1. 300 µl P2 was added and mixed by inverting the tube several times. 300 µl P3 were added and mixed again. Cell fragments were pelleted for 10 min at 13.000 rpm in a tabletop centrifuge, and the supernatant was transferred to a new tube. 650 µl isopropanol was added and incubated for 10 min at RT. After centrifugation for 10 min at 13.000 rpm, the supernatant was aspired and the pellet washed with 70% ethanol, dried in a speedvac, and solubilized in TE. The DNA preparation was checked by restriction digestion.

5.4.6 Restriction digestion

Usually 2 – 300 ng plasmid DNA was digested with 5 units of one or more restriction enzymes (Roche or Fermentas) in a total volume of 15 µl for one hour (reaction conditions

like buffer and temperature as suggested for the enzymes by the manufacturer). For subcloning, the vector was dephosphorylated with 1 unit shrimp alkaline phosphatase (Roche) for 10 min at 37°C. Subsequently, the enzyme was deactivated for 15 min at 65°C. The digests were analyzed by agarose gel electrophoresis.

5.4.7 Site directed mutagenesis

Site directed mutagenesis was done with the QuickChange XL site directed mutagenesis kit (Stratagene) according to the manufacturers manual.

5.4.8 Gateway cloning

PCR products with attB recombination sites were recombined with a donor vector using BP clonase mix (Invitrogen) according to the manual creating an entry vector. Alternatively, standard restriction cloning methods were used to clone the ORF of interest into an entry vector. Subsequently, the ORF was recombined into a destination vector with LR clonase mix (Invitrogen) to create an expression clone. Gateway reaction products were transformed into chemically competent *E. coli* or electroporated into electrocompetent *E. coli*. The *E. coli* strain DB3.1 was used for maintaining stocks of the empty Gateway vectors.

5.4.9 Transformation of E. coli by electroporation

Bacteria were inoculated into 5 ml LB-medium and incubated at 37°C overnight with shaking. The culture was diluted into 500 ml LB-medium and grown at 37°C to an OD_{600} of 0.5. The cells were chilled on ice for 30 min and pelleted by centrifugation at 4000 g for 10 min at 4°C. Subsequently the pellet was resuspended in 300 ml 10% glycerol and pelleted again. The procedure was repeated with 150 ml and 10 ml. Finally, the cells were resuspended in 2 ml 10% glycerol, divided into aliquots and stored at -80°C.

For transformation, electroporation cuvettes were cleaned with soap and then washed with dH_2O and 70% ethanol. Subsequently, the cuvettes were irradiated for at least one hour with UV light. Frozen electrocompetent cells were thawed on ice. 50 µl cells were mixed with plasmid DNA on ice and transferred to a clean electroporation cuvette. Electroporation with a gene pulser (BioRad) at 1.7 V, 25 µFD and 200 Ω resulted in time constants between 3.7 and 4.3. The cells were mixed with 1 ml SOC-Medium, revived for

30 min at 37°C with shaking, pelleted by centrifugation and plated onto selective medium. The plates were incubated for up to 2 days at 37°C.

5.5 Biochemical techniques

5.5.1 Coupled in vitro transcription/translation

For the N-terminal GST-fusions analyzed regarding their prenylation status, DNA was amplified by PCR with puReTaq Ready-To-Go PCR Beads (Amersham Biosciences) using a 5'-primer containing a T7-promoter and a Kozak consensus sequence. It anneals at the 5'-end of the DNA encoding the GST-tag:

5' gcgtaatacgactcactatagggagaccacc**atg**tcccctatacttaggttattgg 3'

The bold region represents the start codon of the GST-tag. The 3'-primer was designed to anneal in pGEX-vectors downstream of the insert, allowing the use of the same primer pair for all proteins:

5' agatcgtcagtcagtcacgat 3'

For C-terminal GST fusions analyzed for myristoylation, DNA was amplified by PCR using a 5'-primer annealing to the T7 promoter cloned upstream of the start codons:

5' gcgtaatacgactcactatagggagaccacc 3'

A 3'-primer was designed to anneal downstream of the insert:

5' ccctcactaaagggaacaaaagc 3'

For analysis of lipid modifications, the radioactive label of choice, that is 20 µCi [^{3}H]mevalonate, 10 µCi [^{3}H]FPP, or 10 µCi [^{3}H]GGPP for prenylation or 20 µCi [^{3}H]myristic acid for myristoylation (all purchased from American Radiolabeled Chemicals), was transferred to Eppendorf tubes and dried in a speedvac under vacuum at room temperature to remove the ethanol which could disrupt the transcription/translation. 20 µl rabbit reticulocyte lysate, 0.5 µl PCR-Enhancer, and 0.5 µl methionine were added which were all supplied with the TNT Quick Coupled Transcription/Translation Kit (Promega). For preliminary translation tests, [^{35}S]-methionine (Amersham) was used without radioactive lipids.

The reaction was started by addition of 2.5 µl of the PCR reaction and incubated at 30 °C (4 h for prenylation, 2 h for myristoylation). For purification of the translated protein, 50µl glutathione sepharose 4B-beads (75% slurry, Amersham Biosciences) were separately resuspended in 0.5 ml PBS and spun down in a microcentrifuge at 1.600 rpm for one minute. The supernatant was removed and the washing step repeated once to equilibrate the beads for protein binding. The whole TNT reaction-mix and PBS to a final volume of 200 µl was added. After resuspension, the beads were incubated with gentle agitation at room temperature for 1 hour. Afterwards, they were washed 5 times with 0.5 ml PBS. Following the last washing step, 50 µl of GEB buffer were added and incubated again for 1 hour with agitation. The supernatant was removed, mixed with an appropriate volume of sample buffer,incubated for 5 min at 95°C, and resolved by SDS-PAGE. For myristoylation targets, purification was skipped. Instead, the reaction mix was diluted to a total volume of 100 µl with PBS, mixed with an appropriate volume of sample buffer, incubated for 15 min at 60°C and resolved by SDS-PAGE. The protein was transferred from the gel to a nitrocellulose membrane by electroblotting. The membrane was left to dry. Each lane was scanned separately for 20 min using a Berthold TLC linear analyzer LB 282. Total protein yield was detected by Western Blot with anti-GST antibody (Anti-GST-HRP-conjugate, Amersham Biosciences, 1:5.000).

5.5.2 Co-Immunoprecipitation

A 10 cm dish of N2A cells (~80% confluent) was transiently transfected with the desired expression clones. The next day, cells were detached from the dish with trypsin. Medium was removed by centrifugation at 500 g for 5 min at 4°C. The cells were washed with 1 ml PBS and resuspended in 500 µl Hunt-buffer supplemented with Complete protease inhibitor cocktail (Roche). Lysis was achieved by freezing in liquid nitrogen, thawing at 37°C, and another step with freezing and thawing at RT. Cellular debris was removed by centrifugation at 13.000 rpm in a tabletop centrifuge for 10 min at 4°C. The lysate was split in two aliquots and 50 µl anti-mec-17 antibody was added to one aliquot. After incubation on a rotor at 4°C for 1 h, 50 µl anti-rabbit IgG-beads (100 µl suspension, Dynabeads M-280, sheep anti-rabbit IgG, Invitrogen) for each aliquot were equilibrated in Hunt-buffer and incubated with the lysate for 1 h at 4°C. The beads were washed three times with 500 µl Hunt-buffer, and then protein was eluted by addition of 50 µl 2-fold sample buffer and incubation at 95°C for 5 min. Protein was resolved by SDS-PAGE and detected by Western Blot.

5.5.3 SDS-PAGE

Separation gel	10%	15%	**Stacking gel**	
H_2O	12	8	H_2O	6,8
1M Tris-HCl, pH8.8	7	7	0,5M Tris-HCl, pH6,8	1,25
AA (30%) 37,5:1	10	15	AA (30%) 37,5:1	1,7
10% SDS	0,3	0,3	10% SDS	0,1
TEMED (µl)	25	25	TEMED (µl)	10
APS 20% (µl)	150	150	APS 20% (µl)	50

The recipes are for eight gels. All volumes are in ml unless otherwise noted. All components were mixed according to the recipe adding NNN'N'-Tetramethylethylenediamine (TEMED) and ammoniumpersulfate (APS) last. Separation gel was poured, overlaid with butanol, and left for polymerization at RT for at least 15 min. Subsequently, butanol was removed and the stacking gel cast. For electrophoresis, gels were inserted into a Mini-PROTEAN 3 cell (BioRad) after washing the slots with running buffer. Gels were run at a constant current of 30 – 50 mA per gel.

5.5.4 Western Blot

Proteins were transferred from the gel to a nitrocellulose membrane by semi-dry electroblotting in SDS-PAGE running buffer for 2 h at a constant current of 150 mA. The membrane was blocked with 5 % skim milk powder in PBS-T for 1 h at RT with gentle agitation. The membrane was rinsed in PBS-T and incubated with primary antibody diluted into PBS-T for 1 h at RT or alternatively overnight at 4°C. It was washed three times for 10 min in PBS-T. If required, incubation with secondary antibody was done for 1 h at RT followed by washing. The wet membrane was incubated with ECL plus Western Blotting Detection solution and exposed with Hyperfilm ECL (Amersham Biosciences) for appropriate time.

5.5.5 Protein expression profile of M. m. mec-17

A ready-to-use mouse mixed tissue Western Blot (Zyagen) was blocked, incubated with anti-mec17 antibody (1:1000) as primary antibody and anti-rabbit-HRP-conjugate (1:10.000, Amersham) as secondary antibody. Detection was performed as described.

5.6 Cell culture techniques

Cells were cultured in SOP-medium in 100 mm dishes at 37°C and 5% CO_2. For dilution of confluent cells, the medium was aspired and the cells were washed with 10 ml PBS. To detach the cells from the dishes, they were incubated with 1 ml 0.05% trypsin (Gibco) for 5 min at 37°C. Afterwards, they were diluted with 9 ml medium, and an appropriate volume was transferred to a new dish. For microscopy, cells were seeded onto cover slips placed in 6 well plates. Transfection was done with Lipofectamine Plus (Invitrogen) according to the manual.

5.7 Fluorescence microscopy of GFP-constructs

Cells were cultured on cover slips and transfected transiently with GFP-fusion constructs. The day after transfection, the cells were rinsed in PBS, fixed in PBS containing 2% formaldehyde for 15 – 20 min, washed again, and permeabilized with PBS containing 0.1% Triton X-100 for 10 min. After a last wash with PBS, the cover slides were rinsed in dH_2O and mounted on microscope slides using Vectashield hard-set mounting medium H1500 (Vector Laboratories). Fluorescence microscopy was carried out with an Axioplan 2 Imaging Microscope (Zeiss). Images were acquired with a Coolsnap HQ camera (Photometrics) and analyzed using the software Metamorph 6.2r4 (Universal Imaging Corp.).

5.8 Yeast 2-hybrid screen

All plasmids needed for the screen were kindly provided by Andreas Hartig:

- pEG202 (bait vector, N-terminal LexA fusion)
- pSH18-34 (reporter plasmid, lacZ downstream of LexA-operators)
- pRFHM-1 (negative control, LexA fusion of fly protein bicoid)
- pSH17-4 (positive control, LexA fusion of GAL4)
- pJK101 (test plasmid for repression assay, constitutive promoter in front of LexA-operators and lacZ)

All plasmids were checked by restriction digestion. A mouse brain cDNA library cloned into the prey vector pJG4-5 was kindly provided by Egon Ogris as well as the yeast strain EGY48, the bacterial strain KC8, and LexA antibody.

5.8.1 Amplification of the cDNA library

20 ml of chemically competent DH5α were transformed with 20 µg library DNA in aliquots of 0.5 ml and plated onto 14 LB-Amp plates (45 x 45 cm). Transformation efficiency was checked by plating a serial dilution of an aliquot. After incubation overnight at 37°C, transformation efficiency was determined (4 mio. colonies in total, library theoretically has 3.6 mio. independent clones). The colonies were scraped into 300 ml LB-Amp and diluted to 800 ml to give an OD_{600} of 4.0. The cells were incubated for 3 h at 37°C and harvested by centrifugation at 6000 g for 15 min. DNA was prepared with a total of 16 Maxi-Prep columns (QIAGEN Plasmid Maxi Kit) to yield a total amount of ~4 mg library DNA. The DNA was checked by restriction digestion.

5.8.2 Yeast one-step transformation

Fresh cells are taken from a plate and mixed with 100 µl of one-step buffer as well as 2 µl plasmid DNA and 5µl hs-DNA (herring sperm). The mix was incubated at 45°C for 30 min, plated onto selective medium, and incubated at 30°C for 2 days.

5.8.3 β-galactosidase filter assay

Colonies were picked and streaked onto new plates with selective medium and grown at 30°C. A nitrocellulose membrane was put onto the plate and softly pressed on the agar to transfer the colonies to the membrane. The membrane was frozen in liquid nitrogen to break the cells and thawed at RT. Afterwards, the membrane was put on a piece of whatman paper soaked in Z-buffer containing 1 mg/ml X-Gal (stock 100 mg/ml in DMF) and incubated at 30°C. Color was monitored for 1 h.

5.8.4 Total protein lysate from yeast

A preculture was grown at 30°C overnight. 15 ml selective medium were inoculated at an OD_{600} of 0.2 and grown to ~ 0.6. The cells were harvested by centrifugation at 10.000 g for 5 min. Medium was decanted and the cells resuspended in the residual medium. After transfer to screw-cap tubes, they were pelleted, frozen in liquid nitrogen, and thawed at RT. Cells were resuspended in 200 µl lysis buffer A, and ~ 200 µl sterile glass beads were added. Cells were broken in the Fast-Prep two times for 10 sec at speed 6. The lysate was separated from the beads by centrifugation.

5.8.5 Large scale yeast transformation

Yeast already containing the bait plasmid was grown in 750 ml selective medium over night at 30°C to an OD_{600} of ~5. The pre-culture was used to inoculate 12.5 L YPD medium to an OD of 0.2. The culture was grown at 30°C for ~3.5 h to an OD of 0.6. Cells were harvested by centrifugation at 1000 g for 5 min, washed in dH_2O, and split into 10 aliquots. Those were resuspended in 5 ml TE/LiOAc each. Hs-DNA (10 mg/ml) was heated for 5 min at 95°C and then cooled on ice. To each aliquot, 5 mg Hs-DNA and 50 µg library DNA were added prior to 30 ml of TE/LiOAC/PEG. The mixture was incubated at 30°C with moderate agitation for 30 min. After addition of 3.5 ml dimethylsulfoxide (DMSO) to each aliquot, heat shock was done at 45°C in a water bath for 15 min followed by 2 min on ice. The cells were harvested by centrifugation, resuspended in 500 ml YPD, and revived at 30°C for 3 h. Cells were pelleted again, resuspended in 32 ml TE, and plated onto 16 plates (45 x 45 cm) with galactose medium (to induce expression of the library) selective for the plasmids and also lacking Leu to select for interaction of the proteins.

5.8.6 Plasmid isolation from yeast

2 ml selective medium were inoculated with one colony and grown at 30°C overnight. 1.5 ml were pelleted at 13.000 rpm in a tabletop centrifuge. Supernatant was decanted and the pellet resuspended in the residual liquid. 200 µl lysis buffer (TE plus 2% Triton X-100, 1% SDS, 100 mM NaCl) and 200 µl phenol/chloroform/isoamylalcohol (25:24:1) were added. After addition of ~0.3 g acid washed glass beads and vortexing for 2 min, the samples were centrifuged at 13.000 rpm for 5 min. 200 µl of the upper phase were transferred to a new tube and mixed with 20 µl 3 M NaOAc pH 5.5 and 440 µl 95% ethanol by vortexing. DNA was pelleted at 13.000 rpm for 20 min, washed with 200 µl 70% ethanol, dried, and resuspended in TE.

5.8.7 Liquid β-galactosidase assay

3 independent colonies for each clone were inoculated into 1.5 ml selective medium and grown at 30°C overnight. 3 ml medium were inoculated with the overnight culture to give an OD_{600} of 0.1 and grown for ~5 h to give an OD of 0.5 – 0.8. 1.5 ml were pelleted at 13.000 rpm for 1 min, washed with 1 ml Z-buffer, and resuspended in 300 µl Z-buffer. OD was measured again to correct for losses. 100 µl were transferred to a new tube, frozen in liquid nitrogen and thawed at 37°C. The procedure was repeated three times. 700 µl of Z-buffer with β-mercaptoethanol and 160 µl freshly prepared ONPG in Z-buffer (4 mg/ml) were added, mixed by inversion, and incubated at 30°C for 30 min (5 min for positive control). The reaction was stopped by addition of 400 µl 1 M Na_2CO_3. Cell debris was removed by centrifugation at 13.000 rpm for 10 min and OD_{420} was measured. β-galactosidase activity was calculated according to the following formula:

$$1000 \times OD_{420}/(t \times V \times OD_{600} \times \text{concentration factor})$$

Time is given in min, volume in ml.

6 Table of Figures

TABLE OF FIGURES

7 Abbreviations

A, Ala	alanine
ADP/ATP	adenosine diphosphate/adenosine triphosphate
AnkRep	ankyrin repeat
Bp	base pairs
C, Cys	cysteine
cAMP	cyclo-adenosine monophosphate
cDNA	complementary DNA
C. e.	*Caenorhabditis elegans*
Ci	Curie
CoA	coenzyme A
D, Asp	aspartate
Da	dalton
DAPI	4′,6-diamidino-2-phenylindol
DNA	deoxyribonucleic acid
D. m.	*Drosophila melanogaster*
DMSO	dimethylsulfoxide
DTT	dithiothreitol
E. coli	*Escherichia coli*
EDTA	ethylendiaminetetraacetic acid
ELISA	enzyme-linked immunosorbent assay
ER	endoplasmatic reticulum
F, Phe	phenylalanine
FPP	farnesylpyrophosphate
FT	farnesyltransferase
G, Gly	glycine
GFP	green fluorescent protein
GGPP	geranylgeranylpyrophosphate
GGT	geranlgeranyltransferase
GPCR	G protein coupled receptor
GPI	glycosylphosphatidylinositol
GST	glutathione-S-transferase
GTP	guanosine triphosphate
H, His	histidine
HA	hemagglutinin
HAT	histone acetyltransferase
HDAC	histone deacetylase
HeLa	Henrietta Lacks
HIV	human immunodeficiency virus

H. s.	*Homo sapiens*
I, Ile	isoleucine
IPTG	isopropyl-β-D-thiogalactopyranoside
K, Lys	lysine
L, Leu	leucine
M, Met	methionine
MAF	membrane attachment factor
M. m.	*Mus musculus*
mRNA	messenger RNA
N, Asn	asparagine
NLS	nuclear localization sequence
NMT	N-myristoyltransferase
OD	optical density
PAT	palmitoyl acyltransferase
PBR	polybasic region
PBS	phosphate-buffered saline
PCR	polymerase chain reaction
Pfu	*Pyrococcus furiosus*
PTM	posttranslational modification
Q, Gln	glutamine
R, Arg	arginine
RNA	ribonucleic acid
RNAi	RNA interference
RT	room temperature
S, Ser	serine
S. c.	*Saccharomyces cerevisiae*
SDS	sodium dodecylsulfate
SDS-PAGE	sodium dodecylsulfate polyacrylamide gel electrophoresis
SNP	single nucleotide polymorphism
T, Thr	threonine
Taq	*Thermophilus aquaticus*
TLC	thin layer chromatography
TNT	transcription and translation
Tris	tris(hydroxymethyl)aminomethane
V, Val	valine
W, Trp	tryptophane
X-Gal	5-bromo-4-chloro-3-indolyl-β-D-galactoside
Y, Tyr	tyrosine

8 Curriculum vitae

23. 08. 1981	Born in Vienna
1987 –1991	Elementary school, VS St. Elisabeth, 1020 Vienna
1991 – 1999	Grammar school, 1100 Vienna, BRG Laaerbergstraße
06/1999	Graduation from high school („Fachbereichsarbeit" in chemistry)
10/1999 – 05/2000	Military service
10/2000 – 09/2003	Studies of Chemistry, University of Vienna, introductory part
10/2003 – 03/2005	specialization part, focus on biochemistry and analytical chemistry
04/2005 – 03/2006	Diploma thesis at the department of biochemistry of the university of Vienna in cooperation with the research institute of molecular pathology (IMP), Vienna
04/2006 – 03/2009	PhD thesis at the research institute of molecular pathology (IMP) and Max F. Perutz Laboratories (MFPL), Vienna

9 Publications

Benetka W., Koranda M., Maurer-Stroh S., Pittner F., Eisenhaber F.: **Farnesylation or Geranylgeranylation? Efficient assays for Testing Protein Prenylation in vitro and in vivo.** BMC Biochem. 2006 Feb 28; 7: 6.

Maurer-Stroh S., Koranda M., Benetka W., Schneider G., Sirota F.L., Eisenhaber F.: **Towards complete sets of farnesylated and geranylgeranylated proteins.** PLoS Comput Biol. 2007 Apr 6; 3(4): e66.

Benetka W., Koranda M., Eisenhaber F.: **Protein Prenylation: An (Almost) Comprehensive Overview on Discovery History, Enzymology, and Significance in Physiology and Disease.** Monatshefte für Chemie, 2006 Sep 30; 137: 1241.

Benetka W., Mehlmer N., Maurer-Stroh S., Sammer M., Koranda M., Neumüller R., Betschiger J., Knoblich J.A., Teige M., Eisenhaber F.: **Experimental testing of predicted myristoylation targets involved in asymmetric cell division and calcium-dependent signaling.** Cell Cycle. 2008 Dec 13; 7(23): Epub ahead of print.

Eisenhaber B., Sammer M., Benetka W., Uddin M.S., Lee H.K., Eisenhaber F., Koranda M.: **Regulated mobilization for nuclear import of a lipid-modified transcription factor: The case of NFAT5a.** In preparation

10 Bibliography

1. Benetka,W., Koranda,M. & Eisenhaber,F. Protein Prenylation: An (Almost) Comprehensive Overview on Discovery History, Enzymology, and Significance in Physiology and Disease. *Monatshefte für Chemie/Chemical Monthly* **137**, 1241-1281 (2006).

2. Aitken,A. *et al.* Identification of the NH2-terminal blocking group of calcineurin B as myristic acid. *FEBS Lett.* **150**, 314-318 (1982).

3. Carr,S.A., Biemann,K., Shoji,S., Parmelee,D.C. & Titani,K. n-Tetradecanoyl is the NH2-terminal blocking group of the catalytic subunit of cyclic AMP-dependent protein kinase from bovine cardiac muscle. *Proc. Natl. Acad. Sci. U. S. A* **79**, 6128-6131 (1982).

4. Kamps,M.P., Buss,J.E. & Sefton,B.M. Mutation of NH2-terminal glycine of p60src prevents both myristoylation and morphological transformation. *Proc. Natl. Acad. Sci. U. S. A* **82**, 4625-4628 (1985).

5. Towler,D.A., Eubanks,S.R., Towery,D.S., Adams,S.P. & Glaser,L. Amino-terminal processing of proteins by N-myristoylation. Substrate specificity of N-myristoyl transferase. *J. Biol. Chem.* **262**, 1030-1036 (1987).

6. Olson,E.N., Towler,D.A. & Glaser,L. Specificity of fatty acid acylation of cellular proteins. *J. Biol. Chem.* **260**, 3784-3790 (1985).

7. Towler,D. & Glaser,L. Protein fatty acid acylation: enzymatic synthesis of an N-myristoylglycyl peptide. *Proc. Natl. Acad. Sci. U. S. A* **83**, 2812-2816 (1986).

8. Magee,A.I. & Courtneidge,S.A. Two classes of fatty acid acylated proteins exist in eukaryotic cells. *EMBO J.* **4**, 1137-1144 (1985).

9. Wilcox,C., Hu,J.S. & Olson,E.N. Acylation of proteins with myristic acid occurs cotranslationally. *Science* **238**, 1275-1278 (1987).

10. McIlhinney,R.A., Pelly,S.J., Chadwick,J.K. & Cowley,G.P. Studies on the attachment of myristic and palmitic acid to cell proteins in human squamous carcinoma cell lines: evidence for two pathways. *EMBO J.* **4**, 1145-1152 (1985).

11. da Silva,A.M. & Klein,C. A rapid posttranslational myristylation of a 68-kD protein in D. discoideum. *J. Cell Biol.* **111**, 401-407 (1990).

12. Zha,J., Weiler,S., Oh,K.J., Wei,M.C. & Korsmeyer,S.J. Posttranslational N-myristoylation of BID as a molecular switch for targeting mitochondria and apoptosis. *Science* **290**, 1761-1765 (2000).

13. Utsumi,T., Sakurai,N., Nakano,K. & Ishisaka,R. C-terminal 15 kDa fragment of cytoskeletal actin is posttranslationally N-myristoylated upon caspase-mediated cleavage and targeted to mitochondria. *FEBS Lett.* **539**, 37-44 (2003).

14. Sakurai,N. & Utsumi,T. Posttranslational N-myristoylation is required for the anti-apoptotic activity of human tGelsolin, the C-terminal caspase cleavage product of human gelsolin. *J. Biol. Chem.* **281**, 14288-14295 (2006).

15. Vilas,G.L. *et al.* Posttranslational myristoylation of caspase-activated p21-activated protein kinase 2 (PAK2) potentiates late apoptotic events. *Proc. Natl. Acad. Sci. U. S. A* **103**, 6542-6547 (2006).

16. Manenti,S., Sorokine,O., Van Dorsselaer,A. & Taniguchi,H. Demyristoylation of the major substrate of protein kinase C (MARCKS) by the cytoplasmic fraction of brain synaptosomes. *J. Biol. Chem.* **269**, 8309-8313 (1994).

17. Farazi,T.A., Waksman,G. & Gordon,J.I. The biology and enzymology of protein N-myristoylation. *J. Biol. Chem.* **276**, 39501-39504 (2001).

18. Peitzsch,R.M. & McLaughlin,S. Binding of acylated peptides and fatty acids to phospholipid vesicles: pertinence to myristoylated proteins. *Biochemistry* **32**, 10436-10443 (1993).

19. Dunphy,J.T. & Linder,M.E. Signalling functions of protein palmitoylation. *Biochim. Biophys. Acta* **1436**, 245-261 (1998).

20. Dunphy,J.T., Greentree,W.K., Manahan,C.L. & Linder,M.E. G-protein palmitoyltransferase activity is enriched in plasma membranes. *J. Biol. Chem.* **271**, 7154-7159 (1996).

21. Murray,D., Ben Tal,N., Honig,B. & McLaughlin,S. Electrostatic interaction of myristoylated proteins with membranes: simple physics, complicated biology. *Structure.* **5**, 985-989 (1997).

22. Murray,D. *et al.* Electrostatics and the membrane association of Src: theory and experiment. *Biochemistry* **37**, 2145-2159 (1998).

23. Resh,M.D. Fatty acylation of proteins: new insights into membrane targeting of myristoylated and palmitoylated proteins. *Biochim. Biophys. Acta* **1451**, 1-16 (1999).

24. Ames,J.B. *et al.* Molecular mechanics of calcium-myristoyl switches. *Nature* **389**, 198-202 (1997).

25. Goldberg,J. Structural basis for activation of ARF GTPase: mechanisms of guanine nucleotide exchange and GTP-myristoyl switching. *Cell* **95**, 237-248 (1998).

26. Zhou,W. & Resh,M.D. Differential membrane binding of the human immunodeficiency virus type 1 matrix protein. *J. Virol.* **70**, 8540-8548 (1996).

27. Hermida-Matsumoto,L. & Resh,M.D. Human immunodeficiency virus type 1 protease triggers a myristoyl switch that modulates membrane binding of Pr55(gag) and p17MA. *J. Virol.* **73**, 1902-1908 (1999).

28. Liemann,S., Chandran,K., Baker,T.S., Nibert,M.L. & Harrison,S.C. Structure of the reovirus membrane-penetration protein, Mu1, in a complex with is protector protein, Sigma3. *Cell* **108**, 283-295 (2002).

29. Seykora,J.T., Myat,M.M., Allen,L.A., Ravetch,J.V. & Aderem,A. Molecular determinants of the myristoyl-electrostatic switch of MARCKS. *J. Biol. Chem.* **271**, 18797-18802 (1996).

30. McLaughlin,S. & Aderem,A. The myristoyl-electrostatic switch: a modulator of reversible protein-membrane interactions. *Trends Biochem. Sci.* **20**, 272-276 (1995).

31. Hanakam,F., Gerisch,G., Lotz,S., Alt,T. & Seelig,A. Binding of hisactophilin I and II to lipid membranes is controlled by a pH-dependent myristoyl-histidine switch. *Biochemistry* **35**, 11036-11044 (1996).

32. McCabe,J.B. & Berthiaume,L.G. Functional roles for fatty acylated amino-terminal domains in subcellular localization. *Mol. Biol. Cell* **10**, 3771-3786 (1999).

33. Denny,P.W., Gokool,S., Russell,D.G., Field,M.C. & Smith,D.F. Acylation-dependent protein export in Leishmania. *J. Biol. Chem.* **275**, 11017-11025 (2000).

34. Shahinian,S. & Silvius,J.R. Doubly-lipid-modified protein sequence motifs exhibit long-lived anchorage to lipid bilayer membranes. *Biochemistry* **34**, 3813-3822 (1995).

35. Schroeder,H., Leventis,R., Shahinian,S., Walton,P.A. & Silvius,J.R. Lipid-modified, cysteinyl-containing peptides of diverse structures are efficiently S-acylated at the plasma membrane of mammalian cells. *J. Cell Biol.* **134**, 647-660 (1996).

36. van't Hof,W. & Resh,M.D. Rapid plasma membrane anchoring of newly synthesized p59fyn: selective requirement for NH2-terminal myristoylation and palmitoylation at cysteine-3. *J. Cell Biol.* **136**, 1023-1035 (1997).

37. Brown,D.A. & London,E. Functions of lipid rafts in biological membranes. *Annu. Rev. Cell Dev. Biol.* **14**, 111-136 (1998).

38. Zacharias,D.A., Violin,J.D., Newton,A.C. & Tsien,R.Y. Partitioning of lipid-modified monomeric GFPs into membrane microdomains of live cells. *Science* **296**, 913-916 (2002).

39. Melkonian,K.A., Ostermeyer,A.G., Chen,J.Z., Roth,M.G. & Brown,D.A. Role of lipid modifications in targeting proteins to detergent-resistant membrane rafts. Many raft proteins are acylated, while few are prenylated. *J. Biol. Chem.* **274**, 3910-3917 (1999).

40. McCabe,J.B. & Berthiaume,L.G. N-terminal protein acylation confers localization to cholesterol, sphingolipid-enriched membranes but not to lipid rafts/caveolae. *Mol. Biol. Cell* **12**, 3601-3617 (2001).

41. Escriba,P.V., Wedegaertner,P.B., Goni,F.M. & Vogler,O. Lipid-protein interactions in GPCR-associated signaling. *Biochim. Biophys. Acta* **1768**, 836-852 (2007).

42. Chen,C.A. & Manning,D.R. Regulation of G proteins by covalent modification. *Oncogene* **20**, 1643-1652 (2001).

43. Wedegaertner,P.B. Lipid modifications and membrane targeting of G alpha. *Biol. Signals Recept.* **7**, 125-135 (1998).

44. Vogler,O. *et al.* The Gbetagamma dimer drives the interaction of heterotrimeric Gi proteins with nonlamellar membrane structures. *J. Biol. Chem.* **279**, 36540-36545 (2004).

45. van der Wel,P.C. *et al.* Tryptophan-anchored transmembrane peptides promote formation of nonlamellar phases in phosphatidylethanolamine model membranes in a mismatch-dependent manner. *Biochemistry* **39**, 3124-3133 (2000).

46. Funari,S.S., Prades,J., Escriba,P.V. & Barcelo,F. Farnesol and geranylgeraniol modulate the structural properties of phosphatidylethanolamine model membranes. *Mol. Membr. Biol.* **22**, 303-311 (2005).

47. Oh,P. & Schnitzer,J.E. Segregation of heterotrimeric G proteins in cell surface microdomains. G(q) binds caveolin to concentrate in caveolae, whereas G(i) and G(s) target lipid rafts by default. *Mol. Biol. Cell* **12**, 685-698 (2001).

48. Matsubara,M., Titani,K., Taniguchi,H. & Hayashi,N. Direct involvement of protein myristoylation in myristoylated alanine-rich C kinase substrate (MARCKS)-calmodulin interaction. *J. Biol. Chem.* **278**, 48898-48902 (2003).

49. Hayashi,N., Izumi,Y., Titani,K. & Matsushima,N. The binding of myristoylated N-terminal nonapeptide from neuro-specific protein CAP-23/NAP-22 to calmodulin does not induce the globular structure observed for the calmodulin-nonmyristylated peptide complex. *Protein Sci.* **9**, 1905-1913 (2000).

50. Hayashi,N. *et al.* Nef of HIV-1 interacts directly with calcium-bound calmodulin. *Protein Sci.* **11**, 529-537 (2002).

51. Kennedy,M.T., Brockman,H. & Rusnak,F. Contributions of myristoylation to calcineurin structure/function. *J. Biol. Chem.* **271**, 26517-26521 (1996).

52. Andriotis,V.M. & Rathjen,J.P. The Pto kinase of tomato, which regulates plant immunity, is repressed by its myristoylated N terminus. *J. Biol. Chem.* **281**, 26578-26586 (2006).

53. Nagar,B. *et al.* Structural basis for the autoinhibition of c-Abl tyrosine kinase. *Cell* **112**, 859-871 (2003).

54. Hantschel,O. *et al.* A myristoyl/phosphotyrosine switch regulates c-Abl. *Cell* **112**, 845-857 (2003).

55. Preininger,A.M., Parello,J., Meier,S.M., Liao,G. & Hamm,H.E. Receptor-Mediated Changes at the Myristoylated Amino Terminus of Galphail Proteins. *Biochemistry* (2008).

56. Preininger,A.M. *et al.* The myristoylated amino terminus of Galpha(i)(1) plays a critical role in the structure and function of Galpha(i)(1) subunits in solution. *Biochemistry* **42**, 7931-7941 (2003).

57. Webb,Y., Hermida-Matsumoto,L. & Resh,M.D. Inhibition of protein palmitoylation, raft localization, and T cell signaling by 2-bromopalmitate and polyunsaturated fatty acids. *J. Biol. Chem.* **275**, 261-270 (2000).

58. Bolen,J.B., Veillette,A., Schwartz,A.M., DeSeau,V. & Rosen,N. Activation of pp60c-src protein kinase activity in human colon carcinoma. *Proc. Natl. Acad. Sci. U. S. A* **84**, 2251-2255 (1987).

59. Park,J., Meisler,A.I. & Cartwright,C.A. c-Yes tyrosine kinase activity in human colon carcinoma. *Oncogene* **8**, 2627-2635 (1993).

60. Magnuson,B.A., Raju,R.V., Moyana,T.N. & Sharma,R.K. Increased N-myristoyltransferase activity observed in rat and human colonic tumors. *J. Natl. Cancer Inst.* **87**, 1630-1635 (1995).

61. Raju,R.V., Moyana,T.N. & Sharma,R.K. N-Myristoyltransferase overexpression in human colorectal adenocarcinomas. *Exp. Cell Res.* **235**, 145-154 (1997).

62. Selvakumar,P., Pasha,M.K., Ashakumary,L., Dimmock,J.R. & Sharma,R.K. Myristoyl-CoA:protein N-myristoyltransferase: a novel molecular approach for cancer therapy (Review). *Int. J. Mol. Med.* **10**, 493-500 (2002).

63. Selvakumar,P. *et al.* Potential role of N-myristoyltransferase in cancer. *Prog. Lipid Res.* **46**, 1-36 (2007).

64. Batistic,O., Sorek,N., Schultke,S., Yalovsky,S. & Kudla,J. Dual fatty acyl modification determines the localization and plasma membrane targeting of CBL/CIPK Ca2+ signaling complexes in Arabidopsis. *Plant Cell* **20**, 1346-1362 (2008).

65. Lakshmikuttyamma,A., Selvakumar,P., Tuchek,J. & Sharma,R.K. Myristoyltransferase and calcineurin: novel molecular therapeutic target for epilepsy. *Prog. Neurobiol.* **84**, 77-84 (2008).

66. Weinberg,R.A. *et al.* Genetic studies reveal that myristoylCoA:protein N-myristoyltransferase is an essential enzyme in Candida albicans. *Mol. Microbiol.* **16**, 241-250 (1995).

67. Lodge,J.K., Jackson-Machelski,E., Toffaletti,D.L., Perfect,J.R. & Gordon,J.I. Targeted gene replacement demonstrates that myristoyl-CoA: protein N-myristoyltransferase is essential for viability of Cryptococcus neoformans. *Proc. Natl. Acad. Sci. U. S. A* **91**, 12008-12012 (1994).

68. Price,H.P. *et al.* Myristoyl-CoA:protein N-myristoyltransferase, an essential enzyme and potential drug target in kinetoplastid parasites. *J. Biol. Chem.* **278**, 7206-7214 (2003).

69. Panethymitaki,C. *et al.* Characterization and selective inhibition of myristoyl-CoA:protein N-myristoyltransferase from Trypanosoma brucei and Leishmania major. *Biochem. J.* **396**, 277-285 (2006).

70. Lodge,J.K. *et al.* Genetic and biochemical studies establish that the fungicidal effect of a fully depeptidized inhibitor of Cryptococcus neoformans myristoyl-CoA:protein N-myristoyltransferase (Nmt) is Nmt-dependent. *J. Biol. Chem.* **273**, 12482-12491 (1998).

71. Devadas,B. *et al.* Novel biologically active nonpeptidic inhibitors of myristoylCoA:protein N-myristoyltransferase. *J. Med. Chem.* **41**, 996-1000 (1998).

72. Sikorski,J.A. *et al.* Selective peptidic and peptidomimetic inhibitors of Candida albicans myristoylCoA: protein N-myristoyltransferase: a new approach to antifungal therapy. *Biopolymers* **43**, 43-71 (1997).

73. Lodge,J.K. *et al.* N-myristoylation of Arf proteins in Candida albicans: an in vivo assay for evaluating antifungal inhibitors of myristoyl-CoA: protein N-myristoyltransferase. *Microbiology* **143 (Pt 2)**, 357-366 (1997).

74. Masubuchi,M. *et al.* Design and synthesis of novel benzofurans as a new class of antifungal agents targeting fungal N-myristoyltransferase. Part 1. *Bioorg. Med. Chem. Lett.* **11**, 1833-1837 (2001).

75. Kawasaki,K. *et al.* Design and synthesis of novel benzofurans as a new class of antifungal agents targeting fungal N-myristoyltransferase. Part 3. *Bioorg. Med. Chem. Lett.* **13**, 87-91 (2003).

76. Maurer-Stroh,S., Eisenhaber,B. & Eisenhaber,F. N-terminal N-myristoylation of proteins: refinement of the sequence motif and its taxon-specific differences. *J. Mol. Biol.* **317**, 523-540 (2002).

77. Maurer-Stroh,S. & Eisenhaber,F. Myristoylation of viral and bacterial proteins. *Trends Microbiol.* **12**, 178-185 (2004).

78. Bruss,V., Hagelstein,J., Gerhardt,E. & Galle,P.R. Myristylation of the large surface protein is required for hepatitis B virus in vitro infectivity. *Virology* **218**, 396-399 (1996).

79. Chen,B., Lian,M., Xu,S., Luo,M. & Zheng,X. A chemical lipid modification of recombinant preS antigen to study the mechanism of HBV attachment to the host cell. *J. Biotechnol.* (2008).

80. Hogle,J.M. Poliovirus cell entry: common structural themes in viral cell entry pathways. *Annu. Rev. Microbiol.* **56**, 677-702 (2002).

81. Chen,X.S., Stehle,T. & Harrison,S.C. Interaction of polyomavirus internal protein VP2 with the major capsid protein VP1 and implications for participation of VP2 in viral entry. *EMBO J.* **17**, 3233-3240 (1998).

82. Moscufo,N., Simons,J. & Chow,M. Myristoylation is important at multiple stages in poliovirus assembly. *J. Virol.* **65**, 2372-2380 (1991).

83. Henderson,L.E., Krutzsch,H.C. & Oroszlan,S. Myristyl amino-terminal acylation of murine retrovirus proteins: an unusual post-translational proteins modification. *Proc. Natl. Acad. Sci. U. S. A* **80**, 339-343 (1983).

84. Rein,A., McClure,M.R., Rice,N.R., Luftig,R.B. & Schultz,A.M. Myristylation site in Pr65gag is essential for virus particle formation by Moloney murine leukemia virus. *Proc. Natl. Acad. Sci. U. S. A* **83**, 7246-7250 (1986).

85. Schultz,A. & Oroszlan,S. Myristylation of gag-onc fusion proteins in mammalian transforming retroviruses. *Virology* **133**, 431-437 (1984).

86. Lindwasser,O.W. & Resh,M.D. Multimerization of human immunodeficiency virus type 1 Gag promotes its localization to barges, raft-like membrane microdomains. *J. Virol.* **75**, 7913-7924 (2001).

87. Ravanello,M.P. & Hruby,D.E. Characterization of the vaccinia virus L1R myristylprotein as a component of the intracellular virion envelope. *J. Gen. Virol.* **75 (Pt 6)**, 1479-1483 (1994).

88. Schultz,A.M., Henderson,L.E., Oroszlan,S., Garber,E.A. & Hanafusa,H. Amino terminal myristylation of the protein kinase p60src, a retroviral transforming protein. *Science* **227**, 427-429 (1985).

89. Greenway,A.L. *et al.* HIV-1 Nef control of cell signalling molecules: multiple strategies to promote virus replication. *J. Biosci.* **28**, 323-335 (2003).

90. Nimchuk,Z. *et al.* Eukaryotic fatty acylation drives plasma membrane targeting and enhances function of several type III effector proteins from Pseudomonas syringae. *Cell* **101**, 353-363 (2000).

91. Takamune,N., Hamada,H., Misumi,S. & Shoji,S. Novel strategy for anti-HIV-1 action: selective cytotoxic effect of N-myristoyltransferase inhibitor on HIV-1-infected cells. *FEBS Lett.* **527**, 138-142 (2002).

92. Glover,C.J., Hartman,K.D. & Felsted,R.L. Human N-myristoyltransferase amino-terminal domain involved in targeting the enzyme to the ribosomal subcellular fraction. *J. Biol. Chem.* **272**, 28680-28689 (1997).

93. Duronio,R.J., Towler,D.A., Heuckeroth,R.O. & Gordon,J.I. Disruption of the yeast N-myristoyl transferase gene causes recessive lethality. *Science* **243**, 796-800 (1989).

94. Towler,D.A. *et al.* Purification and characterization of yeast myristoyl CoA:protein N-myristoyltransferase. *Proc. Natl. Acad. Sci. U. S. A* **84**, 2708-2712 (1987).

95. Bhatnagar,R.S. *et al.* Structure of N-myristoyltransferase with bound myristoylCoA and peptide substrate analogs. *Nat. Struct. Biol.* **5**, 1091-1097 (1998).

96. Rudnick,D.A. *et al.* Kinetic and structural evidence for a sequential ordered Bi Bi mechanism of catalysis by Saccharomyces cerevisiae myristoyl-CoA:protein N-myristoyltransferase. *J. Biol. Chem.* **266**, 9732-9739 (1991).

97. Rudnick,D.A. *et al.* Use of photoactivatable peptide substrates of Saccharomyces cerevisiae myristoyl-CoA:protein N-myristoyltransferase (Nmt1p) to characterize a myristoyl-CoA-Nmt1p-peptide ternary complex and to provide evidence for an ordered reaction mechanism. *Proc. Natl. Acad. Sci. U. S. A* **90**, 1087-1091 (1993).

98. Farazi,T.A., Waksman,G. & Gordon,J.I. Structures of Saccharomyces cerevisiae N-myristoyltransferase with bound myristoylCoA and peptide provide insights about substrate recognition and catalysis. *Biochemistry* **40**, 6335-6343 (2001).

99. Fierke,C.A. & Jencks,W.P. Two functional domains of coenzyme A activate catalysis by coenzyme A transferase. Pantetheine and adenosine 3'-phosphate 5'-diphosphate. *J. Biol. Chem.* **261**, 7603-7606 (1986).

100. Bhatnagar,R.S., Jackson-Machelski,E., McWherter,C.A. & Gordon,J.I. Isothermal titration calorimetric studies of Saccharomyces cerevisiae myristoyl-CoA:protein N-myristoyltransferase. Determinants of binding energy and catalytic discrimination among acyl-CoA and peptide ligands. *J. Biol. Chem.* **269**, 11045-11053 (1994).

101. Wu,J. *et al.* Crystal structures of Saccharomyces cerevisiae N-myristoyltransferase with bound myristoyl-CoA and inhibitors reveal the functional roles of the N-terminal region. *J. Biol. Chem.* **282**, 22185-22194 (2007).

102. Rudnick,D.A. *et al.* Analogs of palmitoyl-CoA that are substrates for myristoyl-CoA:protein N-myristoyltransferase. *Proc. Natl. Acad. Sci. U. S. A* **89**, 10507-10511 (1992).

103. Rudnick,D.A., Johnson,R.L. & Gordon,J.I. Studies of the catalytic activities and substrate specificities of Saccharomyces cerevisiae myristoyl-coenzyme A: protein N-myristoyltransferase deletion mutants and human/yeast Nmt chimeras in Escherichia coli and S. cerevisiae. *J. Biol. Chem.* **267**, 23852-23861 (1992).

104. Farazi,T.A., Manchester,J.K. & Gordon,J.I. Transient-state kinetic analysis of Saccharomyces cerevisiae myristoylCoA:protein N-myristoyltransferase reveals that a step after chemical transformation is rate limiting. *Biochemistry* **39**, 15807-15816 (2000).

105. Rocque,W.J., McWherter,C.A., Wood,D.C. & Gordon,J.I. A comparative analysis of the kinetic mechanism and peptide substrate specificity of human and Saccharomyces cerevisiae myristoyl-CoA:protein N-myristoyltransferase. *J. Biol. Chem.* **268**, 9964-9971 (1993).

106. Kishore,N.S. *et al.* Comparison of the acyl chain specificities of human myristoyl-CoA synthetase and human myristoyl-CoA:protein N-myristoyltransferase. *J. Biol. Chem.* **268**, 4889-4902 (1993).

107. Eisenhaber,B. & Eisenhaber,F. Posttranslational modifications and subcellular localization signals: indicators of sequence regions without inherent 3D structure? *Curr. Protein Pept. Sci.* **8**, 197-203 (2007).

108. Eisenhaber,B., Eisenhaber,F., Maurer-Stroh,S. & Neuberger,G. Prediction of sequence signals for lipid post-translational modifications: insights from case studies. *Proteomics.* **4**, 1614-1625 (2004).

109. Maurer-Stroh,S., Eisenhaber,B. & Eisenhaber,F. N-terminal N-myristoylation of proteins: prediction of substrate proteins from amino acid sequence. *J. Mol. Biol.* **317**, 541-557 (2002).

110. Maurer-Stroh,S. *et al.* MYRbase: analysis of genome-wide glycine myristoylation enlarges the functional spectrum of eukaryotic myristoylated proteins. *Genome Biol.* **5**, R21 (2004).

111. Pavlopoulos,E. *et al.* neuralized Encodes a peripheral membrane protein involved in delta signaling and endocytosis. *Dev. Cell* **1**, 807-816 (2001).

112. Takimoto,K., Yang,E.K. & Conforti,L. Palmitoylation of KChIP splicing variants is required for efficient cell surface expression of Kv4.3 channels. *J. Biol. Chem.* **277**, 26904-26911 (2002).

113. Ueda,T., Yamaguchi,M., Uchimiya,H. & Nakano,A. Ara6, a plant-unique novel type Rab GTPase, functions in the endocytic pathway of Arabidopsis thaliana. *EMBO J.* **20**, 4730-4741 (2001).

114. Gonzalez,E., Kou,R., Lin,A.J., Golan,D.E. & Michel,T. Subcellular targeting and agonist-induced site-specific phosphorylation of endothelial nitric-oxide synthase. *J. Biol. Chem.* **277**, 39554-39560 (2002).

115. Furuya,T., Kashuba,C., Docampo,R. & Moreno,S.N. A novel phosphatidylinositol-phospholipase C of Trypanosoma cruzi that is lipid modified and activated during trypomastigote to amastigote differentiation. *J. Biol. Chem.* **275**, 6428-6438 (2000).

116. Peterson,C.L. & Laniel,M.A. Histones and histone modifications. *Curr. Biol.* **14**, R546-R551 (2004).

117. Kornberg,R.D. Structure of chromatin. *Annu. Rev. Biochem.* **46**, 931-954 (1977).

118. McGhee,J.D. & Felsenfeld,G. Nucleosome structure. *Annu. Rev. Biochem.* **49**, 1115-1156 (1980).

119. Horn,P.J. & Peterson,C.L. Molecular biology. Chromatin higher order folding--wrapping up transcription. *Science* **297**, 1824-1827 (2002).

120. Hansen,J.C. Conformational dynamics of the chromatin fiber in solution: determinants, mechanisms, and functions. *Annu. Rev. Biophys. Biomol. Struct.* **31**, 361-392 (2002).

121. Luger,K., Mader,A.W., Richmond,R.K., Sargent,D.F. & Richmond,T.J. Crystal structure of the nucleosome core particle at 2.8 A resolution. *Nature* **389**, 251-260 (1997).

122. Yang,Z., Zheng,C. & Hayes,J.J. The core histone tail domains contribute to sequence-dependent nucleosome positioning. *J. Biol. Chem.* **282**, 7930-7938 (2007).

123. Tse,C. & Hansen,J.C. Hybrid trypsinized nucleosomal arrays: identification of multiple functional roles of the H2A/H2B and H3/H4 N-termini in chromatin fiber compaction. *Biochemistry* **36**, 11381-11388 (1997).

124. Schwarz,P.M., Felthauser,A., Fletcher,T.M. & Hansen,J.C. Reversible oligonucleosome self-association: dependence on divalent cations and core histone tail domains. *Biochemistry* **35**, 4009-4015 (1996).

125. Parseghian,M.H. & Hamkalo,B.A. A compendium of the histone H1 family of somatic subtypes: an elusive cast of characters and their characteristics. *Biochem. Cell Biol.* **79**, 289-304 (2001).

126. Ramakrishnan,V. Histone H1 and chromatin higher-order structure. *Crit Rev. Eukaryot. Gene Expr.* **7**, 215-230 (1997).

127. Belmont,A.S., Sedat,J.W. & Agard,D.A. A three-dimensional approach to mitotic chromosome structure: evidence for a complex hierarchical organization. *J. Cell Biol.* **105**, 77-92 (1987).

128. Belmont,A.S. & Bruce,K. Visualization of G1 chromosomes: a folded, twisted, supercoiled chromonema model of interphase chromatid structure. *J. Cell Biol.* **127**, 287-302 (1994).

129. Tumbar,T., Sudlow,G. & Belmont,A.S. Large-scale chromatin unfolding and remodeling induced by VP16 acidic activation domain. *J. Cell Biol.* **145**, 1341-1354 (1999).

130. Muller,W.G., Walker,D., Hager,G.L. & McNally,J.G. Large-scale chromatin decondensation and recondensation regulated by transcription from a natural promoter. *J. Cell Biol.* **154**, 33-48 (2001).

131. Clarkson,M.J., Wells,J.R., Gibson,F., Saint,R. & Tremethick,D.J. Regions of variant histone His2AvD required for Drosophila development. *Nature* **399**, 694-697 (1999).

132. Dhillon,N. & Kamakaka,R.T. A histone variant, Htz1p, and a Sir1p-like protein, Esc2p, mediate silencing at HMR. *Mol. Cell* **6**, 769-780 (2000).

133. Adam,M., Robert,F., Larochelle,M. & Gaudreau,L. H2A.Z is required for global chromatin integrity and for recruitment of RNA polymerase II under specific conditions. *Mol. Cell Biol.* **21**, 6270-6279 (2001).

134. Fan,J.Y., Gordon,F., Luger,K., Hansen,J.C. & Tremethick,D.J. The essential histone variant H2A.Z regulates the equilibrium between different chromatin conformational states. *Nat. Struct. Biol.* **9**, 172-176 (2002).

135. Bustin,M. Chromatin unfolding and activation by HMGN(*) chromosomal proteins. *Trends Biochem. Sci.* **26**, 431-437 (2001).

136. Peterson,C.L. & Workman,J.L. Promoter targeting and chromatin remodeling by the SWI/SNF complex. *Curr. Opin. Genet. Dev.* **10**, 187-192 (2000).

137. Berger,S.L. Histone modifications in transcriptional regulation. *Curr. Opin. Genet. Dev.* **12**, 142-148 (2002).

138. Braunstein,M., Sobel,R.E., Allis,C.D., Turner,B.M. & Broach,J.R. Efficient transcriptional silencing in Saccharomyces cerevisiae requires a heterochromatin histone acetylation pattern. *Mol. Cell Biol.* **16**, 4349-4356 (1996).

139. Cheung,P., Allis,C.D. & Sassone-Corsi,P. Signaling to chromatin through histone modifications. *Cell* **103**, 263-271 (2000).

140. Strahl,B.D. & Allis,C.D. The language of covalent histone modifications. *Nature* **403**, 41-45 (2000).

141. Sims,R.J., III, Nishioka,K. & Reinberg,D. Histone lysine methylation: a signature for chromatin function. *Trends Genet.* **19**, 629-639 (2003).

142. Shi,Y. *et al.* Histone demethylation mediated by the nuclear amine oxidase homolog LSD1. *Cell* **119**, 941-953 (2004).

143. Nightingale,K.P., O'Neill,L.P. & Turner,B.M. Histone modifications: signalling receptors and potential elements of a heritable epigenetic code. *Curr. Opin. Genet. Dev.* **16**, 125-136 (2006).

144. Vogelauer,M., Wu,J., Suka,N. & Grunstein,M. Global histone acetylation and deacetylation in yeast. *Nature* **408**, 495-498 (2000).

145. Workman,J.L. & Kingston,R.E. Alteration of nucleosome structure as a mechanism of transcriptional regulation. *Annu. Rev. Biochem.* **67**, 545-579 (1998).

146. Verdone,L., Caserta,M. & Di Mauro,E. Role of histone acetylation in the control of gene expression. *Biochem. Cell Biol.* **83**, 344-353 (2005).

147. Awad,S. & Hassan,A.H. The Swi2/Snf2 bromodomain is important for the full binding and remodeling activity of the SWI/SNF complex on H3- and H4-acetylated nucleosomes. *Ann. N. Y. Acad. Sci.* **1138**, 366-375 (2008).

148. Bannister,A.J. *et al.* Selective recognition of methylated lysine 9 on histone H3 by the HP1 chromo domain. *Nature* **410**, 120-124 (2001).

149. Brehm,A., Tufteland,K.R., Aasland,R. & Becker,P.B. The many colours of chromodomains. *Bioessays* **26**, 133-140 (2004).

150. Couture,J.F. & Trievel,R.C. Histone-modifying enzymes: encrypting an enigmatic epigenetic code. *Curr. Opin. Struct. Biol.* **16**, 753-760 (2006).

151. ALLFREY,V.G., FAULKNER,R. & MIRSKY,A.E. ACETYLATION AND METHYLATION OF HISTONES AND THEIR POSSIBLE ROLE IN THE REGULATION OF RNA SYNTHESIS. *Proc. Natl. Acad. Sci. U. S. A* **51**, 786-794 (1964).

152. Garcia-Ramirez,M., Rocchini,C. & Ausio,J. Modulation of chromatin folding by histone acetylation. *J. Biol. Chem.* **270**, 17923-17928 (1995).

153. Walia,H., Chen,H.Y., Sun,J.M., Holth,L.T. & Davie,J.R. Histone acetylation is required to maintain the unfolded nucleosome structure associated with transcribing DNA. *J. Biol. Chem.* **273**, 14516-14522 (1998).

154. Eberharter,A. & Becker,P.B. Histone acetylation: a switch between repressive and permissive chromatin. Second in review series on chromatin dynamics. *EMBO Rep.* **3**, 224-229 (2002).

155. Zeng,L. & Zhou,M.M. Bromodomain: an acetyl-lysine binding domain. *FEBS Lett.* **513**, 124-128 (2002).

156. Jeanmougin,F., Wurtz,J.M., Le Douarin,B., Chambon,P. & Losson,R. The bromodomain revisited. *Trends Biochem. Sci.* **22**, 151-153 (1997).

157. Yang,X.J. Lysine acetylation and the bromodomain: a new partnership for signaling. *Bioessays* **26**, 1076-1087 (2004).

158. Brownell,J.E. *et al.* Tetrahymena histone acetyltransferase A: a homolog to yeast Gcn5p linking histone acetylation to gene activation. *Cell* **84**, 843-851 (1996).

159. Kuo,M.H. & Allis,C.D. Roles of histone acetyltransferases and deacetylases in gene regulation. *Bioessays* **20**, 615-626 (1998).

160. Marmorstein,R. Structure of histone acetyltransferases. *J. Mol. Biol.* **311**, 433-444 (2001).

161. Vetting,M.W. *et al.* Structure and functions of the GNAT superfamily of acetyltransferases. *Arch. Biochem. Biophys.* **433**, 212-226 (2005).

162. Tanner,K.G. *et al.* Catalytic mechanism and function of invariant glutamic acid 173 from the histone acetyltransferase GCN5 transcriptional coactivator. *J. Biol. Chem.* **274**, 18157-18160 (1999).

163. Lau,O.D. *et al.* p300/CBP-associated factor histone acetyltransferase processing of a peptide substrate. Kinetic analysis of the catalytic mechanism. *J. Biol. Chem.* **275**, 21953-21959 (2000).

164. Tanner,K.G., Langer,M.R., Kim,Y. & Denu,J.M. Kinetic mechanism of the histone acetyltransferase GCN5 from yeast. *J. Biol. Chem.* **275**, 22048-22055 (2000).

165. Yan,Y., Harper,S., Speicher,D.W. & Marmorstein,R. The catalytic mechanism of the ESA1 histone acetyltransferase involves a self-acetylated intermediate. *Nat. Struct. Biol.* **9**, 862-869 (2002).

166. Grant,P.A. *et al.* Yeast Gcn5 functions in two multisubunit complexes to acetylate nucleosomal histones: characterization of an Ada complex and the SAGA (Spt/Ada) complex. *Genes Dev.* **11**, 1640-1650 (1997).

167. Galarneau,L. *et al.* Multiple links between the NuA4 histone acetyltransferase complex and epigenetic control of transcription. *Mol. Cell* **5**, 927-937 (2000).

168. Grant,P.A. *et al.* Expanded lysine acetylation specificity of Gcn5 in native complexes. *J. Biol. Chem.* **274**, 5895-5900 (1999).

169. Balasubramanian,R., Pray-Grant,M.G., Selleck,W., Grant,P.A. & Tan,S. Role of the Ada2 and Ada3 transcriptional coactivators in histone acetylation. *J. Biol. Chem.* **277**, 7989-7995 (2002).

170. Sterner,D.E. *et al.* Functional organization of the yeast SAGA complex: distinct components involved in structural integrity, nucleosome acetylation, and TATA-binding protein interaction. *Mol. Cell Biol.* **19**, 86-98 (1999).

171. Brown,C.E. *et al.* Recruitment of HAT complexes by direct activator interactions with the ATM-related Tra1 subunit. *Science* **292**, 2333-2337 (2001).

172. Gu,W. & Roeder,R.G. Activation of p53 sequence-specific DNA binding by acetylation of the p53 C-terminal domain. *Cell* **90**, 595-606 (1997).

173. Juan,L.J. *et al.* Histone deacetylases specifically down-regulate p53-dependent gene activation. *J. Biol. Chem.* **275**, 20436-20443 (2000).

174. Luo,J., Su,F., Chen,D., Shiloh,A. & Gu,W. Deacetylation of p53 modulates its effect on cell growth and apoptosis. *Nature* **408**, 377-381 (2000).

175. Glozak,M.A., Sengupta,N., Zhang,X. & Seto,E. Acetylation and deacetylation of non-histone proteins. *Gene* **363**, 15-23 (2005).

176. Yao,Y.L., Yang,W.M. & Seto,E. Regulation of transcription factor YY1 by acetylation and deacetylation. *Mol. Cell Biol.* **21**, 5979-5991 (2001).

177. Munshi,N. *et al.* Acetylation of HMG I(Y) by CBP turns off IFN beta expression by disrupting the enhanceosome. *Mol. Cell* **2**, 457-467 (1998).

178. Pasheva,E. *et al.* In vitro acetylation of HMGB-1 and -2 proteins by CBP: the role of the acidic tail. *Biochemistry* **43**, 2935-2940 (2004).

179. Thevenet,L. *et al.* Regulation of human SRY subcellular distribution by its acetylation/deacetylation. *EMBO J.* **23**, 3336-3345 (2004).

180. Luhrs,H. *et al.* Modulation of HMG-N2 binding to chromatin by butyrate-induced acetylation in human colon adenocarcinoma cells. *Int. J. Cancer* **97**, 567-573 (2002).

181. Wang,R., Cherukuri,P. & Luo,J. Activation of Stat3 sequence-specific DNA binding and transcription by p300/CREB-binding protein-mediated acetylation. *J. Biol. Chem.* **280**, 11528-11534 (2005).

182. Yuan,Z.L., Guan,Y.J., Chatterjee,D. & Chin,Y.E. Stat3 dimerization regulated by reversible acetylation of a single lysine residue. *Science* **307**, 269-273 (2005).

183. Patel,J.H. *et al.* The c-MYC oncoprotein is a substrate of the acetyltransferases hGCN5/PCAF and TIP60. *Mol. Cell Biol.* **24**, 10826-10834 (2004).

184. Fu,M. *et al.* Androgen receptor acetylation governs trans activation and MEKK1-induced apoptosis without affecting in vitro sumoylation and trans-repression function. *Mol. Cell Biol.* **22**, 3373-3388 (2002).

185. Gaughan,L., Logan,I.R., Cook,S., Neal,D.E. & Robson,C.N. Tip60 and histone deacetylase 1 regulate androgen receptor activity through changes to the acetylation status of the receptor. *J. Biol. Chem.* **277**, 25904-25913 (2002).

186. Wang,C. *et al.* Direct acetylation of the estrogen receptor alpha hinge region by p300 regulates transactivation and hormone sensitivity. *J. Biol. Chem.* **276**, 18375-18383 (2001).

187. Boyes,J., Byfield,P., Nakatani,Y. & Ogryzko,V. Regulation of activity of the transcription factor GATA-1 by acetylation. *Nature* **396**, 594-598 (1998).

188. Hayakawa,F. *et al.* Functional regulation of GATA-2 by acetylation. *J. Leukoc. Biol.* **75**, 529-540 (2004).

189. Yamagata,T. *et al.* Acetylation of GATA-3 affects T-cell survival and homing to secondary lymphoid organs. *EMBO J.* **19**, 4676-4687 (2000).

190. Zhang,W. & Bieker,J.J. Acetylation and modulation of erythroid Kruppel-like factor (EKLF) activity by interaction with histone acetyltransferases. *Proc. Natl. Acad. Sci. U. S. A* **95**, 9855-9860 (1998).

191. Zhang,W., Kadam,S., Emerson,B.M. & Bieker,J.J. Site-specific acetylation by p300 or CREB binding protein regulates erythroid Kruppel-like factor transcriptional activity via its interaction with the SWI-SNF complex. *Mol. Cell Biol.* **21**, 2413-2422 (2001).

192. Chen,X. & Bieker,J.J. Unanticipated repression function linked to erythroid Kruppel-like factor. *Mol. Cell Biol.* **21**, 3118-3125 (2001).

193. Sartorelli,V. *et al.* Acetylation of MyoD directed by PCAF is necessary for the execution of the muscle program. *Mol. Cell* **4**, 725-734 (1999).

194. Polesskaya,A. *et al.* CREB-binding protein/p300 activates MyoD by acetylation. *J. Biol. Chem.* **275**, 34359-34364 (2000).

195. Martinez-Balbas,M.A., Bauer,U.M., Nielsen,S.J., Brehm,A. & Kouzarides,T. Regulation of E2F1 activity by acetylation. *EMBO J.* **19**, 662-671 (2000).

196. Marzio,G. *et al.* E2F family members are differentially regulated by reversible acetylation. *J. Biol. Chem.* **275**, 10887-10892 (2000).

197. Costanzo,A. *et al.* DNA damage-dependent acetylation of p73 dictates the selective activation of apoptotic target genes. *Mol. Cell* **9**, 175-186 (2002).

198. Bernassola,F. *et al.* Ubiquitin-dependent degradation of p73 is inhibited by PML. *J. Exp. Med.* **199**, 1545-1557 (2004).

199. Nguyen,D.X., Baglia,L.A., Huang,S.M., Baker,C.M. & McCance,D.J. Acetylation regulates the differentiation-specific functions of the retinoblastoma protein. *EMBO J.* **23**, 1609-1618 (2004).

200. Chen,L., Fischle,W., Verdin,E. & Greene,W.C. Duration of nuclear NF-kappaB action regulated by reversible acetylation. *Science* **293**, 1653-1657 (2001).

201. Chen,L.F., Mu,Y. & Greene,W.C. Acetylation of RelA at discrete sites regulates distinct nuclear functions of NF-kappaB. *EMBO J.* **21**, 6539-6548 (2002).

202. Kiernan,R. *et al.* Post-activation turn-off of NF-kappa B-dependent transcription is regulated by acetylation of p65. *J. Biol. Chem.* **278**, 2758-2766 (2003).

203. Jeong,J.W. *et al.* Regulation and destabilization of HIF-1alpha by ARD1-mediated acetylation. *Cell* **111**, 709-720 (2002).

204. Gronroos,E., Hellman,U., Heldin,C.H. & Ericsson,J. Control of Smad7 stability by competition between acetylation and ubiquitination. *Mol. Cell* **10**, 483-493 (2002).

205. Maruta,H., Greer,K. & Rosenbaum,J.L. The acetylation of alpha-tubulin and its relationship to the assembly and disassembly of microtubules. *J. Cell Biol.* **103**, 571-579 (1986).

206. Schulze,E., Asai,D.J., Bulinski,J.C. & Kirschner,M. Posttranslational modification and microtubule stability. *J. Cell Biol.* **105**, 2167-2177 (1987).

207. Bannister,A.J., Miska,E.A., Gorlich,D. & Kouzarides,T. Acetylation of importin-alpha nuclear import factors by CBP/p300. *Curr. Biol.* **10**, 467-470 (2000).

208. Cohen,H.Y. *et al.* Acetylation of the C terminus of Ku70 by CBP and PCAF controls Bax-mediated apoptosis. *Mol. Cell* **13**, 627-638 (2004).

209. Bali,P. *et al.* Inhibition of histone deacetylase 6 acetylates and disrupts the chaperone function of heat shock protein 90: a novel basis for antileukemia activity of histone deacetylase inhibitors. *J. Biol. Chem.* **280**, 26729-26734 (2005).

210. Kovacs,J.J. *et al.* HDAC6 regulates Hsp90 acetylation and chaperone-dependent activation of glucocorticoid receptor. *Mol. Cell* **18**, 601-607 (2005).

211. Zhang,Q., Yao,H., Vo,N. & Goodman,R.H. Acetylation of adenovirus E1A regulates binding of the transcriptional corepressor CtBP. *Proc. Natl. Acad. Sci. U. S. A* **97**, 14323-14328 (2000).

212. Madison,D.L., Yaciuk,P., Kwok,R.P. & Lundblad,J.R. Acetylation of the adenovirus-transforming protein E1A determines nuclear localization by disrupting association with importin-alpha. *J. Biol. Chem.* **277**, 38755-38763 (2002).

213. Mu,J.J. *et al.* The small delta antigen of hepatitis delta virus is an acetylated protein and acetylation of lysine 72 may influence its cellular localization and viral RNA synthesis. *Virology* **319**, 60-70 (2004).

214. Kouzarides,T. Acetylation: a regulatory modification to rival phosphorylation? *EMBO J.* **19**, 1176-1179 (2000).

215. Eisenhaber,B., Bork,P. & Eisenhaber,F. Prediction of potential GPI-modification sites in proprotein sequences. *J. Mol. Biol.* **292**, 741-758 (1999).

216. Maurer-Stroh,S. & Eisenhaber,F. Refinement and prediction of protein prenylation motifs. *Genome Biol.* **6**, R55 (2005).

217. Benetka,W., Koranda,M., Maurer-Stroh,S., Pittner,F. & Eisenhaber,F. Farnesylation or geranylgeranylation? Efficient assays for testing protein prenylation in vitro and in vivo. *BMC. Biochem.* **7**, 6 (2006).

218. Hancock,J.F. Reticulocyte lysate assay for in vitro translation and posttranslational modification of Ras proteins. *Methods Enzymol.* **255**, 60-65 (1995).

219. Wang,D.A. & Sebti,S.M. Palmitoylated cysteine 192 is required for RhoB tumor-suppressive and apoptotic activities. *J. Biol. Chem.* **280**, 19243-19249 (2005).

220. Maurer-Stroh,S. *et al.* Towards complete sets of farnesylated and geranylgeranylated proteins. *PLoS. Comput. Biol.* **3**, e66 (2007).

221. Hsu,L.C. & Chang,W.C. Sequencing and expression of the human ALDH8 encoding a new member of the aldehyde dehydrogenase family. *Gene* **174**, 319-322 (1996).

222. Neel,V.A. & Young,M.W. Igloo, a GAP-43-related gene expressed in the developing nervous system of Drosophila. *Development* **120**, 2235-2243 (1994).

223. Uemura,T., Shepherd,S., Ackerman,L., Jan,L.Y. & Jan,Y.N. Numb, A Gene Required in Determination of Cell Fate During Sensory Organ Formation in Drosophila Embryos. *Cell* **58**, 349-360 (1989).

224. Rhyu,M.S., Jan,L.Y. & Jan,Y.N. Asymmetric Distribution of Numb Protein During Division of the Sensory Organ Precursor Cell Confers Distinct Fates to Daughter Cells. *Cell* **76**, 477-491 (1994).

225. Guo,S. & Kemphues,K.J. par-1, a gene required for establishing polarity in C. elegans embryos, encodes a putative Ser/Thr kinase that is asymmetrically distributed. *Cell* **81**, 611-620 (1995).

226. Huynh,J.R., Shulman,J.M., Benton,R. & St Johnston,D. PAR-1 is required for the maintenance of oocyte fate in Drosophila. *Development* **128**, 1201-1209 (2001).

227. Shulman,J.M., Benton,R. & St Johnston,D. The Drosophila homolog of C. elegans PAR-1 organizes the oocyte cytoskeleton and directs oskar mRNA localization to the posterior pole. *Cell* **101**, 377-388 (2000).

228. Tomancak,P. *et al.* A Drosophila melanogaster homologue of Caenorhabditis elegans par-1 acts at an early step in embryonic-axis formation. *Nat. Cell Biol.* **2**, 458-460 (2000).

229. Le Borgne,R. & Schweisguth,F. Unequal segregation of neuralized biases notch activation during asymmetric cell division. *Developmental Cell* **5**, 139-148 (2003).

230. Koutelou,E. *et al.* Neuralized-like 1 (Neurl1) targeted to the plasma membrane by N-myristoylation regulates the Notch ligand Jagged1. *J. Biol. Chem.* **283**, 3846-3853 (2008).

231. Vaccari,T. & Ephrussi,A. The fusome and microtubules enrich Par-1 in the oocyte, where it effects polarization in conjunction with Par-3, BicD, Egl, and dynein. *Curr. Biol.* **12**, 1524-1528 (2002).

232. Karin,M. & Ben Neriah,Y. Phosphorylation meets ubiquitination: the control of NF-[kappa]B activity. *Annu. Rev. Immunol.* **18**, 621-663 (2000).

233. Osborne,T.F. Cholesterol homeostasis: clipping out a slippery regulator. *Curr. Biol.* **7**, R172-R174 (1997).

234. Tong,E.H. *et al.* Regulation of nucleocytoplasmic trafficking of transcription factor OREBP/TonEBP/NFAT5. *J. Biol. Chem.* **281**, 23870-23879 (2006).

235. Zhang,Y. *et al.* Identification of genes expressed in C. elegans touch receptor neurons. *Nature* **418**, 331-335 (2002).

236. Chalfie,M. & Au,M. Genetic control of differentiation of the Caenorhabditis elegans touch receptor neurons. *Science* **243**, 1027-1033 (1989).

237. Way,J.C. & Chalfie,M. The mec-3 gene of Caenorhabditis elegans requires its own product for maintained expression and is expressed in three neuronal cell types. *Genes Dev.* **3**, 1823-1833 (1989).

238. Ivanov,D. *et al.* Eco1 is a novel acetyltransferase that can acetylate proteins involved in cohesion. *Curr. Biol.* **12**, 323-328 (2002).

239. He,H., Tan,C.K., Downey,K.M. & So,A.G. A tumor necrosis factor alpha- and interleukin 6-inducible protein that interacts with the small subunit of DNA polymerase delta and proliferating cell nuclear antigen. *Proc. Natl. Acad. Sci. U. S. A* **98**, 11979-11984 (2001).

240. Sun,D. *et al.* Identification of a phylogenetically conserved Sug1 CAD family member that is differentially expressed in the mouse nervous system. *J. Neurobiol.* **33**, 877-890 (1997).

241. Masuyama,H. & MacDonald,P.N. Proteasome-mediated degradation of the vitamin D receptor (VDR) and a putative role for SUG1 interaction with the AF-2 domain of VDR. *J. Cell Biochem.* **71**, 429-440 (1998).

242. Fraser,R.A., Rossignol,M., Heard,D.J., Egly,J.M. & Chambon,P. SUG1, a putative transcriptional mediator and subunit of the PA700 proteasome regulatory complex, is a DNA helicase. *J. Biol. Chem.* **272**, 7122-7126 (1997).

243. Lee,D. *et al.* The proteasome regulatory particle alters the SAGA coactivator to enhance its interactions with transcriptional activators. *Cell* **123**, 423-436 (2005).

244. Bhat,K.P. *et al.* The 19S proteasome ATPase Sug1 plays a critical role in regulating MHC class II transcription. *Mol. Immunol.* **45**, 2214-2224 (2008).

245. Jang,W., Weber,J.S., Tokito,M.K., Holzbaur,E.L. & Meisler,M.H. Mouse p150Glued (dynactin 1) cDNA sequence and evaluation as a candidate for the neuromuscular disease mutation mnd2. *Biochem. Biophys. Res. Commun.* **231**, 344-347 (1997).

246. Lai,C. *et al.* The G59S mutation in p150(glued) causes dysfunction of dynactin in mice. *J. Neurosci.* **27**, 13982-13990 (2007).

247. Stagi,M., Gorlovoy,P., Larionov,S., Takahashi,K. & Neumann,H. Unloading kinesin transported cargoes from the tubulin track via the inflammatory c-Jun N-terminal kinase pathway. *FASEB J.* **20**, 2573-2575 (2006).

248. Terada,N. *et al.* Protein 4.1B localizes on unmyelinated axonal membranes in the mouse enteric nervous system. *Neurosci. Lett.* **366**, 15-17 (2004).

249. Gieffers,C., Korioth,F., Heimann,P., Ungermann,C. & Frey,J. Mitofilin is a transmembrane protein of the inner mitochondrial membrane expressed as two isoforms. *Exp. Cell Res.* **232**, 395-399 (1997).

250. Kim,S.C. *et al.* Substrate and functional diversity of lysine acetylation revealed by a proteomics survey. *Mol. Cell* **23**, 607-618 (2006).

251. Kimmelman,A.C., Osada,M. & Chan,A.M. R-Ras3, a brain-specific Ras-related protein, activates Akt and promotes cell survival in PC12 cells. *Oncogene* **19**, 2014-2022 (2000).

252. Kimmelman,A.C., Nunez,R.N. & Chan,A.M. R-Ras3/M-Ras induces neuronal differentiation of PC12 cells through cell-type-specific activation of the mitogen-activated protein kinase cascade. *Mol. Cell Biol.* **22**, 5946-5961 (2002).